Research toward Multi-Site Characterization Of Sky Obscuration by Clouds

Janet E. Shields, Monette E. Karr, Art R. Burden, Richard W. Johnson, Vincent W. Mikuls, Jacob R. Streeter, and William S. Hodgkiss

Marine Physical Laboratory
Scripps Institution of Oceanography
291 Rosecrans Street
San Diego, CA 92106

July 2009

Final Report

Grant N00244-07-1-009

For the Period
28 June 2007 – 31 October 2008

Report Documentation Page

Form Approved
OMB No. 0704-0188

1. REPORT DATE	2. REPORT TYPE	3. DATES COVERED
01 JUL 2009	**Final**	**28-06-2007 to 31-10-2008**

4. TITLE AND SUBTITLE
Research toward Multi-site Characterization of Sky Obscuration by Clouds

5a. CONTRACT NUMBER
N00244-07-1-0009

5b. GRANT NUMBER

5c. PROGRAM ELEMENT NUMBER

6. AUTHOR(S)
Janet Shields; Monette Karr; Art Burden; Richard Johnson; Vincent Mikuls

5d. PROJECT NUMBER

5e. TASK NUMBER

5f. WORK UNIT NUMBER

7. PERFORMING ORGANIZATION NAME(S) AND ADDRESS(ES)
Marine Physical Laboratory,Scripps Institution of Oceanography/University of California, San Diego,291 Rosecrans St.,San Diego,CA,92106

8. PERFORMING ORGANIZATION REPORT NUMBER

9. SPONSORING/MONITORING AGENCY NAME(S) AND ADDRESS(ES)
Naval Postgraudate School c/o Fleet Industrial and Supply Center (FISC), San Diego Regional Office, Code 230, 930 N. Harbor Drive, Bldg 1, Ste. 60, San Diego, CA, 92132-0060

10. SPONSOR/MONITOR'S ACRONYM(S)
NPS

11. SPONSOR/MONITOR'S REPORT NUMBER(S)

12. DISTRIBUTION/AVAILABILITY STATEMENT
Approved for public release; distribution unlimited

13. SUPPLEMENTARY NOTES

14. ABSTRACT
This report describes the work done for the Naval Post Graduate School and in association with Starfire Optical Range, Kirtland Air Force Base, under NPS Grant N00244-07-1-0009. This work relates to the Air Force?s need to characterize the cloud distribution during day and night, for a variety of applications. These applications include support of research into the impact of clouds on laser communication and support of satellite tracking.

15. SUBJECT TERMS

16. SECURITY CLASSIFICATION OF:			17. LIMITATION OF ABSTRACT	18. NUMBER OF PAGES	19a. NAME OF RESPONSIBLE PERSON
a. REPORT	b. ABSTRACT	c. THIS PAGE			
unclassified	**unclassified**	**unclassified**	**2**	**94**	

Standard Form 298 (Rev. 8-98)
Prescribed by ANSI Std Z39-18

Research toward Multi-Site Characterization Of Sky Obscuration by Clouds

Table of Contents

List of Illustrations

List of Tables

Research toward Multi-Site Characterization Of Sky Obscuration by Clouds

Janet E. Shields, Monette E. Karr, Art R. Burden, Richard W. Johnson, Vincent W. Mikuls, Jacob R. Streeter, and William S. Hodgkiss

1. Introduction

This report describes the work done for the Naval Post Graduate School and in association with Starfire Optical Range, Kirtland Air Force Base, under NPS Grant N00244-07-1-009, between 28 June 2007 and 31 October 2008.

This work relates to the Air Force's need to characterize the cloud distribution during day and night, for a variety of applications. These applications include support of research into the impact of clouds on laser communication and support of satellite tracking. This contract followed Contract N00014-01-D-0043 DO #4, which is documented in Shields et al. 2007a, Technical Note 271, Contract N00014-01-D-0043 DO #11, which is documented in Shields et al. 2007b, Technical Note 272, and Contract N00014-01-D-0043 DO #13, which is documented in Shields et al. 2007c, Technical Note 273.

Under the NPS Grant, we finished preparing a refurbished Whole Sky Imager (WSI), Unit 8, and fielded it at Air Force Site 3. This completed deployment to the three sites we were responsible for, Sites 2, 3, and 5. In addition, we repaired the WSI at Site 5 after it was struck by lightning, and got the WSI at the SOR site operational. We upgraded the daytime cloud algorithm to include an adaptive feature to adjust for haze changes, and upgraded the nighttime cloud algorithm to include moonlight conditions in the new high resolution algorithm. We delivered these algorithms so they were running in real time at Sites 3 and 5, and also processed and delivered significant amounts of archival data from these two sites.

A follow-on Contract, FA9451-008-C-0226, was funded through the Air Force Research Laboratory on 1 February 2008. This work helped fund some of the later work mentioned in the paragraph above. The other work under this contract will be reported under a separate report.

2. Background

A series of digital automated Whole Sky Imagers (WSI) have been developed by MPL over many years, beginning in the early 1980's (Johnson et al. 1989 and 1991, and Shields et al. 1993, 1994, 1997a and b). (Published references are listed in Section 12.3.) These systems are designed to acquire accurate imagery of the full upper hemisphere in several spectral filters, in order to assess the presence of clouds at each pixel in the image. A system capable of 24-hour operation, the Day/Night WSI, was developed by MPL under funding from the Air Force, Navy, and Army in the early 1990's (Shields et al. 1998, 2003b and e, 2004 a and b, and 2005b and c). One of the first two units was

fielded at the Air Force's Starfire Optical Range in October 1992. Technical Memo AV06-034t documents the estimated run-time experience with the different systems. (Technical Memos are listed in Section 12.1.) We have approximately 75 system-years, or 650,000 hours of experience with the Day/Night WSI systems at this time.

Related systems have been designed and fielded over the years. These include a Daytime Visible/NIR WSI (Feister et al. 2000, and Shields et al. 2003d), and visible and Short-wave IR systems for airborne use (Shields et al. 2003c). An imaging system for measuring visibility was developed and successfully tested (Shields et al. 2005a and 2006). A field calibration system was developed to enable calibration of the D/N WSI in the field (Shields et al. 2003a).

SOR has funded development of additional instruments and more advanced algorithms, as well as support of instruments in the field, for several years. Under Contract N00014-97-D-0350 DO #2 (September 1997 – June 2001), MPL was funded to develop and provide a new Day/Night WSI, which was designated Unit 12 (Shields et al. 2003b). This was the first system using a Windows operating system and the Series 300 Photometrics cameras. We also analyzed and provided statistical estimates of Cloud Free Line of Sight (CFLOS) and related properties.

Under Contract N00014-97-D-0350 DO #6 (May 1999 – May 2003), we were funded to provide two upgraded instruments, Units 13 and 14 (Shields et al. 2004b). These instruments included integration of the control computer into the outdoor environmental housing, and new software to provide near-real-time cloud processing on an additional processing computer. In addition, we developed a night cloud algorithm based on detection of the contrast between the signal from stars and their background. The concepts had been developed under funding from another sponsor (Shields et al. 2002). Under Delivery Order #6, this concept was expanded to handle moonlight, and converted to a fieldable C-code and installed on Unit 12 running at the SOR site.

Under Contract N00014-01-D-0043 DO #4 (May 2001 – September 2006), documented in Shields et al. 2007a, we fielded WSI Unit 14 at a site in Virginia, and supported this deployment as well as the continued operation of Unit 12 at the SOR site. Also under DO #4 the day algorithm at the SOR site was updated to run in real time (like Units 13 and 14) and include a horizon and occultor mask, and the clear sky background was updated. A stand-alone version of the algorithm was written for in-house data analysis. Under funding from another sponsor, an extensive data base was processed and analyzed to extract CFLOS statistics. This work allowed us to determine the strengths and weaknesses of the daytime cloud algorithm. The night algorithm was further developed to handle the anthropogenic light sources near the SOR site. The new night algorithm was installed to run in real time at the SOR site.

Under DO #4 we also provided an extensive analysis of IR systems and their pros and cons for this program. Most of this analysis concentrated on Long Wave IR (LWIR) systems in the 8 – 12 μm wavelength region, because our analysis showed that Short Wave IR (SWIR) systems near the 1.6 μm wavelength region would not be adequate for

our purposes, and Mid Wave IR (MWIR) systems near the 3 – 5 μm wavelength region had disadvantages with respect to the LWIR systems. The LWIR analysis of theoretical performance and images we had access to show that the LWIR system can be expected to have difficulty in environments other than those that are high and dry, particularly with thin high clouds as well as all clouds near the horizon. This analysis, as well as the other work done under DO #4, is presented in Shields et al. 2007a.

Contract N00014-01-D-0043 DO #11 (September 2004 – April 2006), is documented in Shields et al., 2007b. During this time, we received some of the older DOS-based WSI systems retired from the program we had built them for, and began refurbishing them for use with this project. The refurbishment also included creating the control software and the processing software to enable these older hardware systems to meet the needs of the SOR program. Many new features were added to the software during this time. The first of the refurbished WSI's was operational in June 05, and ran well, but was not fielded because the site was not ready.

We were asked to direct much of the effort under DO #11 toward processing and testing data, and developing methods to evaluate the results. Program SORCloudAssess was developed to enable testing, and day data from the SOR site were processed and found to be very good, with an estimated accuracy of about 98%. This program does not use a blind test, so the numbers could be optimistic, however the program does enable us to quantitatively compare different sites and algorithm versions.

We were challenged to process data for a hazy site, so data from the Virginia site were processed, and the day cloud algorithm also worked well for this site, with an estimated accuracy of about 98%. For the VA data, we updated the day algorithm to use Near Infrared (NIR) data, and also tested an adaptive algorithm concept.

Meanwhile, the night algorithm data were tested using Program SORCloudAssess. The accuracy is more difficult to assess due to the moderate resolution of the night algorithm, however we still got results of about 95% using the "region of sight", as discussed in Technical Note 272. We also developed a method to ground-truth the results using the brightest stars, and developed and tested beginning concepts for a high resolution night algorithm. Much of the work to convert the night algorithm to a transmittance-based algorithm (rather than contrast-based) was done under this contract. Work in several other areas, including evaluating night data in cities, and developing forecasting techniques, was also begun under this contract.

Contract N00014-01-D-0043 DO #13 (April 2006 – July 2007), is documented in Shields et al., 2007c. Under this contract, we fielded the WSI that was refurbished under DO #11, fielding it at Site 2 in May 2006. A second WSI was refurbished and deployed to Site 5 in January 2007, and a third WSI was partially refurbished. The software was upgraded in several ways, and also the QC capabilities and software were more fully developed.

Under DO #13, the field version of the day algorithm was upgraded to allow using the Near Infrared (NIR) data, which often does a better job in heavy haze. This was fielded at Site 2. The algorithm did not yet include a feature for adjusting for the variations in haze amount, but even just the conversion to the NIR was a significant improvement.

More importantly, we developed a new night algorithm based on the earth-to-space transmittance measured at star locations, which provided high resolution cloud results at night. Although we did not have time under this contract to optimize the algorithm for moonlight conditions, it worked very well under starlight conditions. Details of these accomplishments, as well as others, are documented in Technical Note 273. DO #13 was the contract that immediately preceded the grant under discussion in the current report.

The primary goals of the NPS Grant were to complete the refurbishment and deployment of the third WSI, and get working algorithms in the field at all 3 sites.

3. Statement of Work

The Statement of Work for Grant N00244-07-1-009 is given in italics below.

Primary Task:

Task 1. Under the Primary Task funding in the first year from May 1 2007 through April 30 2008, or for 12 months after receipt of grant, support the multi-site research objectives by providing the necessary test hardware.

Subtask 1.1. Refurbish an existing Whole Sky Imager and repair and/or replace failed components and install software/hardware upgrades necessary to ensure 24/7/365 data collection. Begin refurbishment of additional parts/materials to allow for low to moderate-cost repairs for other WSI systems in the field. Test and calibrate the refurbished WSI and software to insure suitability for deployment to a remote field site. Install the refurbished WSI system at CONUS field site #3. During both pre-deployment and post-deployment intervals, adapt the existing software acquisition algorithms as well as the hardware of the deployed all sky cameras to address and circumvent minor problems that arise during the routine operation of the cameras in the field. Problems may include adapting to different background light levels, system sensitivity, and different integration times.

Subtask 1.2. Write technical memoranda to document the system configuration, test results, and related information that may be needed in the field. Provide a report documenting the status of the instrument and providing an overview of the results of the test, with regard to its anticipated performance. Report results at occasional meetings as scheduled by the DoD contacts at Starfire Optical Range.

Task 2. Under the Primary Task funding for the first year from May 1 2007 through April 30 2008, or for 12 months after receipt of grant, support the multi-site research objectives by providing analysis of the acquired data.

Subtask 2.1. For the instrument fielded in Item 1 and a second WSI which is already fielded, perform a daytime clear sky background analysis for the site, lens, detector and system combination, update the cloud algorithm input files to identify cloud obscuration and create cloud decision images. Deliver the appropriate input files to the government for installation in the field to enable near-real time creation of cloud decision images. Evaluate the night data, and extract the star signals, clear sky background, and cloud radiance fields as necessary to update the algorithm input files for creating cloud decision images at night. Deliver the input files to the government for installation in the field. During both pre-deployment and post-deployment intervals, adapt the existing analysis and support software to address and circumvent minor problems that arise during the routine operation of the cameras in the field. Problems include adapting to different haze levels, and issues such as instrument sensitivity that may impact the algorithms. Evaluate the algorithm results, and assess whether they should be improved, and how they might be improved if necessary.

Subtask 2.2. Write technical memoranda to document the processing, analysis and results. Provide a report documenting an overview of the status of the instrument algorithms and the results of analysis. Report results at occasional meetings as scheduled by the DoD contacts at Starfire Optical Range.

The Optional Tasks were not funded, and therefore we have not included them here.

4. Funding Increments

The funding for the primary tasks was received 28 June 2007. The options were not funded. It should also be noted that we received a no-cost extension through 31 October 2008 on 14 April 2008.

5. Major Deliveries and Documentation

This section outlines the major deliveries associated with each task. The details of the hardware and software deliveries and documentation memo numbers are discussed in Sections 6 and 7. The details of the algorithm developments and data analysis and documentation memo numbers are discussed in Sections 8 and 9.

Task 1: This task is directed primarily toward the refurbishment a WSI, and its deployment at Site 3. It also includes modification of hardware and software as necessary, and calibration of the system. This task also allows for refurbishment of additional systems. Task 1.2 requires documentation of this work, both in memos and in a report.

The refurbishment of the unit for Site 3 was delayed due to camera repairs at the manufacturer that took quite some time, however the refurbishment was completed, and the system deployed on April 9 2008. In addition to the standard refurbishments, the

system was modified by adding a ring shade, as will be discussed in Section 6. Calibrations were acquired and analyzed. Also, the unit at Site 5 was hit by lightning in July 2007, so we refurbished it, and redeployed it January 16 2008. We continued monitoring of the Site 2 instrument and data, and also repaired the instrument at the SOR, although it required further repairs a few months later. We prepared a spare WSI unit, Unit 9.

Numerous memos were provided to the sponsor or to SOR, and are listed in Section 12.1. All of the memos written between July 2007 and February 2008 were written with funding from this grant, and the later memos were in many cases at least partially funded by this grant, or they document work done under this grant. These memos document the configuration of the hardware, the software, the use of the instrument, the calibration tests and their results, and so on. The requirement for a report documenting the hardware is met by this report, Technical Note 274. The memos will be referenced in the sections discussing the hardware.

Task 2: This task is directed primarily toward providing algorithms running in real time at Sites 3 and 5. It requires extracting the field data in able to determine the inputs for both day and night algorithms. Task 2.2 requires documentation of this work, both in memos and in a report.

For the day algorithm, we analyzed Site 5 January – May 08 data. We found that in order to get good results, we had to upgrade the day algorithm in order to include an adaptive feature that adjusted for haze amount. This was completed and integrated into the field code as well as the in-house interactive code. The inputs completed and delivered to the sponsors, who installed it August 26 2008. The day algorithm was further updated and installed on October 14 2008. The Site 3 day algorithm extraction and setup was also completed, and fielded October 14 2008. We also processed significant amounts of Site 5 and Site 3 archival data, and delivered it to SOR on October 23 2008.

For the night algorithm, we felt that we needed to upgrade the algorithm to handle moonlight well. This took a good bit of analysis and programming, but the job was completed using IDL code and then converted to C and integrated into the field code. The moonlight algorithm works well. The Site 5 extraction was completed and the code was installed in the field August 26 2008, and further upgraded and reinstalled on September 23 2008. The Site 3 inputs were extracted, and installed in the field October 23 2008. Significant amounts of Site 3 and 5 archival data were processed, and delivered to the SOR on October 23 2008. In addition, we completed an analysis of optical fade at night, and presented the results at the May 2008 meeting. The archival processing and optical fade work were primarily funded by the follow-on contract however.

Numerous memos were provided to the sponsor or to SOR, and are listed in Section 12.1. All of the memos written between July 2007 and February 2008 were written with funding from this grant, and the later memos were in many cases at least partially funded by this grant, or they document work done under this grant. These memos document the format and use of the archival data, and the use of the real time data. They also include

documentation of the new algorithms, and the extracted algorithm inputs. At the request of SOR, many of these algorithm input memos were not written until later at the request of SOR, but they have now been completed, and are referenced below. The requirement for a report documenting the hardware is met by this report, Technical Note 274. The memos will be referenced in the sections discussing the hardware.

It should be noted that both tasks also require attending meetings and presenting results. The primary author attended meetings on Nov 29 2007, Jan 29 2008, Jan 29 2008, Feb 28 2008, Mar 20 2008, May 6 2008, May 29 2008, Sep 11 2008, and Oct 23 2008. She had prepared a talk for the Oct 23 2007 meeting, but a major wildfire near home prevented participation. A total of 11 talks were prepared by the group and presented at these meetings. An overview of the topics of each talk is provided in Section 12.2.

Although this Section 5 discussion documents some of the more significant deliveries, there were numerous additional deliveries, which are documented in the following sections.

We believe we have completed all contract requirements at this time.

This work is discussed more fully in the following Sections 6 – 9.

6. WSI Refurbishment, Deployment, and Support

This section discusses the progress with WSI refurbishment and deployment, QC and support of the fielded instruments under this Grant.

6.1. WSI Refurbishment under the previous contracts

As discussed in Technical Notes 272 and 273, some older WSI systems became available early in 2005, and the decision was made to refurbish these systems for use at three new SOR sites (Sites 2, 3, and 5) for this program. These older instruments were originally built for the Department of Energy (DOE) and used for many years at a variety of sites. Following refurbishment of the instruments, WSI Unit 7 was deployed to Site 2 in May 2006, and Unit 4 was deployed to Site 5 in January 2007. As discussed in Technical Notes 272 and 273, this work included a lot of upgrade of capabilities, as well as repair and preventative maintenance. In addition, quite a bit of work was completed on Unit 8 under the previous contract.

The configurations of the Unit 7 sensor and the controller upon completion of the refurbishment are shown in Figure 1. The left side shows the sensor unit, with its environmental housing and the solar/lunar occultor. This unit has successfully operated for many years in the Arctic, and similar units have operated in other locations, including the tropics and the desert. The right side shows the controller unit, as reconfigured for the SOR project. The other units are quite similar, except for the size of the occultor shade, which depends on the latitude of the site. Also, Units 7 and 8 have glass domes, and Unit 4 has an acrylic dome.


Fig. 1. Sensor and Controller Configuration for Unit 7

These systems were built in the mid-to-late 1990's, and as a result they needed a fair amount of refurbishment. Typical refurbishment tasks include disassembly and cleaning, replacing worn components such as the coolant tubing, replacing any failed components such as arc drive motors, and getting the cameras tested and purged at Photometrics. In many cases, these components were still operational, but it was sensible to replace them prior to redeployment.

6.2. Site 3 Deployment

Under this contract, we continued with the refurbishment of Unit 8. The biggest problem with Unit 8 was that the camera output was intermittent. We sent it to Photometrics in September 2007, however they no longer had the software or knowledge to operate the camera. One of our team members went out to Photometrics and spent several days working with them, and they were able to repair the camera. The camera repair was completed and the camera was returned on 27 November 07. The Photometrics trip and repair procedures are documented in Memo AV07-052t.

Following repair of the camera, we completed the rest of the refurbishment, test, and calibration, and prepared the documentation that is required for fielding. The instrument was fielded during 8 – 10 April 2008. The documentation memos are AV08-004t, which lists the start-up procedures, AV08-005t, which provides a check list, AV08-006t, which provides an overview of the control computer operations, AV08-007t, which provides an overview of the processing computer operations, AV08-008t, which provides the set-up

instructions, AV08-009t, which discusses the system focus and calibration, and AV08-010t, which provides the system overview and parts list. Memo AV08-013t provides the installation report.

The site installation is shown in Fig. 2. We had been told that there were a lot of lights around the horizon, so to address this issue we designed a small ring shade to place around the dome. This ring shade can perhaps be seen in Fig. 2, and is documented in Memo AV09-054t. We tested the imagery both with and without the ring shade. As shown in Fig. 3, the results without shading were quite poor, but with the ring shade installed, the results were excellent. The ring shade blocks the top of the dome from any lights that are 5 degrees above the horizon or less. This results in blocking 12 degrees above the horizon in the field of view, since the base of the dome is lower than the top of the dome.

Fig. 2. Site 3 installation, including WSI, weather instruments, and shed with computers

When the site started getting warm, we had problems with temperature inside the housing. On 3 – 5 June 08, we replaced the Teca cooler with another Teca cooler, as documented in Memo AV08-020t. This did not turn out to solve the problem, indicating that the problem was that the Teca model of cooler is not sufficient for this site. As a result, on 28 – 30 July 08, we made a second trip and completely replaced the environmental housing for another we had refurbished at MPL that included a McLean

cooler. The McLean cooler has twice the BTU of the Teca. This trip is documented in Memo AV08-030t. This solved the cooler problem.

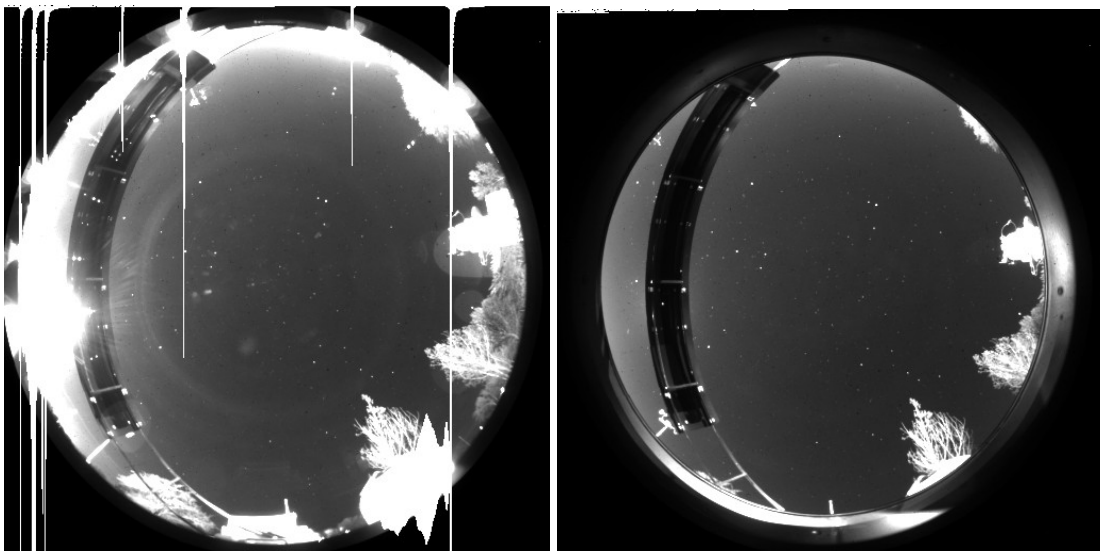

Fig. 3. Raw image at night with no stray light blocking and with stray light blocking

There were also occasional problems with the occultor during this time. The brake power supply was readjusted in the field by the SOR team in May 08. In addition, the occultor stopped working on August 10, and then recovered by itself on September 2, and continued working well throughout the period of the contract. After the end of this contract, some problems occurred again and the occultor was further adjusted.

In spite of the initial start-up problems, most of the data for this site were good. The site statistics chart is shown in Fig. 4. In spite of the problems, the system acquired 85% good data during the first few months, and 98% good data in the last two months of the contract period.

6.3. Site 2 Support

Site 2 had been installed in May 2006, and as reported in Technical Note 273, it worked reasonably well in spite of being an old instrument and the first deployment of a refurbished system. We acquired approximately 85% good data during the period 1 May to 10 December 2006. There was an occultor failure on 11 December 2006. Unfortunately we had insufficient funding to do this repair, however the SOR team was able to repair it with our support in late February 07, as documented in Memo AV07-038t. During the period 28 Feb through 30 Sep 2007, the system acquired 98% good data, as shown in Technical Note 273.

The system continued to run well until February 2008, when the shutter became intermittent. It continued to acquire mostly good data, and the repair was made during 13 – 16 April 2008, as documented in Memo AV08-014t. This repair, and additional repairs made later, were funded by the follow-on contract, however I will document the repairs up until the end of Oct 31 08, which was the end of this contract period. On 10 May, the

control computer failed. We sent a replacement computer, however the site personnel were unable to get it running. We ended up having to replace the processing computer as well, and this was completed 3 – 5 June 2008, as documented in Memo AV08-024t.

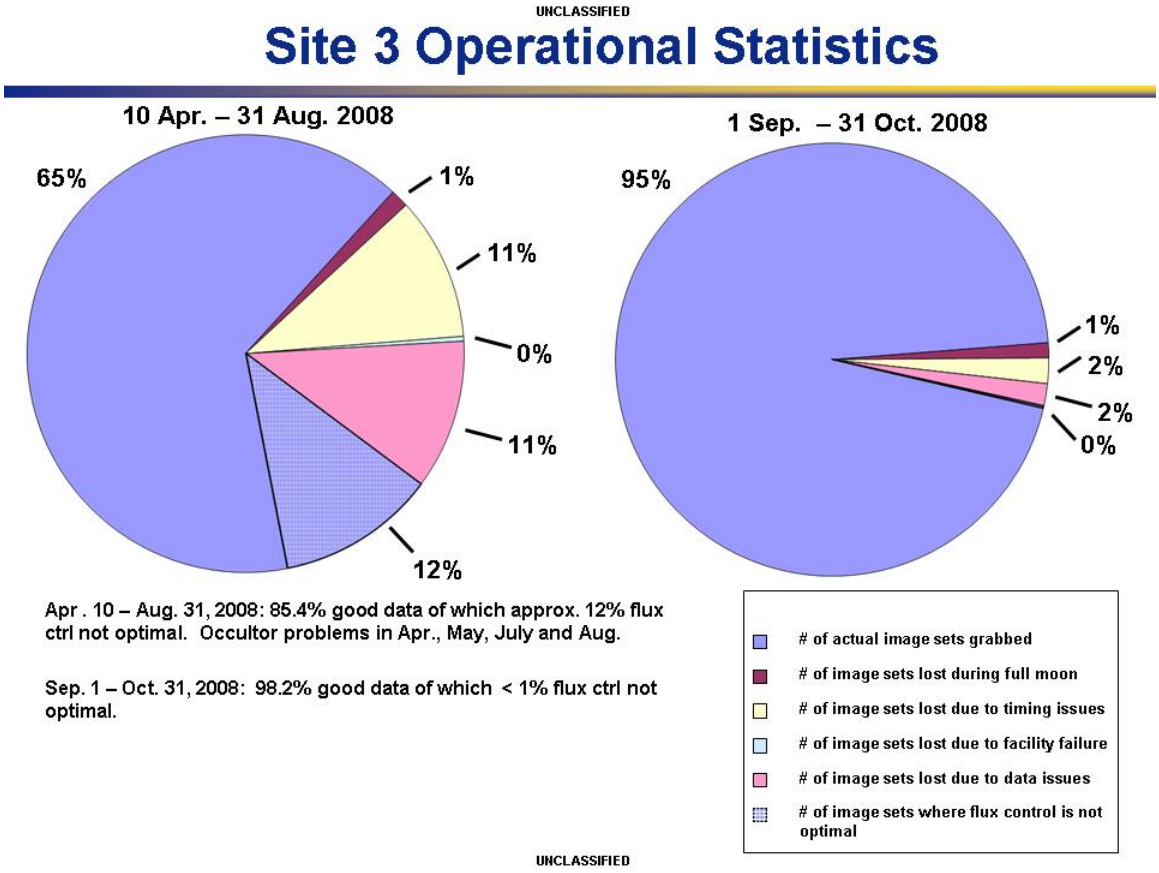

Fig. 4. Site statistics for Site 3 during the contract period

Also, the cooler was destroyed 1 August 2008, as a result of a site power surge, and the system had to be turned off. It was repaired 11 – 14 November 2008, as documented in Memo AV08-046t.

Thus, during the period of the contract from 10 July 2007 through 31 October 2008, this system ran during 10 July 2007 through 10 May 2008 and 3 June through 31 July 2008. The status chart for these periods is shown in Fig. 5. Although the statistics are not optimal, they are reasonable considering that there was not adequate funding to repair this system during much of this contract period. During the first period the system acquired 88% good data, and during the second, it acquired 80% good data.

6.4. Site 5 Support

Site 5 was deployed 31 January 2007, as documented in Technical Note 273. It worked quite well until it was hit by lighting on 23 July 2007. As shown in Technical Note 273, during this interval it acquired 91% good data, and most of the lost data were due to

facility failure, rather than any problems with the WSI. During this interval, there was some routine maintenance, including replacing the external drive, performed on 27 – 28 June 2007, and documented in Memo AV07-039t.

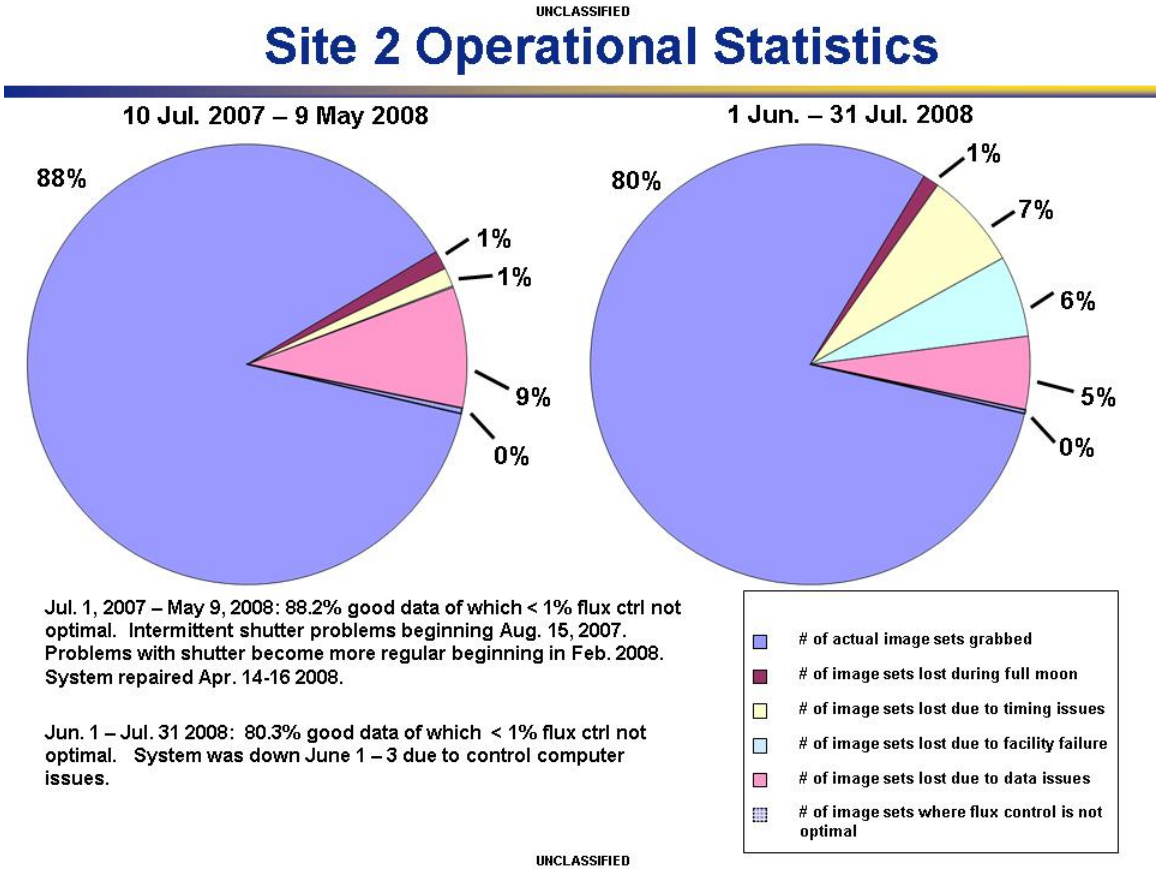

Fig. 5. Site statistics for Site 2 during the contract period

Although this grant was not intended to fund major repairs, repair of the lightning strike was a major priority to the program, and as a result we requested permission to work on this repair. In August, the SOR team went to the site, and returned the computer and both ACP's (Sensor Accessory Control Panel and Occultor Accessory Control Panel, used to electronically control the system). These were repaired at MPL. A trip was made by MPL during October 18 – 19 2007 to reinstall these components, as documented in Memo AV07-050t. On this trip, we tested all the components in detail, and found that the brake power supply and the camera were also dead. On return of these components to MPL, we did further tests of the camera, and then returned it to Photometrics for repair, as documented in Memo AV07-052t. On return, the camera housing was reassembled. We had also had a problem in 2007, in that the daytime images were very slightly out of focus. This was fixed, and the system recalibrated, as documented in Memo AV08-001t. The system was redeployed during 15 – 17 January 2008, as documented in Memo AV08-002t.

The system operated well from 16 January 2008 through 22 May 2008, when the occultor ACP lost power. This was repaired during 30 June through 2 July 2008, as documented in Memo AV08-026t, and a ring shade was added at that time. After that, it operated well through the remainder of the contract period ending 31 October. The status chart is shown in Fig. 6. We achieved 97% good data during 16 Jan – 22 May, and 93% good data during Jul 1 – Oct 31. Most of this data loss was due to the system accidentally being turned off for a few days.

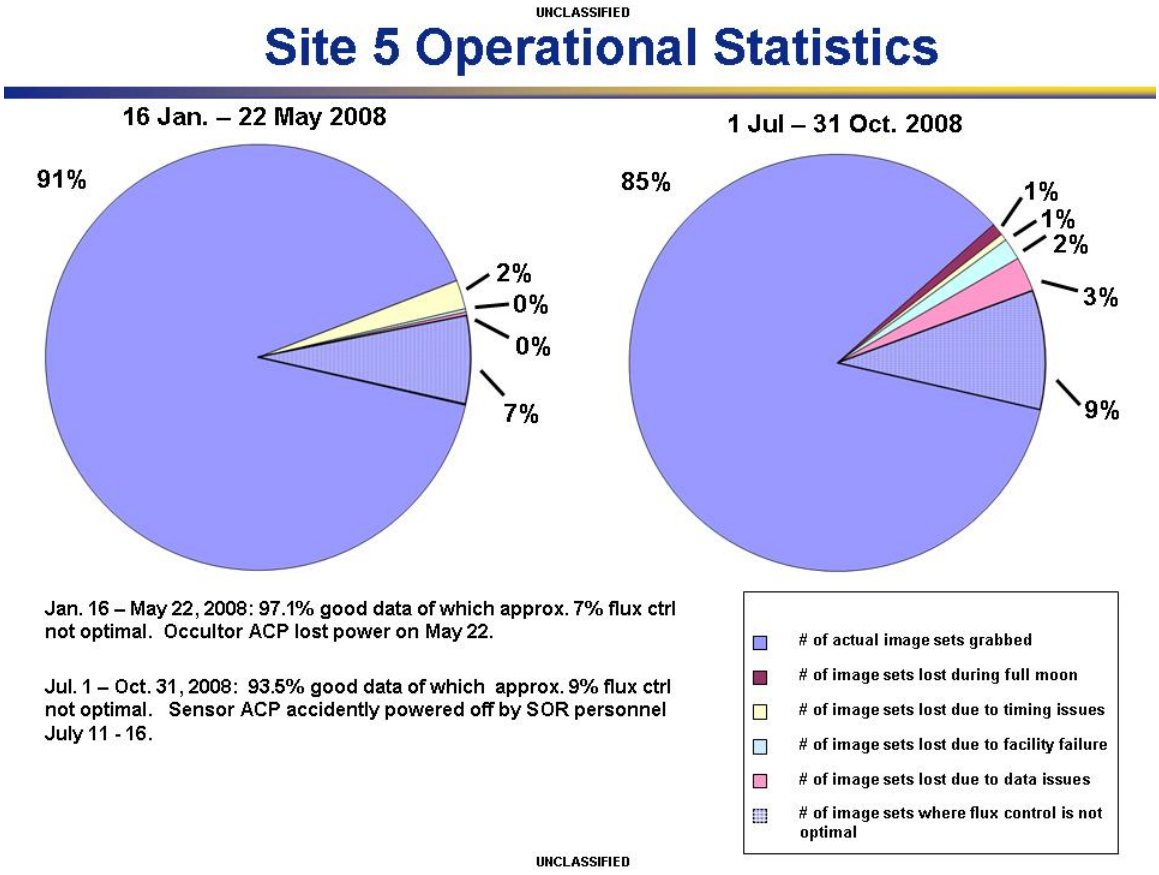

Fig. 6. Site statistics for Site 5 during the contract period

6.5. SOR Site and Virginia Site

We were not funded under this contract to support either of these sites. They had been down for some time due to lack of funding. However, because a team member had to go to the SOR site to give presentations, we were able to provide repairs at no cost to the program. We brought the SOR (Site 7) WSI Unit #12 on-line on 27 September 2007, as documented in Memo AV07-047t. We also did preventative maintenance on 29 November 2007, as documented in Memo AV07-057t. Unfortunately, the system would hang about once a day when acquiring an image. The SOR team tried to diagnose it in December 07, and the system failed.

When the follow-on contract came through in February 2008, we were funded to support the SOR site, although this was lower priority than supporting the other sites. The SOR site was brought on-line during 16 – 18 June 08 with funding from the follow-on contract, as documented in Memo AV08-024t. It continued to work well through the end of the contract period, although we lost quite a bit of data because of power issues at the site. The status chart is shown in Fig. 7.

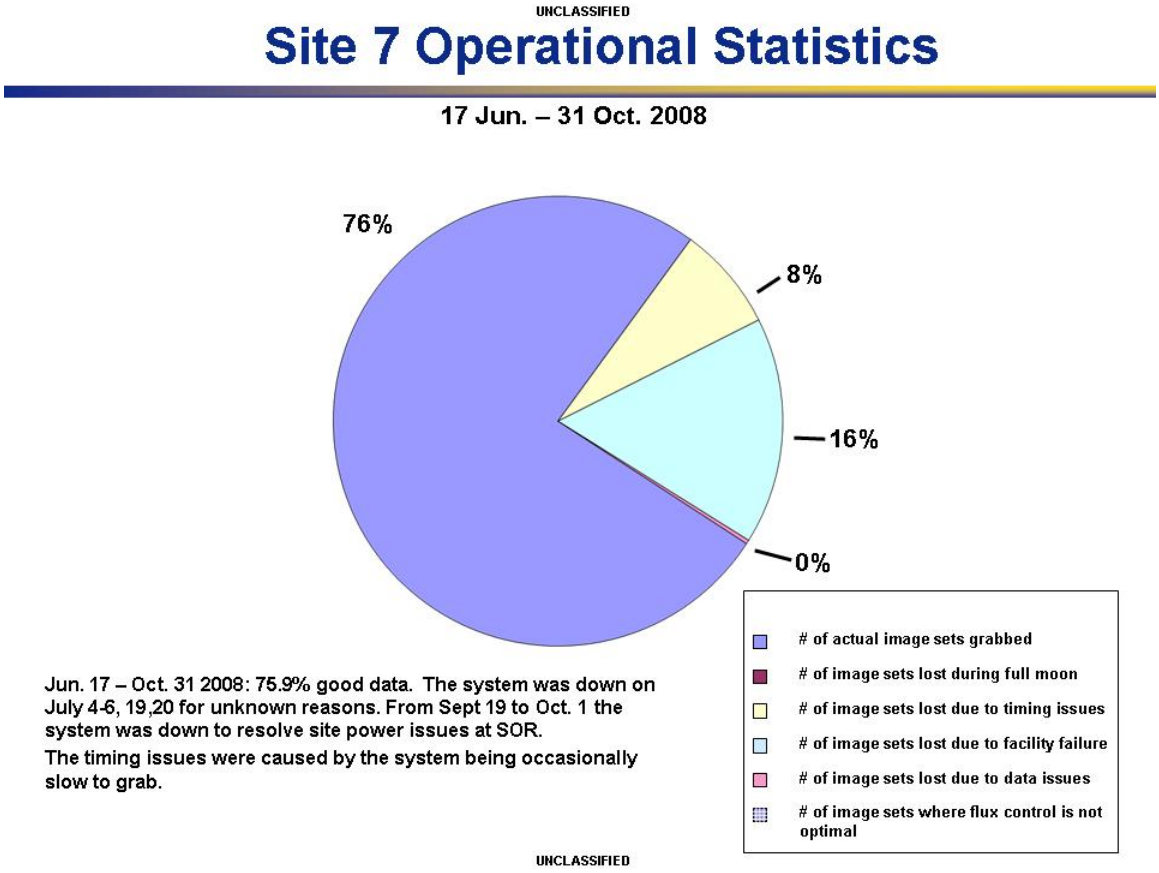

Fig. 7. Site statistics for Site 7 during the contract period

6.6. Hardware Summary

Under this contract, Unit 8 was deployed to Site 3, the last of the main sites. Site 2 was kept in repair, and the Site 5 instrument received extensive repairs following a lightning strike, although this work was partly funded under the follow-on contract. Quite a bit of additional hardware work took place during the interval of the contract, but starting Feb 2008 was mostly funded under the follow-on contract.

7. Software Upgrades and Site Data Processing

This section discusses the upgrades to the field software and the archival and processing of data. Although this section discusses the new algorithm installation, the actual algorithm upgrades are discussed in Sections 8 and 9.

7.1. Field Software Status

There are two primary programs used in the field. RunWSI provides the system control, and ProcWSI provides the result of the real time algorithms that are then sent to SOR via protected ftp. The use of these programs is documented in Memos AV08-006t and -007t, and the quick shut-down is documented in Memo AV08-004t. In addition, an in-house version of the cloud algorithm, AutoProc, is used for testing the day algorithm as it develops, and various IDL programs are used for testing the night algorithm as it develops. Numerous test and data control programs are also present both in the field and in the home analysis facility.

RunWSI is designed to control the instruments. It determines the time and location; calculates the desired occultor position, filter selection and exposure; moves the occultor and filter into position; acquires the images at the proper exposure and in the desired filters; performs initial QC; write status information to a header as well as QC files; and then sends the images to the processing computer. ProcWSI runs on the processing computer. Its primary purpose is to accept the raw imagery, and compute the cloud decision using the algorithms documented in Sections 8 and 9. It performs additional QC checks, and stores these results as well as the processing parameters in the headers. It then archives the data on an external drive, and also ships the data via protected ftp to the SOR site.

The field software was completely upgraded under the previous two contracts, as documented in Technical Notes 272 and 273. As a result, very few upgrades were needed under this contract. The RunWSI program did not require any upgrades during this period. The specific version of each system and its history of fielded software is documented in Memo AV09-005t, which includes both the RunWSI and the ProcWSI history.

The programs write “headers” to the images in order to document the acquisition and processing settings, and also to indicate the results of automated quality control checks. The headers created by RunWSI are documented in Memo AV07-054t. We added new headers to the ProcWSI program. It was installed in the field in Oct 08 at Sites 3 and 5, as documented in Memo AV09-005t. The new headers are documented in Memo AV08-037t. The program updates are documented in Memo AV08-051t.

A new program, QCStat, was written to expedite the quality assessment, and this is documented in Memo AV07-051t. This program made the assessment of field data much easier, and enabled us to start making monthly assessments of the data.

The most significant upgrade to the field software was the addition of the new adaptive day cloud algorithm and the new moonlight algorithm for the night. These upgrades were fielded at Sites 3 and 5 during the August – October 2008 period, as documented in Section 5. The algorithm upgrades are discussed in detail in Sections 8 and 9, and documented in Memos AV09-040t, -041t, and -046t. The details of the software upgrade for ProcWSI are documented in Memo AV08-051t. This upgrade also included addition

of an overall quality indicator. It is important that users of the data base be aware of this indicator, as will be discussed in Section 7.2.

There are many support programs used in handling these large volumes of data, and in extracting the field data and setting up the algorithm inputs. Many of these programs were updated significantly during this period, as documented in Memos AV08-029t, -031t, -032t, -033t, -034t, -035t, -036t, and -039t. However this work was funded under the follow-on contract, and thus is not discussed here.

7.2. Data Archival and Processing

The instruments deployed to Sites 2, 3 and 5 include external hard drives (originally 300 GB, now 500 GB). The primary data archival occurs at SOR, and data are ftp'd directly from the processing computer to the SOR site, where they are archived. The external drives are a redundant backup that provide a second archive, in case of server crashes at the SOR site.

The 300 GB drives must be changed approximately every 6 months, and the 500 GB drives every 9 months. The procedure for changing the drive is documented in Memo AV07-017t.

As discussed in Section 5, our primary goal, in addition to data acquisition, was to get the real time algorithms in the field for Site 3 and 5. In addition, we went ahead and processed archival data as time permitted, since this was a high priority at SOR. The data that were acquired and processed, as well as the delivery of the real time algorithms, is documented in Table 1. Some of the archival processing and algorithm development after 1 Feb 08 was funded by the previous contract.

Table 1 lists the good data that had been acquired as of 31 Oct 08, in columns 1 – 4. In column 3, the entry "Alg Fielded" or "Alg Updated" indicate that we put the real time algorithm into the field. For those archival data that have been processed, as well as the real time algorithms that have been installed, we indicate the date of the delivery in Column 4, the memo which documents what was delivered and how to use it in Column 5, and the memo which documents the determination of the inputs and the results in Column 6.

In the case of Site 3 night, we had not yet processed any of the archival data at the end of October 2008, however we had analyzed it and set up the algorithm inputs. The real time algorithm inputs were based on this analysis, and for this reason we have included the processing memos for these data in the above table. Because the real time algorithm was updated on 12/05/08, we only documented the final delivery in Table 1. The initial algorithm results were nearly as good, however we will be reprocessing the data between 10/23/08 and 12/05/08.

Table 1
Field Data Archival and Processing Status thru 31 Oct 08

Site	Day/Night	Period	Date Delivered	Memo on Delivery	Memo on Processing
2	**Day**	5/2/06 - 12/11/06			
		12/12/06 – 2/26/07	No data		
		2/27/07 - 12/31/07			
		1/1/08 - 7/31/08			
		8/1/08 – 10/31/08	No data		
	Night	5/2/06 - 12/11/06			
		12/12/06 – 2/26/07	No data		
		2/27/07 - 12/31/07			
		1/1/08 - 7/31/08			
		8/1/08 – 10/31/08	No data		
3	**Day**	4/9/08 - 8/4/08	10/23/08	AV08-038t	AV09-008t
		8/5/08 – 10/14/08			
		Alg Fielded	10/14/08	AV09-024t	AV09-008t
	Night	4/9/08 - 7/31/08			AV09-048t
		8/1/08 - 9/1/08			AV09-049t
		9/2/08 - 10/28/08			AV09-050t
		Alg Fielded	10/23/08		AV09-050t
		10/29/08 – 12/05/08			
		Alg Updated	12/05/08	AV09-024t	AV09-050t
5	**Day**	2/1/07 - 7/13/07			
		7/14/07 – 1/15/08	No data		
		1/16/08 - 5/20/08	10/23/08	AV08-038t	AV09-042t
		5/21/08 - 5/22/08			AV09-042t
		5/23/08 – 6/30/08	No data		
		7/1/08 - 10/31/08			AV09-043t
		Alg Fielded	8/26/08		AV09-043t
		Alg Updated	10/14/08	AV09-024t	AV09-043t
	Night	2/1/07 - 7/12/07	10/23/08	AV08-038t	AV09-051t
		7/14/07 – 1/15/08	No data		
		1/17/08 - 2/20/08			AV09-052t
		2/21/08 - 6/30/08	10/23/08	AV08-038t	AV09-052t
		7/1/08 - 8/4/08	10/23/08	AV08-038t	AV09-053t
		8/1/08 - 9/30/08			
		Alg Fielded	8/26/08		AV09-053t
		Alg Updated	9/23/08	AV09-024t	AV09-053t

Memo AV08-038t documents the specific data delivered, and important information such as the geometric calibration equations to use with the data. In addition, Memo AV08-037t provides an overview of the archival format and its use. Memo AV09-024t documents the real time algorithms that were delivered to the field. The memos in Column 6 document the setup of the algorithm inputs for the specific data set, as well as the results. Many of the memos in Column 6 were written much after the contract ended, at the request of SOR. Because we feel that Memos AV08-037t and -038t and AV09-024t are important to the data base user, we have repeated them in Appendices 1 –

3. It should also be noted that we have recently found an error in the night algorithm header where the cloud fraction numbers are reported. We will be correcting all these data and redelivering them. The algorithm results in the pixels are valid, but the summary cloud fraction numbers in the night headers are not.

At the time of writing this report, far more data has been acquired and processed. This will be discussed in the report for the follow-on contract.

The results of the processing are discussed in Sections 8 and 9, which discuss the cloud algorithms and data processing results.

8. Day Algorithm Upgrade and Analysis

During the previous contract, as documented in Technical Note 273, we had processed and evaluated data from Site 2, and set up the real time algorithm running at Site 2. This algorithm used NIR/blue data, because Site 2 was quite hazy, and the NIR results were better. Also during that period, we had updated the algorithm to allow the clear sky background reference value to change as a function of Solar Zenith Angle (SZA). The results were reasonably good, but we felt that it would be very helpful to complete the adaptive algorithm, which would adjust for variable haze amount and its impact on the imagery. Examples and more detailed discussion of these previous results are included in Technical Note 273, Section 8.

When we received funding to begin work on the day algorithm, we began with Site 5, which was the next site that had been fielded. During our time working on Grant N00244-07-1-009, we were able to complete the adaptive algorithm. We also extracted the algorithm inputs for Sites 5 and then 3, got the updated algorithm running in real time at both sites, and processed much of the daytime archival data for these two sites. Processing of the remaining archival data as well as getting the adaptive version of the algorithm running in the field at Site 2, were completed under the follow-on contract. The adaptive algorithm is discussed in Section 8.1. The results for Sites 5 and 3 are discussed in Sections 8.2 and 8.3.

8.1. The Day Adaptive Algorithm that adjusts for variations in Haze Amount

The adaptive algorithm is an update to the D/N WSI's Daytime cloud decision algorithm. It is designed to detect cases with enhanced haze, and adjust the algorithm so that these cases are not identified as thin clouds. Our first version of the adaptive algorithm was programmed for the Daylight Visible/NIR WSI EO System 7 that was built for the Germany's Deutsche WetterDienst. The earlier work was documented in Memo AV04-012t and other memos. An overview of the version of the adaptive algorithm written for the D/N WSI is provided in Memo AV09-040t, and summarized here.

8.1.1. Background

The adaptive algorithm had been adapted and re-programmed for the D/N WSI earlier in 2007 or 2008, but it did not work well, and we did not have the opportunity at that time to look into it in more detail. When we began processing the Site 5 data, however, we found that the haze amount was quite variable for this site, and we really needed to debug the adaptive algorithm and get it working well. As a result, we went ahead and completed this work during July through September 2008, and used it for the Site 5 data analysis.

The Day Thin Cloud algorithm without the adaptive haze feature uses the imagery of the sky measured with blue filters and either red or NIR filters. The initial steps in the algorithm are essentially calibration corrections, which include dark correction, non-uniformity correction. We have found that non-linearity correction is not necessary with this system, because the corrections are so small. From the corrected data, either Red/blue or NIR/blue ratios are computed at each pixel. These can be thresholded to provide detection of opaque clouds. We also check for pixels that are offscale bright or dark, or that have ratios that are offscale.

In our early research, we found that this fixed threshold worked quite well for opaque clouds for all solar zenith angles, and all conditions we have encountered. Originally, we had to apply a zenith-angle-dependent correction, but during this contract, we added the non-uniformity calibration correction, and as a result we no longer have to apply an additional zenith-angle-dependent correction. Thus the correction appears to be due to filter and lens affects that are corrected with the uniformity correction, rather than atmospheric optical effects.

Thin clouds can be better described as having a ratio that's slightly higher than the normal clear sky ratio (as opposed to a fixed ratio such as is used with the opaque clouds). Accordingly, techniques were developed several years ago to characterize the clear sky ratio as a function of look angle and solar zenith angle. This clear sky background ratio is extracted from cloud-free images acquired at the site in the field, and stored as a file of normalized ratios as a function of solar zenith angle and look angle. When field data are processed, a clear sky background ratio image is generated for each field image, based on the current solar zenith angle.

Once the clear sky background image has been generated, those pixels in the current ratio image that are not identified as opaque or offscale are compared with the clear sky ratio. A perturbation ratio is computed for each pixel. This perturbation ratio is the ratio of the current pixel red/blue ratio divided by the clear sky background library ratio. (The perturbation ratio shows how much the current ratio is perturbed or changed with respect to a the clear sky background library ratio for this site, time, and direction.) If the perturbation ratio exceeds a threshold (typically 1.2 or a 20% change), then the pixel is identified as thin cloud. Also, if the clear sky background ratio is higher than the opaque threshold, the pixel will be identified as "indeterminate", meaning that the clear sky ratio in this direction for this solar zenith angle is anticipated to be higher than the ratio for

opaque clouds, and thus we can't identify whether there are clouds there. An example will be shown later.

8.1.2. Requirement for an Adaptive Algorithm

In general, the version of the algorithm described in Section 8.1.1 works quite well. Memos AV06-018t and -020t show results for two sites. The weakness of this earlier version of the algorithm was that when the haze amount is significantly different from that of the cloud-free cases used in extracting the clear background library, the red/blue (and NIR/blue) ratio is higher, and the sky can be falsely identified as thin cloud. Haze will in fact attenuate the signal of anything such as a laser going through the atmosphere, just as thin clouds will, but it attenuates much less in the Short Wave IR than in the visible due to the smaller drop sizes. As a result, we want to be able to distinguish haze from thin cloud, since many applications are in other non-visible wavelengths.

To illustrate the problem, Fig. 8 shows the raw radiances for a reasonably clear day and a fairly hazy day from the same site, which is Site 5. In Fig. 8, we see that the radiances for both the blue and the red are higher with haze (these images were windowed to the same count levels, so the apparent brightness differences are real).

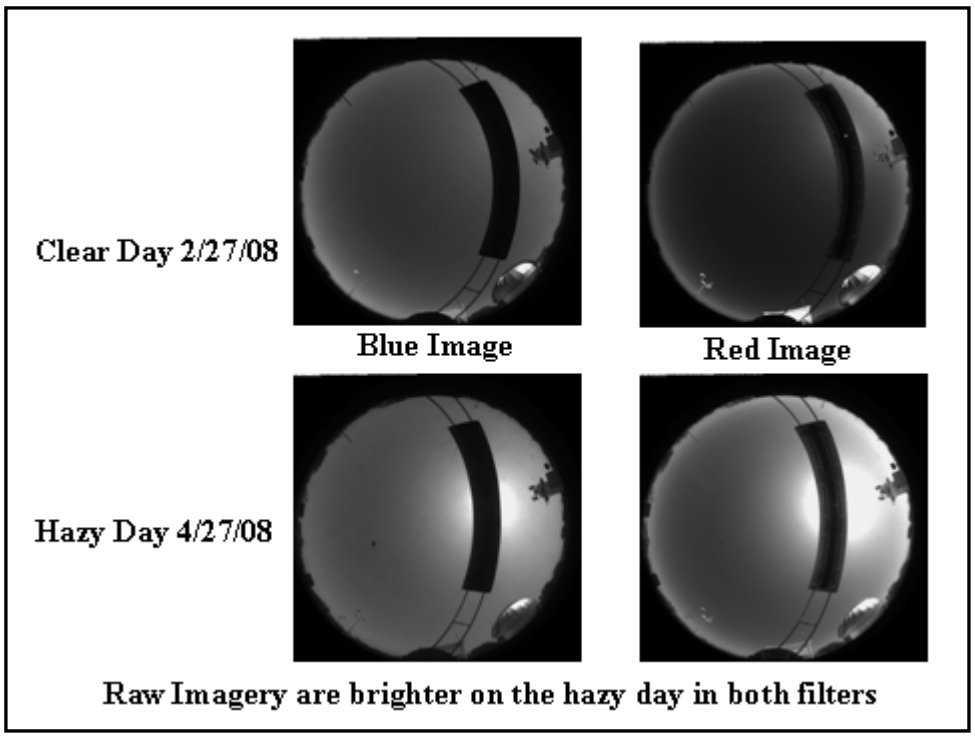

Fig. 8. Raw Imagery, windowed with the same count levels, for a clear day and a hazy day at Site 5. Images acquired at 1700 GMT.

Fig. 9 shows the Red/Blue ratios for these same two cases. Note that the ratio is higher in the hazier case (that is, the sky is not only brighter, but also whiter when it's hazy). Although usually the change with haze is small, in this case, the change was large enough that the whole sky would have been identified as thin cloud.

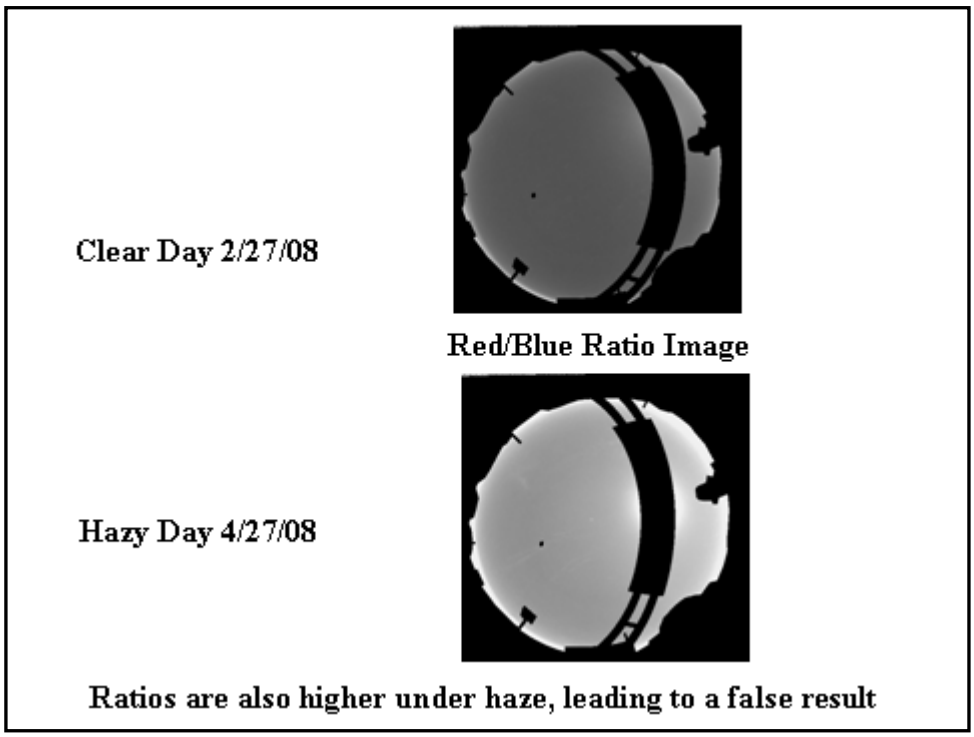

Fig. 9. The Red/Blue ratio image for the same cases as shown in Fig. 8. Note how much higher the ratio is under the very hazy case.

Fig. 10 shows the two cases, and on the left are the results with the previous algorithm, and on the right are the results with the new adaptive algorithm. In Fig. 10, yellow is where the algorithm has called it "thin cloud", and blue is "no cloud". Black is "no data". In the lower right image there is a grey area around the sun. This is a region where the algorithm assigned the category "indeterminate", as discussed in Section 8.1.1.

8.1.3. Concepts Behind the Adaptive Algorithm

When we first evaluated the behavior of clear sky background several years ago, we found that the relative variation in ratio as a function of look angle and solar zenith angle, appears to be nearly independent of haze amount. Only the magnitude changes significantly. The exceptions are right near the aureole, where the drop size distribution will drive the shape of the ratio, and also right near the horizon, where we are probably more affected by the height of the haze boundary layer. This determination was made using both model and data. It's beyond the scope of this memo to show this original work, but I will later show supporting evidence.

As a result, we felt that if we could determine how high or low the ratio for a given field image was in comparison with the clear day library ratio, we could correct our clear day background ratio accordingly. By adjusting the clear sky background up or down according to haze amount, we should be able to use the resulting perturbation ratios over the image to more accurately represent the occurrence of thin clouds.

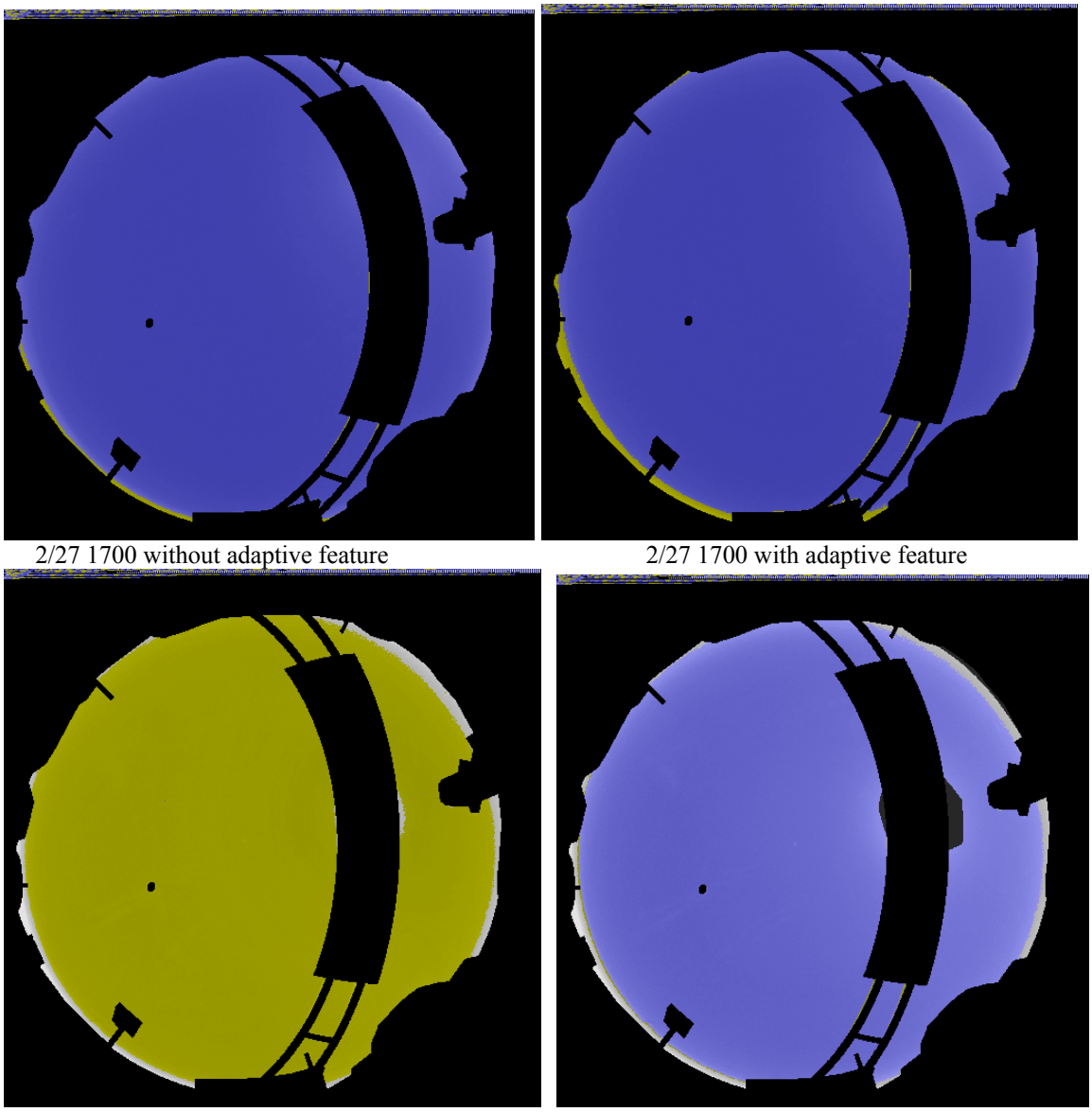

2/27 1700 without adaptive feature

2/27 1700 with adaptive feature

4/27 1700 without adaptive feature

4/27 1700 with adaptive feature

Fig. 10. Cloud Decision Algorithm results for the same cases as shown in Figs. 8 and 9. The results with the previous algorithm are shown on the left, and the adaptive algorithm results are shown on the right. Blue is where the algorithm identified no cloud, and yellow is where the algorithm identified thin cloud.

To evaluate the behavior of the sky ratios as a function of haze, we first evaluated the ratios at two specific points in the sky. In extracting the clear sky background, we always normalize the ratios based on what we call the "beta beta" points. These are two points that are at a scattering angle β that is 45 degrees from the sun, and also at a zenith angle θ of 45 degrees. The locus of points with θ=45° is a ring in the image, half way to the horizon. The locus of points with β =45° is a ring around the sun. These two rings intersect at two points. As part of the processing to generate the clear sky background library, we take the average of the Red/Blue ratio at these two points, and use it as our normalization value for each image used in the library. (When we use the term "Red/Blue", we mean either red/blue or NIR/blue, depending on how the algorithm was

set up.) That is, the clear sky ratios for that image are divided by the normalization constant determined at the beta points. In a later step which is part of generating the clear sky background library, all the normalized ratios that are within ± 1° of a solar zenith angle (SZA) increment of 5° are averaged to represent that solar zenith angle.

In processing field data, when the clear sky background for a given field image is regenerated from the clear sky library, it is interpolated between the nearest two SZA values to the correct SZA value, and then multiplied by the selected normalization constant. The normalized values that are stored in the library are only extracted at every 5° zenith angle and 15° azimuth angle, so when the clear sky background for a given field image is generated, the program also interpolates between these look angles.

Fig. 11 shows the magnitude of the average ratio at the two beta points, for a number of reasonably cloud-free (both clear and hazy) days, and as a function of solar zenith angle. It rises very strongly near sunrise and sunset, corresponding with the whiter (or redder) skies we encounter at these times. In Fig 11, there are 3 best fit curves. In the previous version of the algorithm, we could choose only a single best fit curve to use for the whole data set. As a result, the changes in the normalization constant as a function of SZA were already well handled, but the day-to-day changes resulting from changing haze amount were not handled.

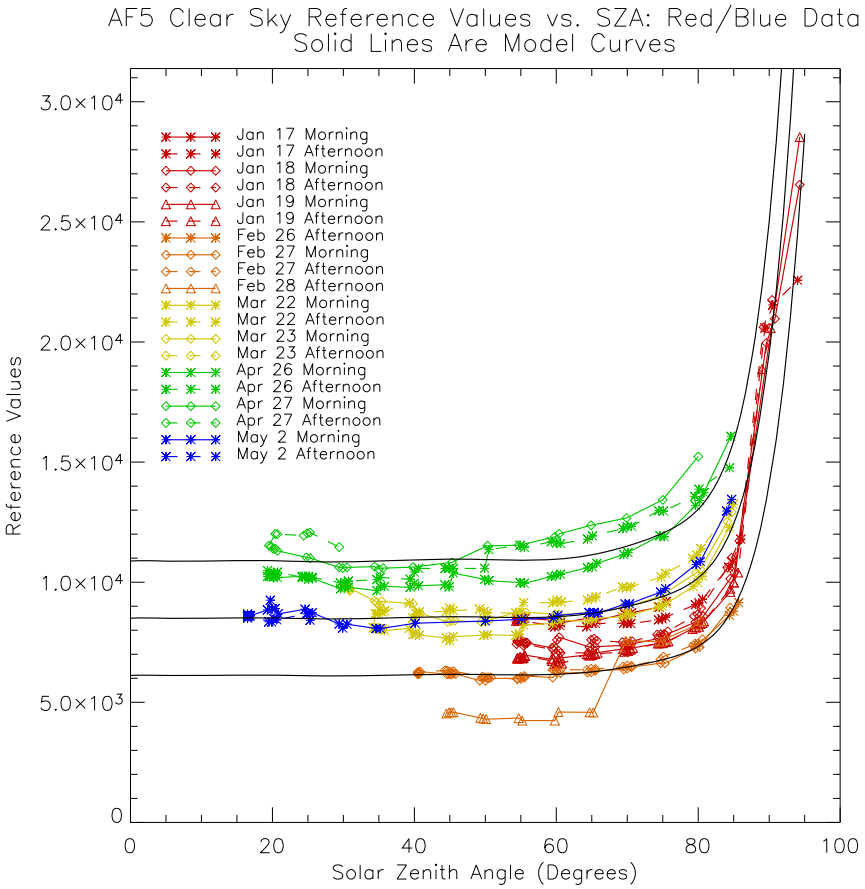

Fig. 11. Reference Values, or Normalization Values, for clear sky ratios during several cloud-free (or nearly cloud-free) days at Site 5.

Note that in general if a given image has a higher or lower reference value than average, it tends to stay that way, to a first approximation, throughout a day. That is, the green curves all stay somewhere near the upper curve, and the blue curve stays near the middle curve, with occasional exceptions as demonstrated by the bottom orange curve. This implies that in general the haze amount tends to persist for at least a few hours.

8.1.4. How the Adaptive Algorithm Works

As described in Section 4, we felt that if we could find a way to predictably determine how much higher or lower the reference curve should be on a given day, we could adjust for the haze. We wanted this to be able to run in the field in real time, which means we couldn't look at the whole day after the fact, but had to use the current image or recent images. We wanted the correction to be tested for each image, in case the haze amount changed during the day. The algorithm should also be flexible enough to work well if a correction cannot be determined for a specific image.

An outline of the adaptive algorithm is as follows. First we first create a line between the two beta points. Then we compute the perturbation ratio along this line. The perturbation ratio is the current ratio divided by the clear sky ratio, and it shows how much the current situation is changed from the clear sky library condition. We look at the Standard Deviation (STD) of the perturbation ratio along the line. If the STD is high, then the region is probably not cloud-free, and is not used to adjust the background. But if the STD is low, and it meets certain other criteria, then it is probably cloud-free, and we determine the correction from the average perturbation ratio along the line. This correction is then multiplied by the full image clear sky background ratio to create the modified clear sky background ratio for that image. And then the cloud algorithm makes its normal checks with respect to this adjusted background.

As part of the check, we also verify that the ratio along the line is not too close to the opaque threshold, nor too close to the sun. The more specific logic of this part of the adaptive algorithm is as follows:

1. If the STD of the perturbation ratio along the line is sufficiently low, and the field ratios are not too high, then we extract the correction from the average of the perturbation along the line.

2. If the STD is too high, we look at segments along the line. If there are any good segments that meet the requirements, then we determine a correction from the average of these segments.

3. If we are not successful, we use the most recent correction, if there is one. Otherwise, the reference correction value of 1 is used.

The above description is somewhat of a simplification, but it is logically correct.

8.1.5. Typical Perturbation Values along the Beta Line

Fig. 12 shows a sample when the day was slightly clearer than the nominal clear day. The green curve shows the magnitude of the field image red/blue ratio along the line, and the purple curve shows the magnitude of the clear sky library ratio along the line. The algorithm chose a correction factor of 0.84 for this case.

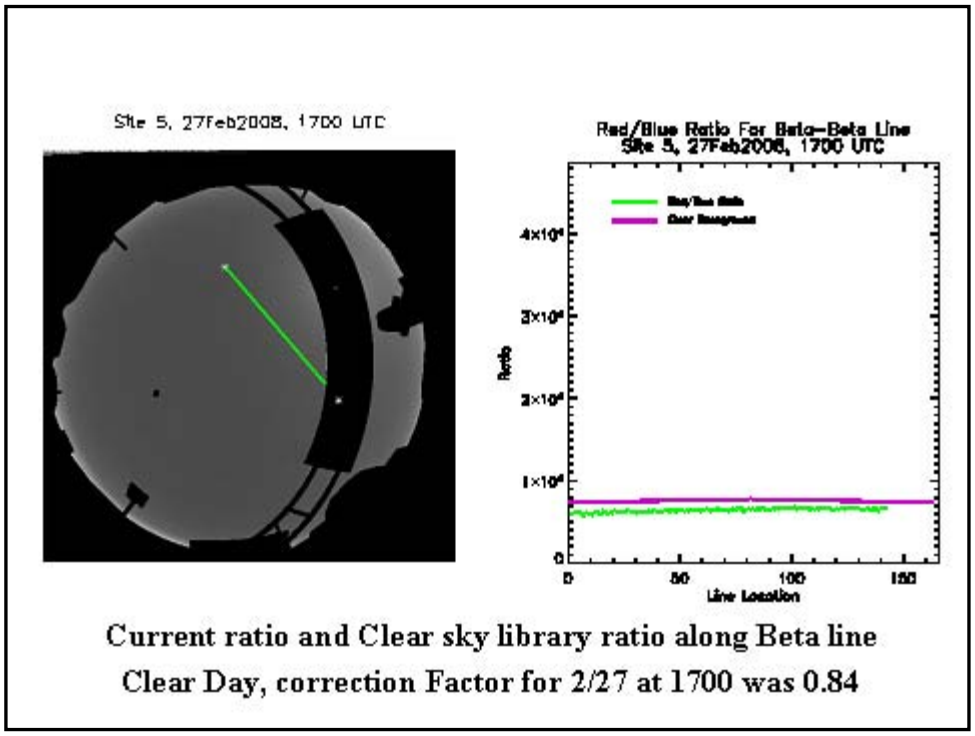

Fig. 12. Sample results for an image on a clear day with low haze amount

In Fig. 13, we show a case for a very hazy day. The field red/blue ratio was significantly higher than the clear sky library ratio along the line, and a correction of 1.42 was chosen by the algorithm.

Fig. 14 shows a case in which there were clouds along some of the beta line. Part of the beta line was reasonably clear, however the STD was a bit too high, and it used a correction of 1.35 extracted two hours previously. However, from the plot we can see that the magnitude of the correction is about right, and we can see that the opaque clouds on part of the line create very large perturbations, which is why they need to be ignored. The fact that the opaque ratio is so different from the clear sky ratio is one reason that the opaque detection is so robust, even as haze amount varies.

The next question is how well the haze correction factor determined from the beta line applies to the whole image. In Figs. 15 and 16, we have shown the field ratio and the clear sky ratio, both for the beta line, and for a line going through the sun. Fig. 15 shows a relatively low-haze day, and Fig. 16 shows a relatively hazy day.

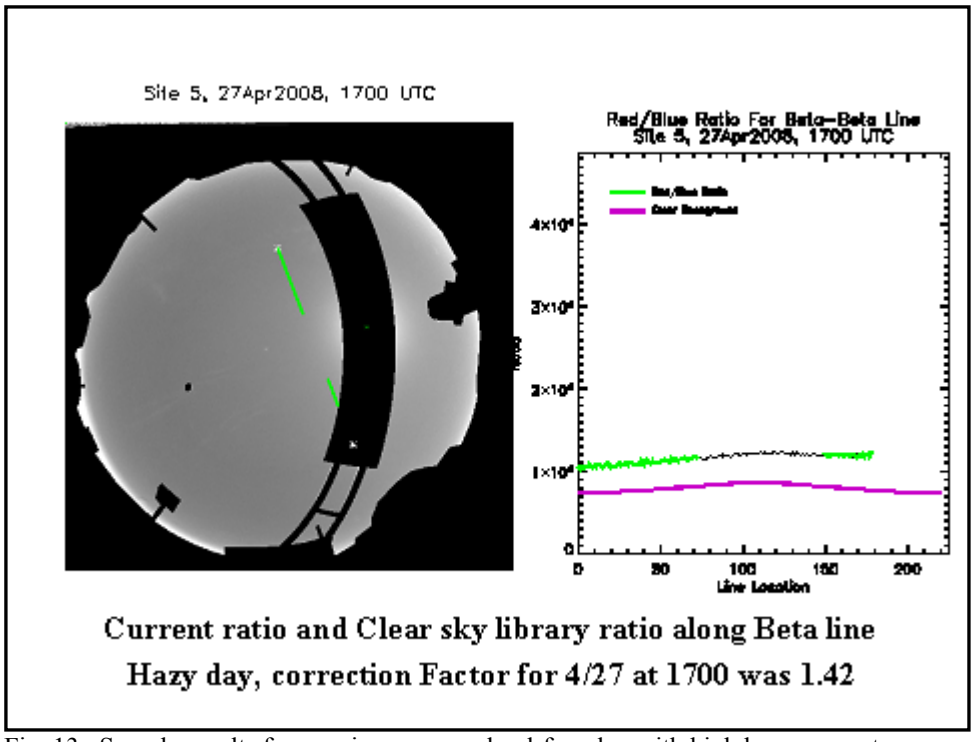

Fig. 13. Sample results for a an image on a cloud-free day with high haze amount

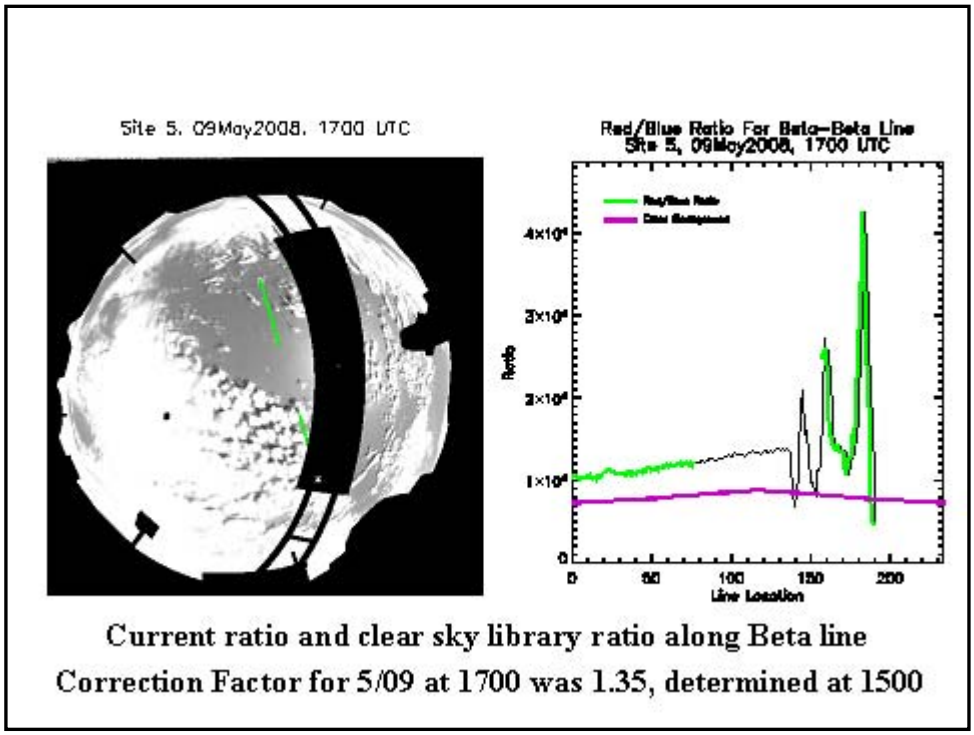

Fig. 14. Sample results for an image with clouds along part of the beta line

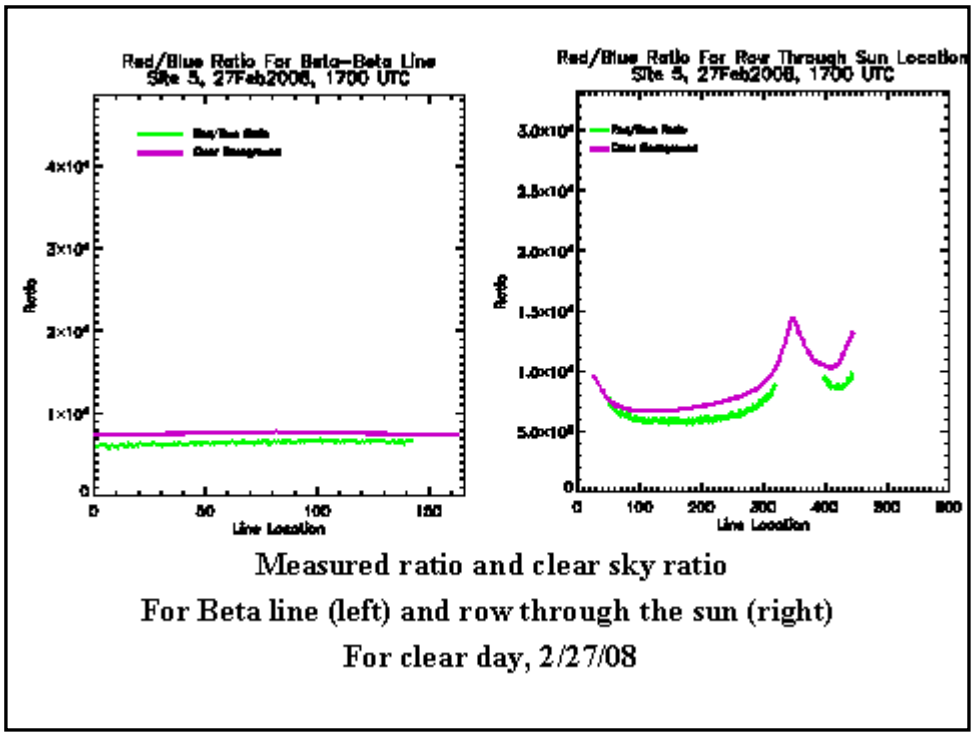

Fig. 15. Red/blue ratio for the current image (green line) and its nominal clear sky background (purple line). Plot on left is for beta line, and plot on right is for line through the sun. This is for a relatively low haze case.

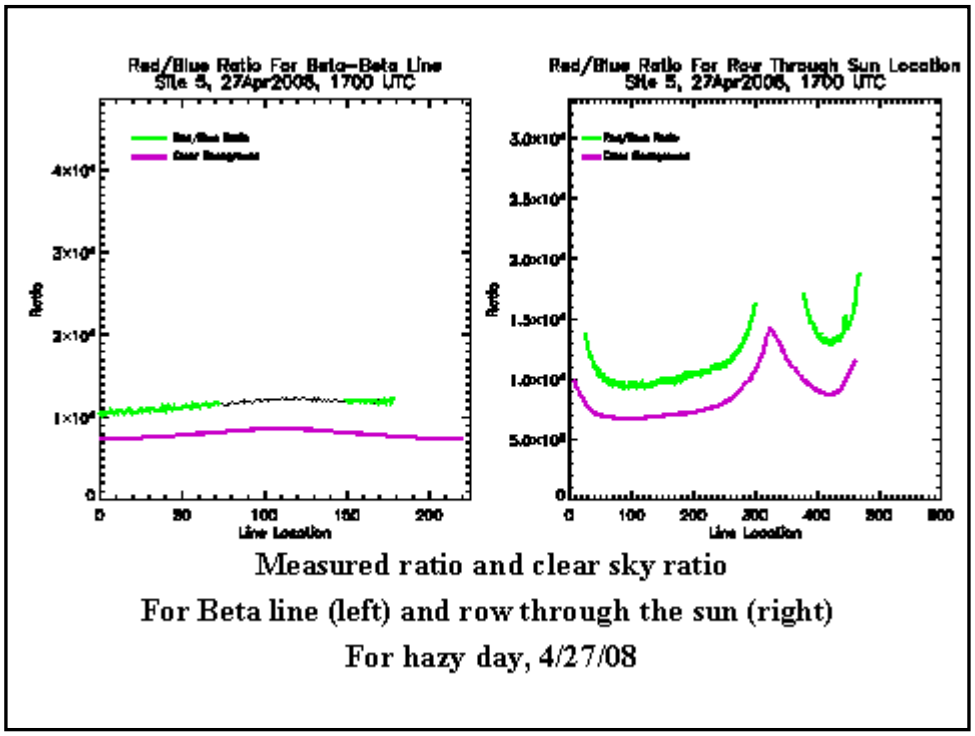

Fig. 16. Red/blue ratio for the current image (green line) and its nominal clear sky background (purple line). Plot on left is for beta line, and plot on right is for line through the sun. This is for a relatively high haze case.

As can be seen in Figs. 15 and 16, the separation between the green and purple lines for the beta line (plot on the left) appears to be reasonably representative of the separation that occurs on a line through the sun and the horizon. That is, the perturbation ratio along the beta line appears to represent the perturbation for other parts of the image quite well. This indicates that the haze correction determined using the beta line should apply reasonably well to the full image. We found that this was the case; that is, the correction works quite well over the whole image in most cases.

8.1.6. Sample Results

Examples for clear skies, both with and without heightened haze, have already been shown in Figs. 8-10. Note in the bottom right image of Fig. 10 that there is a grey circle around the sun. This is a region characterized as "indeterminate". In this case, the clear sky background, as adjusted for the high haze, has a high enough ratio that it cannot readily be separated from opaque cloud. In both of these clear cases, the algorithm did very well. The horizon was very slightly worse in both cases, but the sponsors have told us that they no longer care about the horizon, so we felt that it was not cost-effective to try to improve the horizon.

The results both with and without the adaptive feature of the algorithm for a case with broken clouds are shown in Fig. 17. Other sample results will be shown in the sections discussing the processing of the field data.

The Site 5 Jan – May data set was used to develop the adaptive algorithm. To further test the results of the adaptive algorithm, we ran an additional run with the same input parameters, but with the adaptive feature of the algorithm turned off. We evaluated the hourly data, and found that out of 1401 cases we evaluated, approximately 24% of the cases were significantly better with the adaptive algorithm turned on. Approximately 74% were good with either algorithm, and approximately 2% of the cases were significantly worse with the adaptive algorithm turned on. Most of the cases in which the algorithm did better were in April and May, and were the heavy haze cases. Examples are shown in Fig. 10. Most of the cases in which the algorithm did worse were cases in which there was cirrus, and the algorithm did not pick up as much of the cirrus, although it generally picked up some.

In summary, the new adaptive algorithm evaluates the images on a case by case basis, to adjust for the impact of haze on the image. If it cannot make a current determination, it uses the most recent determination, as corrected for changing solar zenith angle. We found that the new algorithm is not perfect, but is much better than the previous version, in that it avoids calling heavy haze conditions thin cloud.

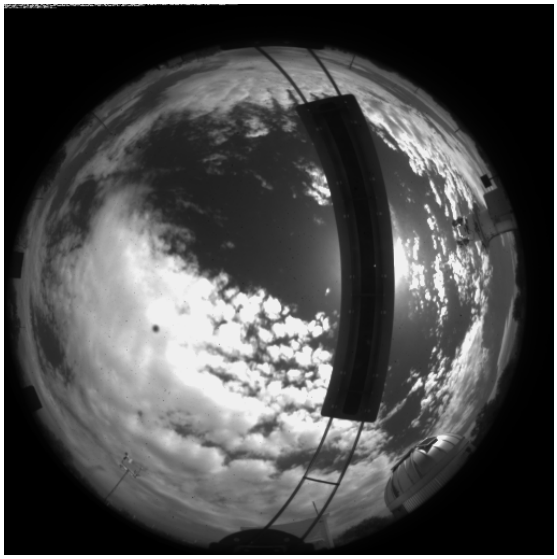

Raw image, 9 May 08 1700

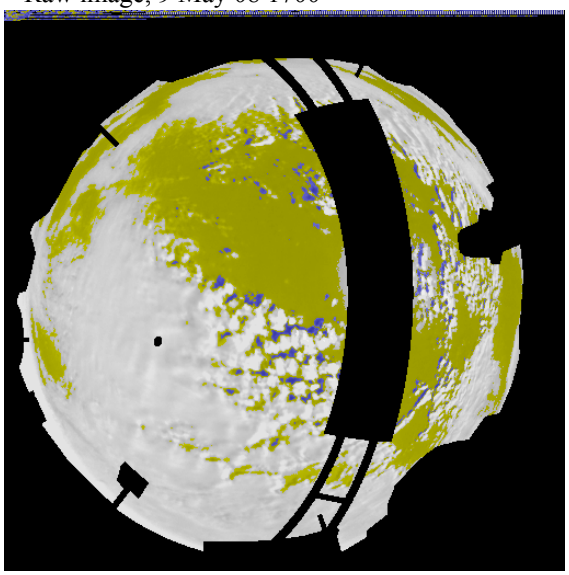

Result without adaptive feature of algorithm

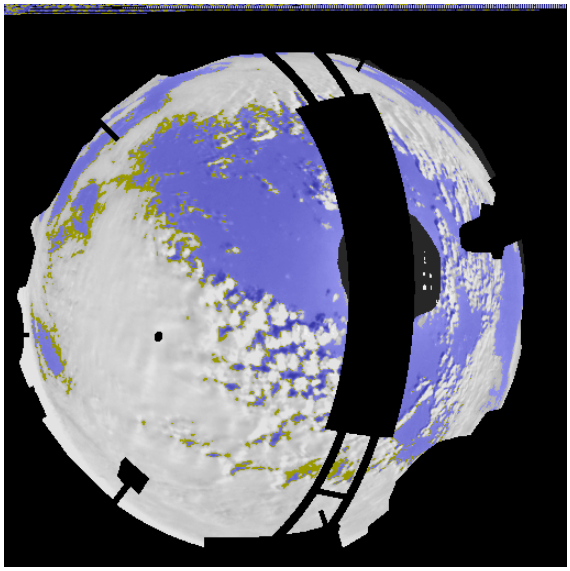

Result with adaptive algorithm

Fig. 17. Sample result for broken clouds, 9 May 08 1700

8.2. Site 5 Daytime Processing and Real Time Algorithm

Under this contract, the archival Daytime Site 5 data for January 16 – May 20 2008 were processed and analyzed and delivered. The instrument was redeployed on January 16 2008, following repair from a lightning strike in 2007. The instrument was down from May 21 through July 1 due to an occultor failure. The post-repair data were evaluated, and the inputs extracted to run the algorithm in real time. The real time algorithm was installed on the system on October 14, 2008. The details of the analysis are documented in Memo AV09-042t. The inputs for the real time algorithm are documented in Memo AV09-043, which also documents the processing of the post-repair data, which was done under the follow-on contract. It should be noted that the documentation of these data was jointly funded with the follow-on contract.

Sample results for two clear days discussed in Section 8.1 are repeated in Figs. 18 and 19. Additional sample results are shown in Figs. 20 - 22. We are very pleased with these results. Fig. 22 shows an excellent case with cirrus forming from contrails, and demonstrates the ability of the WSI to detect contrails.

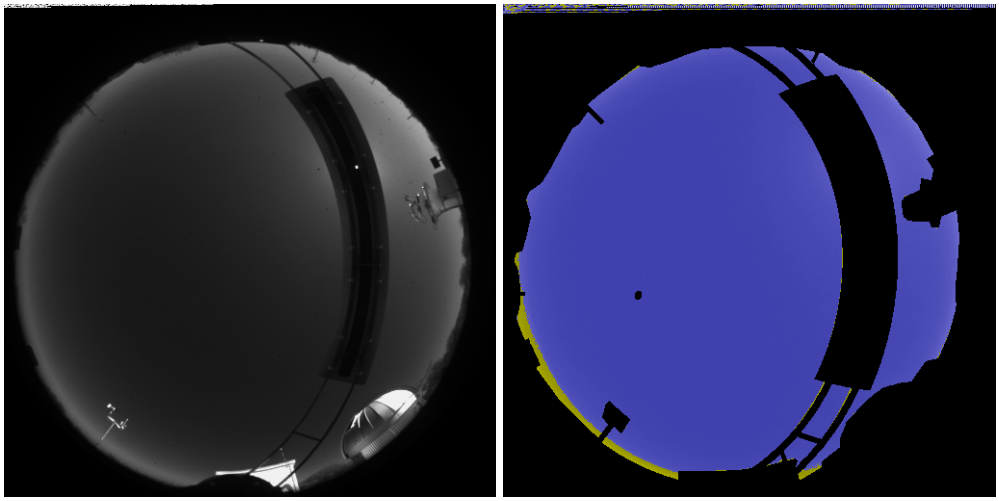

Fig. 18. Raw image and Adaptive Algorithm results for clear case, 2/27/08 at 1700 GMT

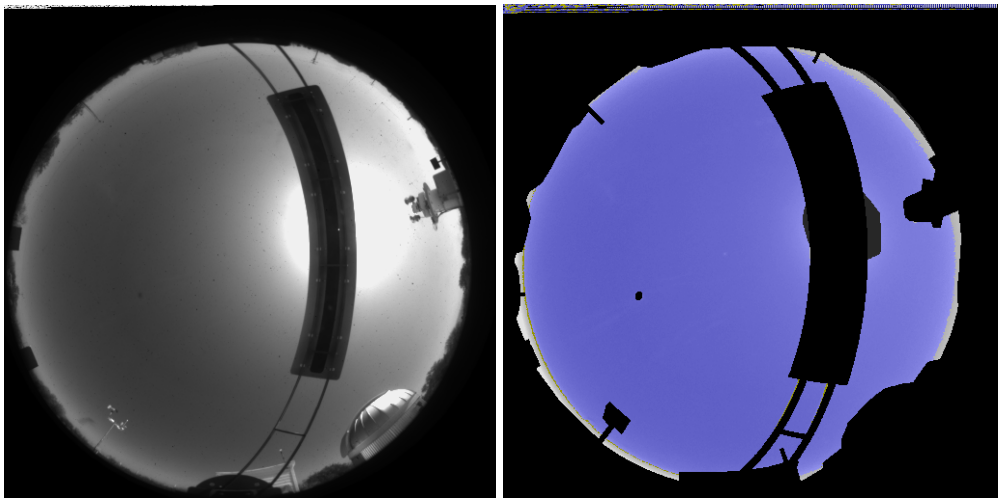

Fig. 19. Raw image and Adaptive Algorithm results for clear case with haze, 4/27/08 at 1700 GMT

The rest of the Site 5 Daytime data was processed under the follow-on contract, and will be discussed in the next report. The format of the archival delivery is documented in Technical Memo AV08-037t, repeated in Appendix 1. The use of the archival data, including the equations for the geometric calibration, is documented in Technical Memo AV08-038t, repeated in Appendix 2. The use of the real time data is documented in Technical Memo AV09-024t.

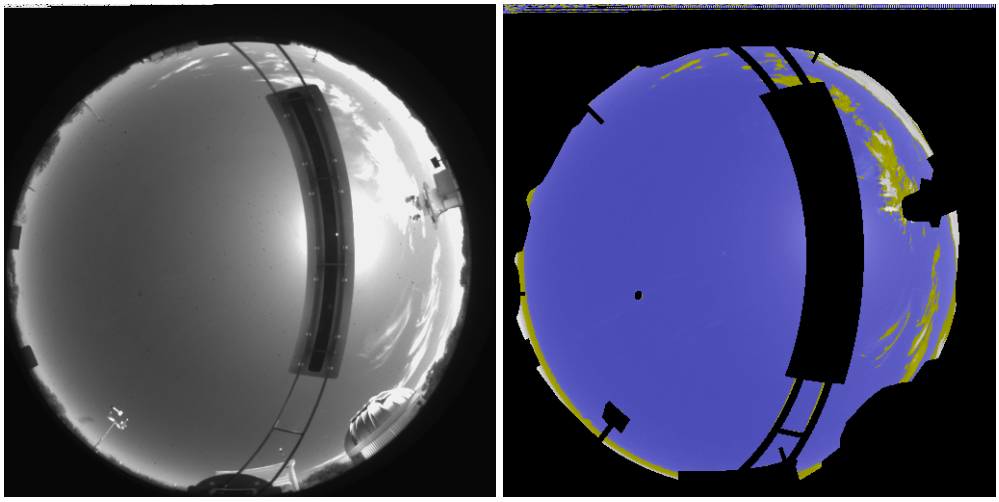

Fig. 20. Raw image and Adaptive Algorithm results for scattered cloud case, 5/4/08 at 1700 GMT

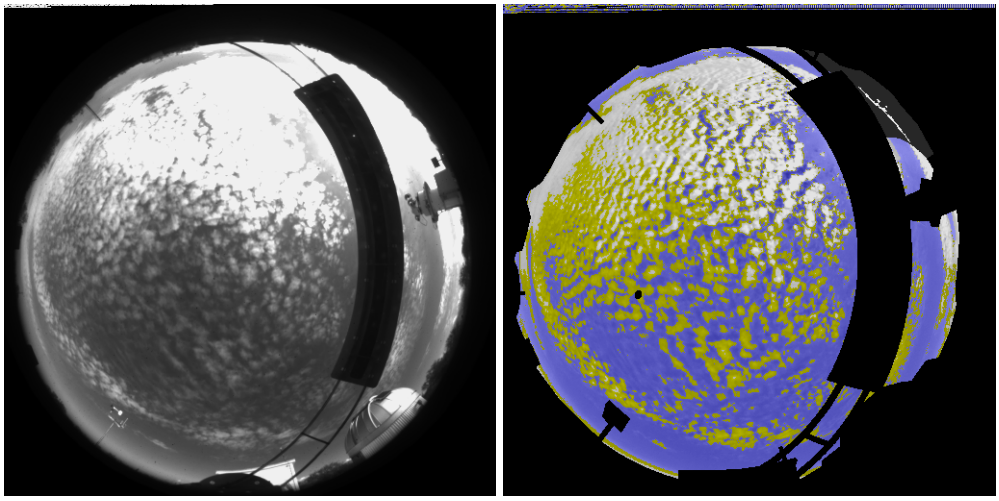

Fig. 21. Raw image and Adaptive Algorithm results for broken cloud, 1/24/08 at 1700 GMT

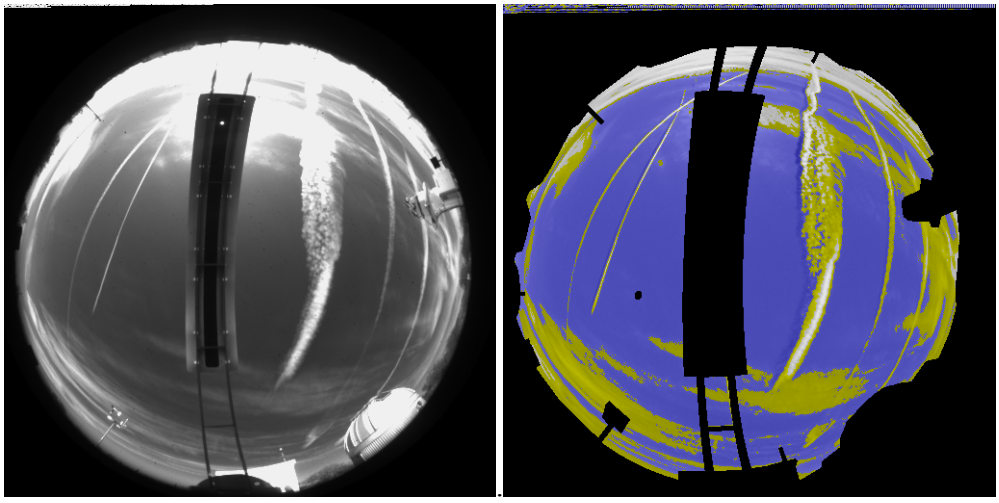

Fig. 22. Raw image and Adaptive Algorithm results for cirrus forming from contrails, 1/20/08 at 2000 GMT

8.3. Site 3 Daytime Processing and Real Time Algorithm

During the time of this contract, the archival Daytime Site 3 data for April 9 – August 4 were processed and analyzed and delivered. The instrument was deployed during 8 – 10 April 2008. The real time algorithm was installed on the system on October 14, 2008 (the same day as for Site 5). It should be noted that the analysis and documentation of these data was jointly funded with the follow-on contract.

The details of the analysis are documented in Memo AV09-008t. These data were somewhat spotty due to occultor and cooler problems, however both problems were repaired. Data marked "Uncertain" in the data header should not be used. If this precaution is taken, then the processed data may be used with good confidence, as it eliminates the cases impacted by the heat and occultor.

Sample results for a clear day and a scattered cloud case are shown in Figs. 23 and 24. Fig. 25 shows a series of hourly images taken over 6 hours, that illustrate that the algorithm generally works well under all conditions. One can also note in this figure that when there were very thin cirrus, the algorithm may not identify them. In general, when this happens the algorithm will identify some of the cirrus, but not all of them. This happens because the thin cloud optical density threshold is not 0; that is, some very thin clouds will be missed. Our sponsors felt that it is reasonable to have a threshold of around 1 dB (transmittance .79). We have estimated the optical density thresholds will at night, as will be discussed further in Section 9. Under the follow-on contract, we began developing methods to quantify the thin cloud optical density associated with the thin cloud threshold for the daytime algorithm, but then we were asked not to make this a priority.

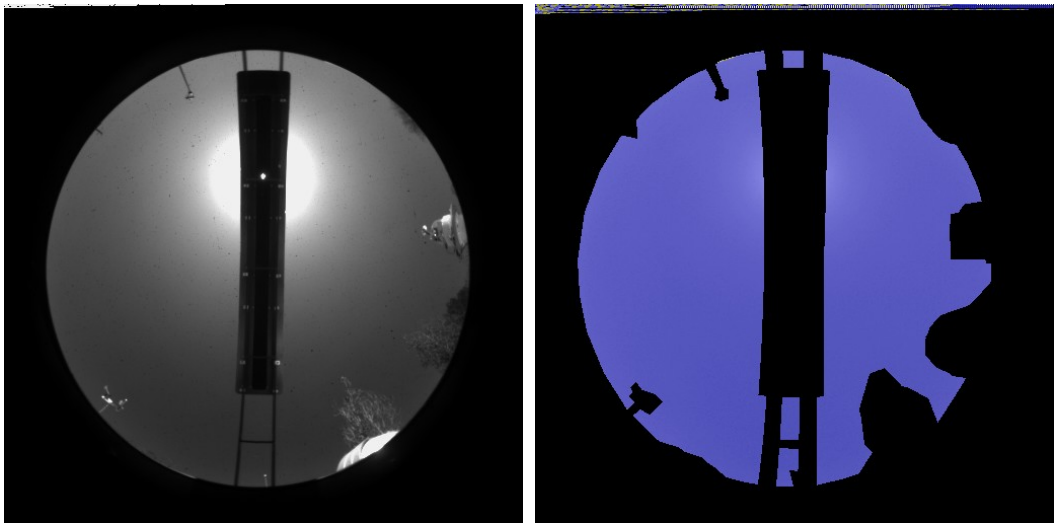

Fig. 23. Clear sky results, 11 April 08 2000.

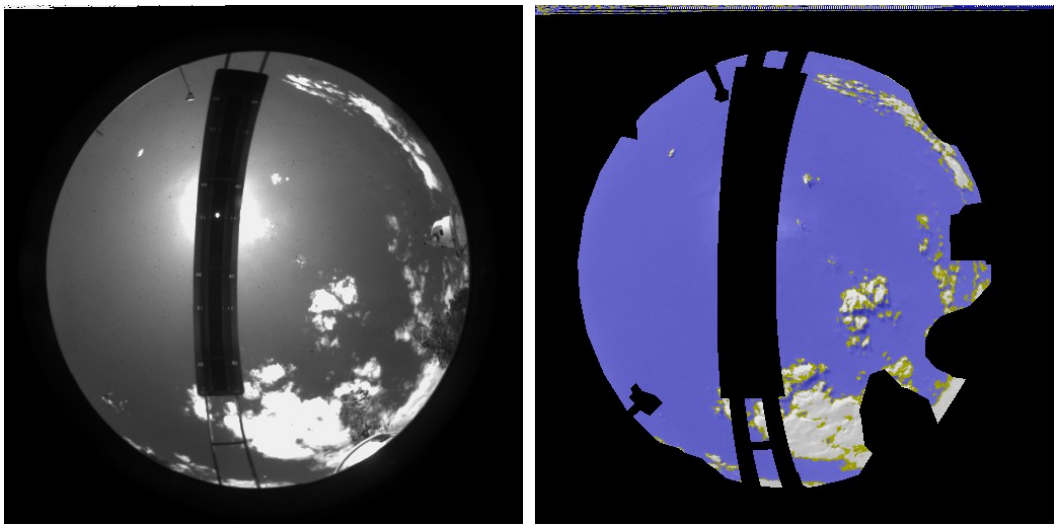

Fig. 24. Mixed cloud results, 22 May 08 2100.

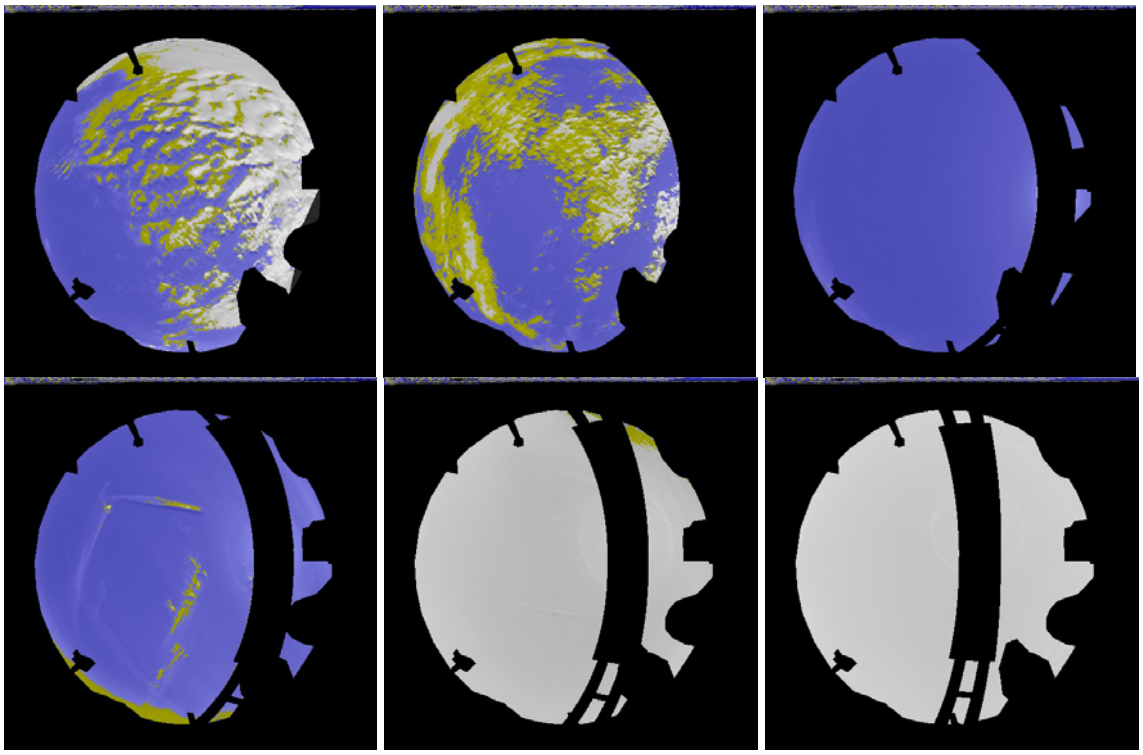

Fig. 25. Hourly time series, 23 May 08 1400 – 1900.

The rest of the Site 3 Daytime data was processed under the follow-on contract, and will be discussed in the next report. The format of the archival delivery is documented in Technical Memo AV08-037t, repeated in Appendix 1. The use of the archival data, including the equations for the geometric calibration, is documented in Technical Memo AV08-038t, repeated in Appendix 2. The use of the real time data is documented in Technical Memo AV09-024t.

8.4. Summary of the Day Algorithm and Accuracy Test Results

The adaptive feature of the daytime cloud algorithm was developed under this contract, and is working very well. Its function is to adjust the algorithm for changes in the aerosol or haze, so that high aerosol (enhanced number of small droplets) will not be identified as thin cloud. Typically, real thin cloud consists of larger droplets, and is often much more variable spatially than haze. We prefer to identify thin cloud as cases with enhanced droplet size, because they will impact the short wave IR as will as the visible.

Under this contract, we were able to get the real time algorithm in the field for Sites 3 and 5, and process part of the archival data. Site 2 already had a working version of the daytime algorithm running in real time (although it did not include the adaptive algorithm). The update to Site 2 was not required under this contract, and it was completed under the follow-on contract. In a test case, we found that the cloud algorithm looked good either with or without the adaptive feature 74% of the time. Results were improved with the adaptive algorithm 24% of the time, and not as good 2% of the time.

At this point we believe the biggest strength of the day cloud algorithm is that it's nearly always correct for clear and opaque cases. It also nearly always identifies most of the cirrus clouds. It does have a non-zero threshold for thin cloud, in that it does not identify the thinnest of the cirrus. Probably the biggest weakness of the algorithm is that we have not yet quantified the optical depth associated with this threshold.

In tests done under the follow-on contract, we wrote a program for doing "blind" tests, to assess the accuracy of the algorithm. In these tests, we identified thin cirrus as "uncertain", because we were not sure whether they should be above or below the threshold. We also identified certain other cases as uncertain, including small holes in opaque clouds, where there can be cloud debris, or small cloud fragments, that are not always obvious in the raw imagery. Of those cases that were not called uncertain, we achieved a 99.3% accuracy rate. The blind test will be documented in the next report.

As a result of this analysis, we felt that the day adaptive algorithm was very accurate and under the follow-on contract, we worked primarily on extracting and processing additional archival data.

9. Night Algorithm Developments and Analysis

During the previous contract, as documented in Technical Note 273, we developed a new high resolution night algorithm. Our previous algorithm provided a result in each of 357 cells over the sky, whereas the new algorithm provides an answer at each pixel. (Although the result is at full pixel resolution, a 5 x 5 smoothing of the image is used during part of the processing, so we refer to it as a "high resolution" algorithm.) It is based on measurement of the earth-to-space beam transmittance determined from the stars in the image, and then the absolute radiance of the image is used to extend it to high resolution.

At the end of the previous contract, the high resolution night algorithm was working very well for starlight conditions, however we had not yet developed good logic for moonlight conditions. Under the grant which is the subject of this report, we completed the development of the moonlight algorithm, and fielded the new algorithm at Sites 3 and 5, as required by the contract. During the interval of this contract, we also processed and delivered the archival data for these sites, however the archival processing was mostly funded under the follow-on contract.

9.1. The High Resolution Algorithm Concept

We have already discussed the development of the high resolution starlight algorithm in some detail in Technical Notes 272 and 273. Therefore we only provide a brief overview in this section of how the starlight algorithm works.

9.1.1 Transmittance

The concept behind the high resolution algorithm was originally tested and documented in Memo AV01-069t. This algorithm requires determination of the absolute value of earth to space beam transmittance for the stars. As discussed in Technical Note 271, we developed the ability to determine the absolute value of earth to space beam transmittance for stars, before working further on the high resolution algorithm. On clear nights, we were able to obtain a correlation of 0.937 between computed inherent star irradiance and measured apparent star irradiance on cloud-free nights, where "inherent" means above the atmosphere, and "apparent" means as measured on the ground. This number was for a data comparison of 43,000 stars, down to magnitude 6, as documented in Memo AV07-037t.

In our next contract, documented in Technical Note 272, we improved the determination of earth to space beam transmittance, and did some studies of the accuracy of the results. We found that the results made sense, in that the clear sky results were reasonable for aerosol transmittance, and the decreases in transmittance were associated with visually detected increases in cloud thickness in the imagery. We were able to determine the transmittance over a wide range down to about a transmittance of .01, and found that the accuracy was about 5% at the high end, although there will be rare "glitch" values in the clouds that are not correct. We felt that these results were sufficiently accurate for identifying the presence of opaque and thin clouds.

9.1.2. Starlight Methods

As discussed in Technical Note 272, we also further tested the concepts for a high resolution algorithm. The concept is basically:

a) Calibrate the night images for absolute radiance.
b) Determine the typical shape of the clear sky radiance distribution under starlight. Call this the "clear shell".

c) Determine the typical shape of the opaque cloud distribution under starlight. Call this the "cloud shell".
d) Using the earth-to-space beam transmittance, identify the likely cloud condition in the direction of the stars as either no cloud, thin cloud, or opaque cloud.
e) Use the radiance at those points identified as no cloud to adjust the clear shell for current conditions.
f) Use the radiance at those points identified as opaque cloud to adjust the opaque shell for current conditions.
g) At pixels not associated with stars, compare the measured radiance with the adjusted clear shell and cloud shell to assess whether that pixel has no cloud, thin cloud, or opaque cloud.

This concept for the high resolution algorithm was developed for the starlight case, and is documented in Technical Note 273. This initial work was done using the data from Site 2. Both the clear and cloud shells were determined from the in-situ data. It was necessary to sort the clear data as a function of hour angle. This site is near a city, and fairly brightly lit. We first found that there was a good separation between the clear and opaque shells, which means that the algorithm concept should work well. Fig. 26 was extracted from TN 273, and illustrates the extracted clear and cloud shells for both the SOR site and Site 2.

For a given site, the background imagery used to create the shells for the night algorithm is obtained by compiling many images that visually appear to be cloud-free, and determining the median value of calibrated radiance at each pixel. The data were sorted into several hour angle ranges and averaged, so there are typically 13 background images for a site to cover the range of possible hour angles.

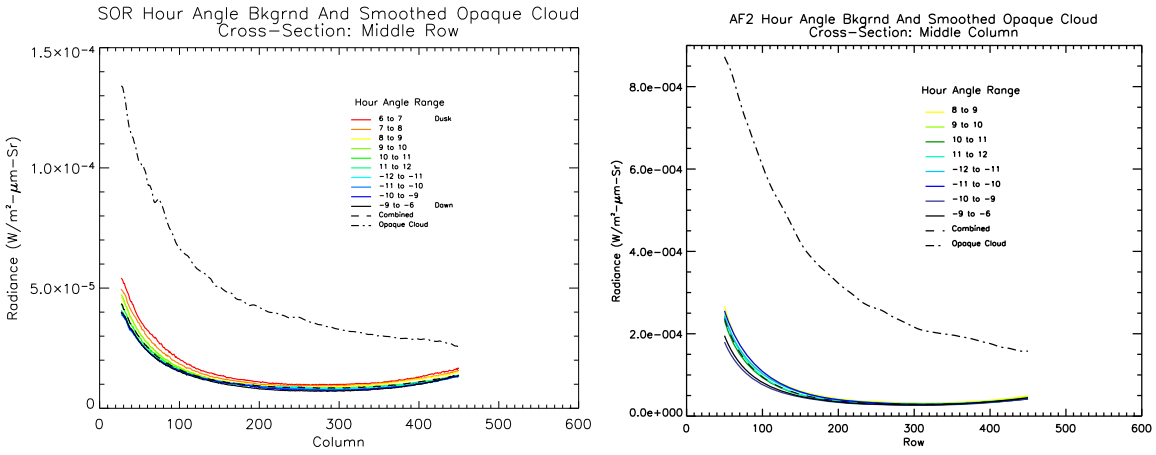

Fig. 26. Typical no-moon clear sky radiance levels for clear sky as a function of hour angle (solid color curves), and typical no-moon cloud radiance levels (dash line). Plot on left is for SOR site, and plot on right is for Site 2. Left plot y-axis scale is 0 to 1.5 10^{-4}. Right plot y axis scale is 0 to 9 10^{-4}.

A similar technique is used to determine the opaque shell, although we did not find it necessary to sort the opaque shell as a function of hour angle. A discussion of the background image determination may be found in Tech. Memo AV05-012t.

A method was also developed to adjust the clear and cloud shells, as outlined in steps e and f above. For each star within 60° of image center identified as not being obscured by cloud, a correction factor was determined from the ratio of the background radiance to the shell radiance at that position. The average correction factor for that image is applied to the shell for that image. If no usable stars are found using the above criteria, a correction from an earlier image is applied. In addition, the clear shell is moved 15% higher. In this way, the radiance at a given pixel must exceed the adaptively adjusted clear shell by 15% in order to be identified as thin cloud. The 15% is an input parameter that can be modified. To more accurately identify thin cloud (at the possible expense of misidentifying some cloud-free regions as thin cloud), the factor may be adjusted down.

The approach is similar for the opaque shell. Also, the cloud shell is further adjusted using a multiplier of .90, so that the cloud shell should be below the actual measured cloud radiances.

Some of the details are provided in Technical Note 273, and more details are provided in Memo AV06-029t. Examples are given in Technical Note 273. The overall results were about 99% accurate at the zenith, and 94% accurate over the whole image. I note that there is an error in Figure 35 of Technical Note 273. Since this is an important figure, showing the accuracy of the high resolution algorithm for no moon, I will show the corrected figure in Fig. 27.

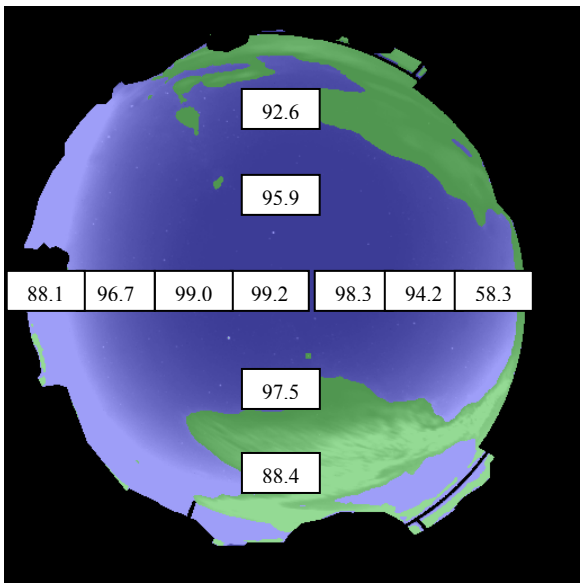

Fig. 27. Fraction of correct answers, in percent, for each Line of Sight for Site 2 Test Data using Program SORCloudAssess, for no moon cases. This is the corrected version of Fig. 35 from Technical Note 273.

As this project developed, our sponsors decided they were less interested in accuracy near the horizons. For those zenith angles of 60 degrees and higher, the results shown above average 95.8%. Sample results are shown in Technical Note 273. We were very pleased with these results.

9.2. Development of the Moonlight High Resolution Night Algorithm

As discussed in Memo AV09-056t, it is considerably more difficult to develop the clear and cloud shells for moonlight, for a number of reasons. One is that there are fewer moonlight cases with full moon, so it is difficult to find clear and cloudy cases. Another is that it is necessary to contend with changes in the phase of the moon. Under clear sky with a full moon the radiance distribution is primarily due to a sum of the light scattered from the moonlight, and the light from man-made or anthropogenic sources.

We used the approach of modeling the shape of the scattered portion of the moonlight imagery. To do this, we first modeled the moonlight sky using the equation:

$$\mathrm{N}(\theta,\phi,\theta_M,\phi_M) = \mathrm{N}_B(\theta,\phi) + RN(\alpha) * N_M(\theta,\phi,\theta_M,\phi_M,\alpha_{\max}) \qquad (1)$$

where

$N(\theta,\phi,\theta_M,\phi_M)$ is the radiance distribution at night as a function of look angle θ,ϕ and the Source (Moon) position θ_M,ϕ_M

$N_B(\theta,\phi)$ is the radiance distribution of the moonless background sky

$RN(\alpha)$ is the relative brightness of the moon as a function of phase angle α

$N_M(\theta,\phi,\theta_M,\phi_M,\alpha_{\max})$ is the radiance distribution of the full-moon-lit sky as a function of look angle θ,ϕ and the Source (Moon) position θ_M,ϕ_M and phase angle.

Using this method, the radiance distribution of the no-moon sky $N_B(\theta,\phi)$ would be the same as previously extracted. The relative brightness of the moon $RN(\alpha)$ is computed as a function of phase angle in our program OccInfo, and takes into account both phase and earth-to-moon distance to determine relative brightness.

Programs were written to enable us to extract the $N_M(\theta,\phi,\theta_S,\phi_S,\alpha)$ radiance distribution of the moonlight sky from night calibrated radiance images. The programs are similar to those used to extract the red/blue ratio distribution for the day algorithm.

When extracting the distribution for a given moonlight case, the image is first corrected for the background radiance that occurs under starlight. Also, the radiance distribution is corrected for the relative moon brightness. Once the clear sky library has been determined for a nominal relative moon brightness of 1, then the radiance for a specific case can be determined using Eqn. 1.

As with the no-moon portion of the algorithm, stars are used to identify portions of the sky with no cloud and opaque cloud, and the radiance in the direction of these stars is used to compute an average correction factor. When corrected, the clear shell should match the current clear sky portions of an image reasonably well, before the additional 15% correction is applies.

In terms of the cloud shell, we found that the cloud shell used during no moon could also be used for moonlight cases. As with the no-moon algorithm, the algorithm adjusts the cloud shell using the radiance at the stars that are identified as being blocked by opaque clouds. In this way, the magnitude of the cloud shell is adjusted from image to image, but the shape of the cloud shell for moonlight is the same as the shape of the cloud shell for starlight. Also, the cloud shell is further adjusted using a multiplier of 0.90.

To determine the algorithm result for a given pixel, if the radiance is higher than the adjusted cloud shell, it is called opaque cloud. If it is lower than the adjusted clear shell, it is called no cloud. If it is between, it is called thin cloud. If a region occurs in which the adjusted clear shell is higher than the adjusted cloud shell, this region is identified as indeterminate. The software also includes a feature that allows the adjusted shell correction determined from one processed image to be applied to other images later in the same day when no usable stars are found in those images.

9.3. Sample Results for Site 5

A typical clear case with moon and the algorithm result is shown in Fig. 28. In this example, the moon is at .61 relative brightness.

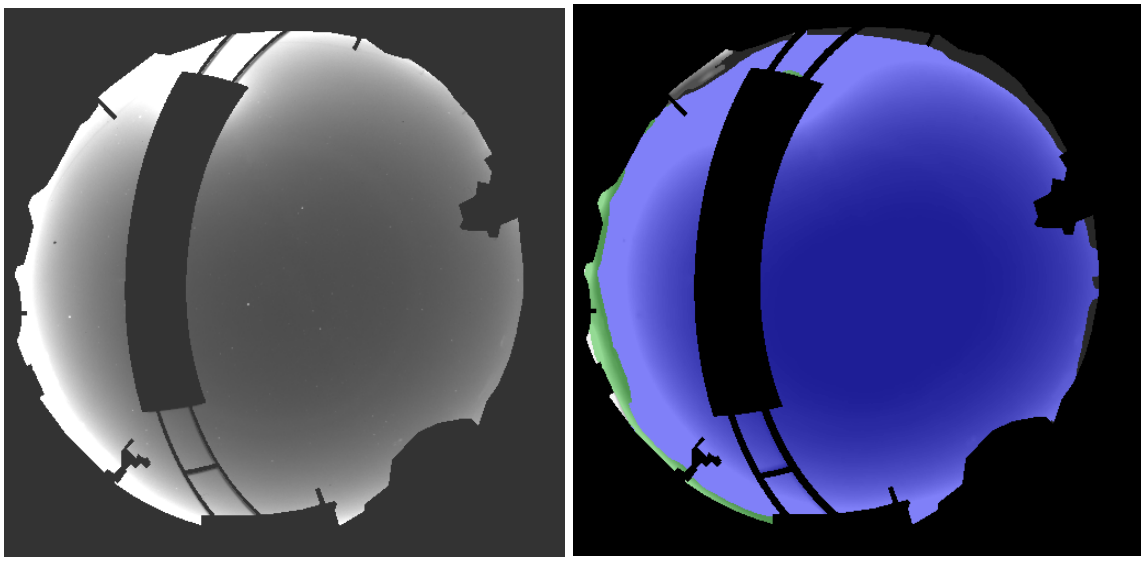

Fig. 28. Raw Image and Cloud Algorithm Results for Site 5, 2 June 2007, 0956 GMT

The algorithm results for the image shown in Fig. 28 is excellent. In this image, blue indicates that the algorithm estimates there to be no cloud, green indicates thin cloud, and grey indicates indeterminate, as defined in Section 3. Opaque cloud, when it occurs, is indicated with white in the algorithm result.

The modeled values for the clear sky radiance and moon radiance for this case are shown in Fig. 29, for a vertical column at x pixel 255 (in the center of the sensor image). On the left hand side, the red is the starlight clear sky background for the hour angle of the image, and the green is the moonlight model clear sky without the starlight radiance, for the moon position and relative brightness of this image. The blue is the combined model

radiance to yield the modeled clear sky radiance for this image. When the starlight and moonlight radiances are combined to show the modeled total radiance in blue, we see that it compares well with the measured radiance, shown in black. Fig. 29 includes the adaptive correction, which is a factor of 0.903 for this sample. We want the model to exceed the measured by 15%, so that we in effect have a 15% threshold. As a result, an additional threshold factor was 1.15 was applied, meaning that the shell image was adjusted upward by 1.038% for use with this particular image. The curves with this correction are shown on the right side of Fig. 29.

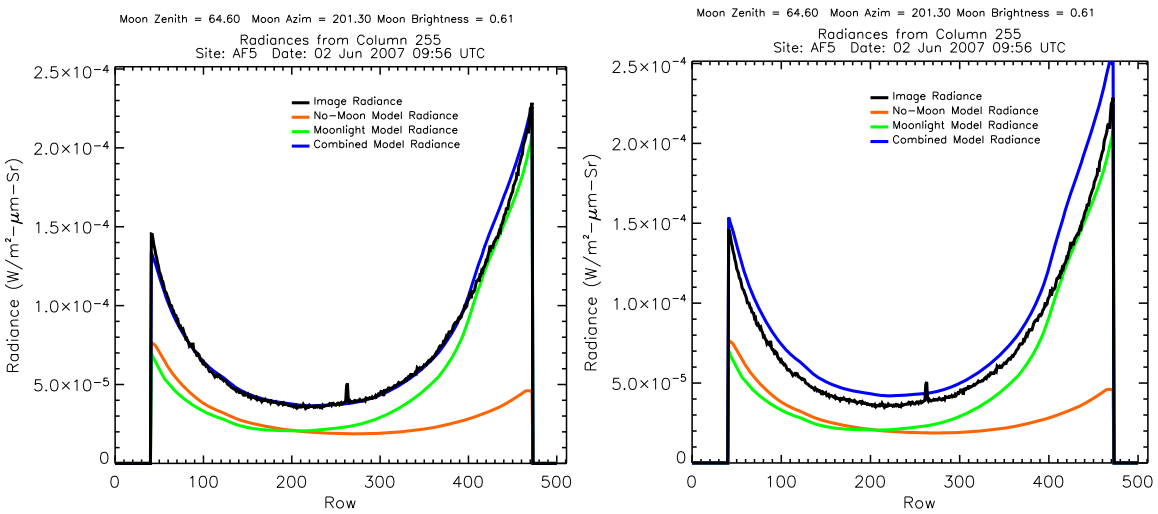

Fig. 29. Model and Measured Radiances, with Adaptive Corr of 1.09 (left) and additional 15% threshold correction (right), for Site 5, 2 June 2007, 0956 GMT These plots are for column 255, i.e. a vertical line through the image. We show the modeled no-moon radiance in orange, the modeled moonlight radiance in green, the combined model radiance with the adaptive correction of 0.903 in blue, and the measured image radiance in black.

One of the reasons for the 1.15 factor for the clear shell and a .90 factor for the cloud shell is that we use one adjustment factor for a whole image. The shape of the shell will never be precisely the same as the shape of the radiances for a given image. This simply means that the threshold for thin cloud detection is not 0 db, but is a finite but very low number. In later research that will be discussed in the report for the follow-on contract, we found that the threshold for optical fade for the thin clouds appears to be about a loss of 0.7 to 1.0 dB (transmittance .85 to .79). The threshold for optical fade for the opaque clouds appears to be a loss of about 8 dB (transmittance .16). We feel these thresholds are appropriate, in that the clouds that are missed are quite thin, and these thresholds help minimize false alarms in clear areas.

To demonstrate the concept for situations with clouds, we have chosen a series with variable conditions that happened a few hours prior to the sample shown in Fig. 29. In Fig. 30, we show a case about 4 ½ hours earlier, in which there were some extremely thin clouds, barely distinguishable in the raw imagery. From the left plot in Fig. 31, we see that the model and measured clear sky match very well in the center of the curve (i.e. near the zenith), where the sky is clear, and the thin clouds can be seen as slight enhancements on the parts of the curve away from the center. The plot with the additional 15% threshold is shown in the right plot in Fig. 31. Much of this very thin

cloud is not above threshold. The algorithm successfully identifies the slightly thicker clouds that are above this threshold. The opaque shell is not shown in Fig. 31, but the pixels are well below the opaque shell. (Examples of the opaque shell will be shown later in this section.)

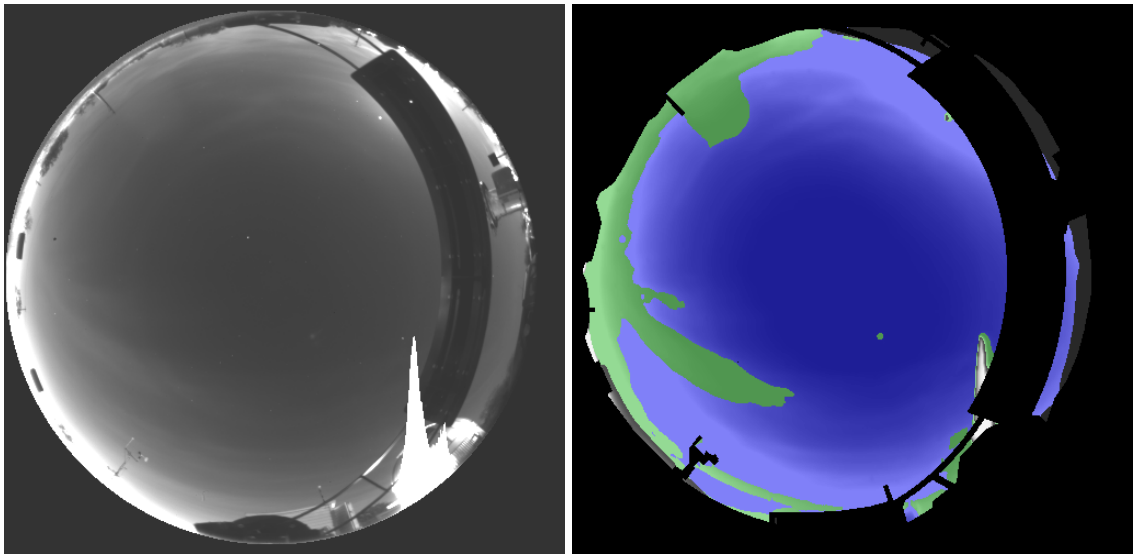

Fig. 30. Raw Image and Cloud Algorithm Results for Site 5, 2 June 2007, 0530 GMT

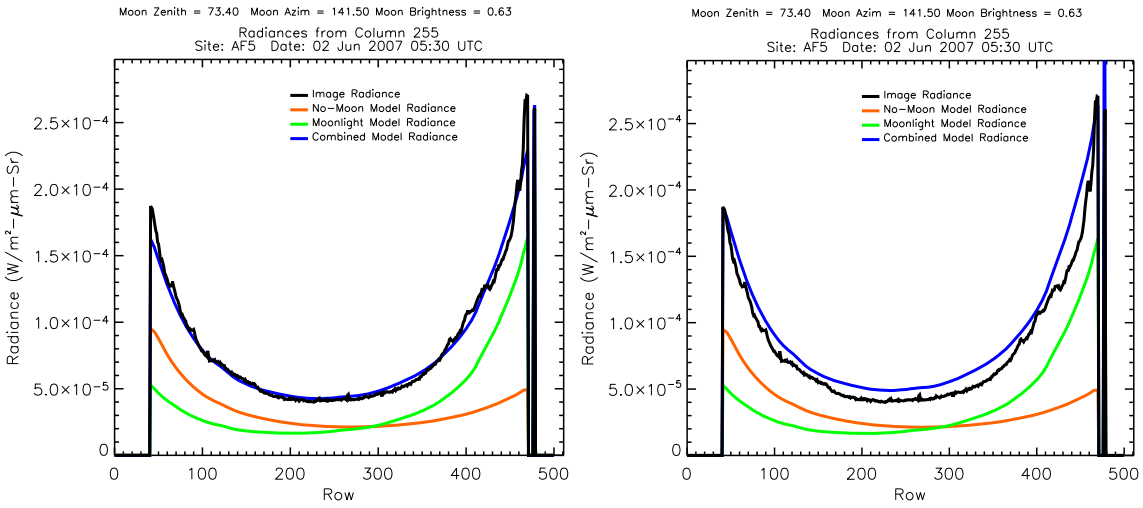

Fig. 31. Model and Measured Radiances, with Adaptive Corr of 1.09 (left) and additional 15% threshold correction (right), for Site 5, 2 June 2007, 0530 GMT

In Figs. 32 and 33, from imagery taken about an hour later, we see that the clouds are somewhat thicker, and a halo has become visible. As seen in Fig. 33, the clouds in the lower part of the image (left side of x axis) are slightly higher than the nominal clear sky, but slightly lower than the shell corrected for the 15% threshold. The upper part of the image clearly has thicker clouds, and these are identified as thin cloud.

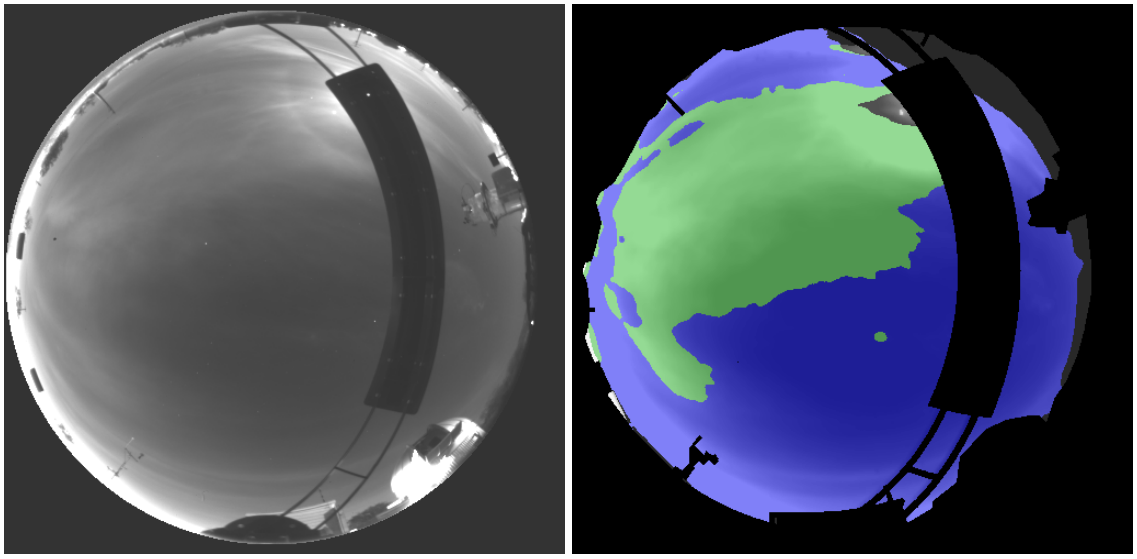

Fig. 32. Raw Image and Cloud Algorithm Results for Site 5, 2 June 2007, 0626 GMT

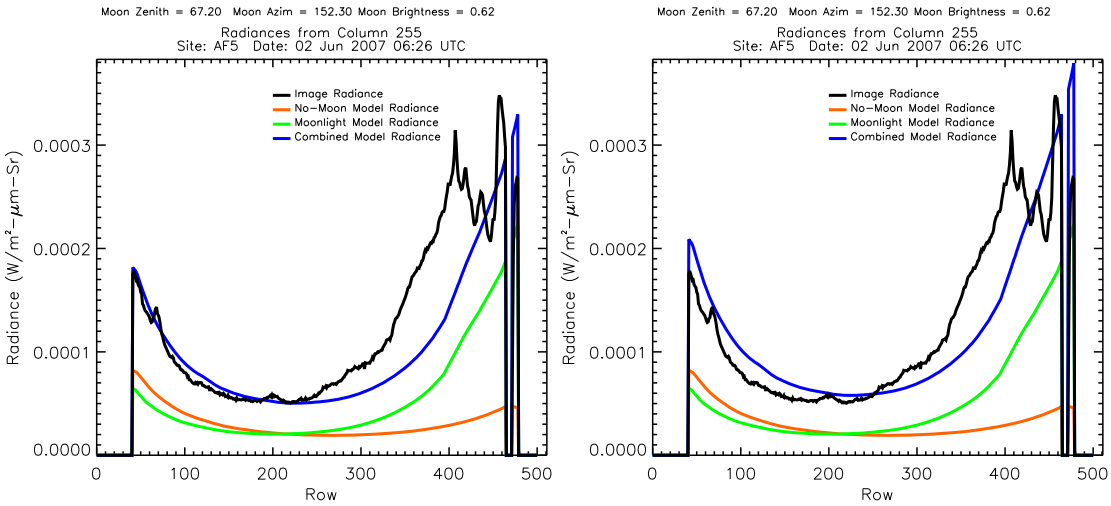

Fig. 33. Model and Measured Radiances, with Adaptive Corr 1.23 (left) and additional 15% threshold correction (right), for Site 5, 2 June 2007, 0626 GMT

Figs. 34 and 35 show the measured transmittances for the stars for these two cases at 0530 and 0626, with the key shown in Fig. 36. We see that indeed the transmittances were lower at 0626, and it is thus reasonable that the algorithm result at 0626 shows more cloud.

Figs. 37 through 40 show the results as the clouds became thicker, and then nearly disappeared except for a very thin cloud near the bottom of the occultor. In Figs. 37 and 38 we see that part of the cloud field has become fairly thick, and this is shown in a fairly high spike in Fig. 38. Although the cloud shell is not shown, this spike is lower than the cloud shell. Also note in these figures that when a reasonably thick cloud appears, as in Fig. 38, the signal is much higher than the clear shell, so the algorithm should work very consistently in identifying the thicker clouds as being cloud. The very thin cloud seen in

Fig. 39 is also seen in Fig. 40, where it appears to be about 20% higher than the adjusted clear shell.

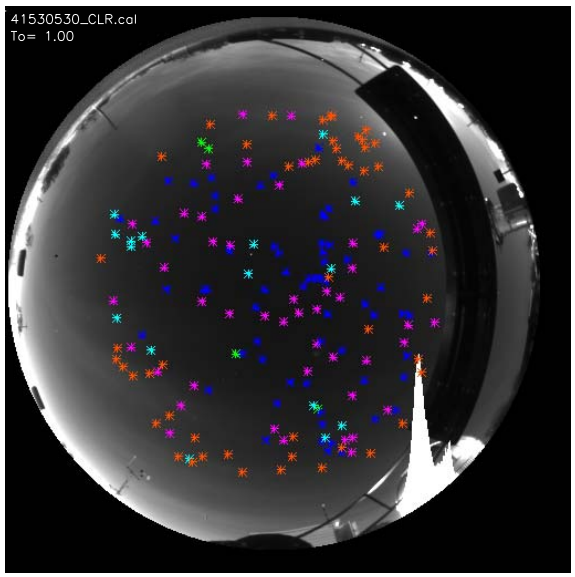

Fig. 34. Transmittance map for 2 June 2008 0530

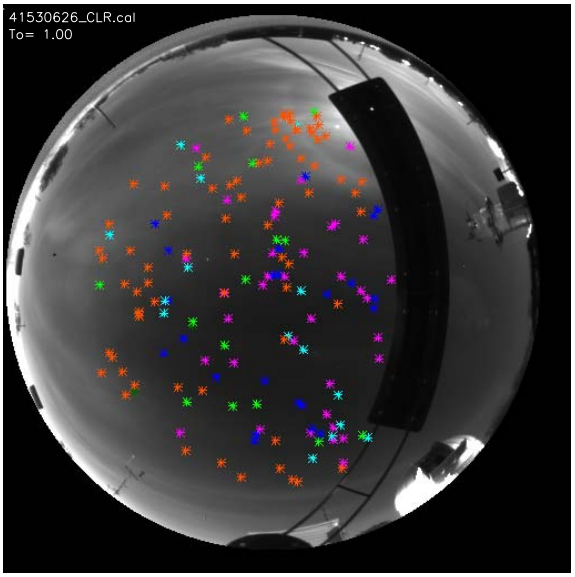

Fig. 35. Transmittance map for 2 June 2008 0626

Fig. 36. Key for Transmittance maps

Results for a moonlight case with some opaque clouds are shown in Figs. 41 and 42. The algorithm worked very well. The plot in Fig. 42 shows the cloud shell as well as the other shells. (We could have shown the cloud shells in the earlier plots, but didn't want to clutter the plots.) The left half of Fig. 42 has been adjusted using the radiances near the stars that were identified as having opaque cloud, so the curve roughly matches the observed radiance. The .90 factor has been applied to the cloud shell in the right side of Fig. 42, which allows the opaque clouds to be identified as opaque.

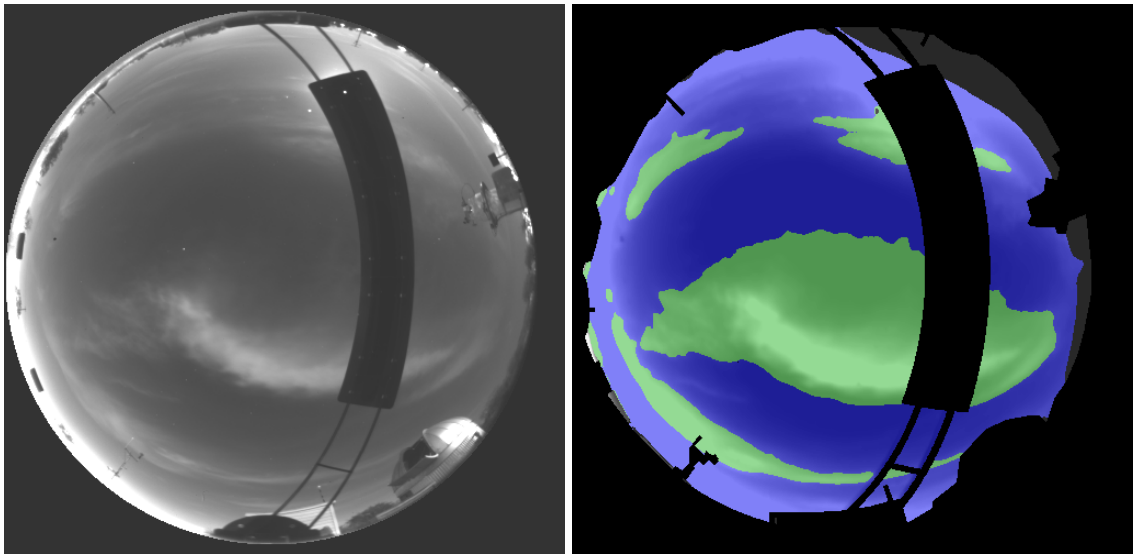

Fig. 37. Raw Image and Cloud Algorithm Results for Site 5, 2 June 2007, 0656 GMT

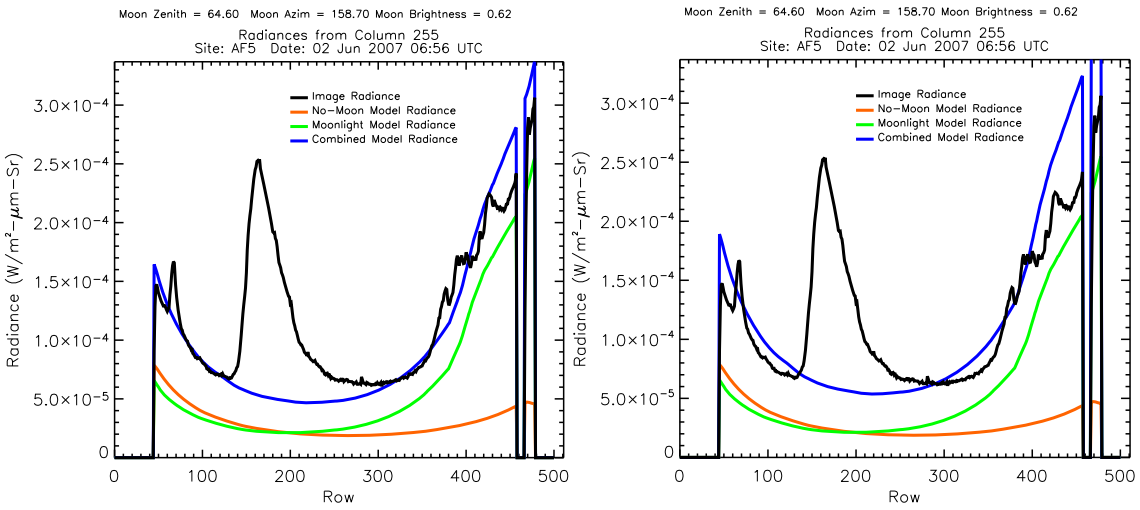

Fig. 38. Model and Measured Radiances, with Adaptive Corr 1.13 (left) and additional 15% threshold correction (right), for Site 5, 2 June 2007, 0656 GMT

Although the no-moon algorithm has not changed appreciably, we would like to show one examples for no moon also. Figs. 43 and 44 show a case with scattered clouds. We feel these results are excellent, like the moonlight cases.

As noted earlier, we are using the same cloud shell for both moonlight and starlight conditions, because the shape of the cloud shell is relatively unchanging. We also note that the adaptive correction for the cloud shell is less than one in the starlight example below, and more than one in the moonlight examples above. This makes sense, because the magnitude of the cloud shell should depend to some extent on the moonlight, and it shows the effectiveness of the adaptive feature of the algorithm.

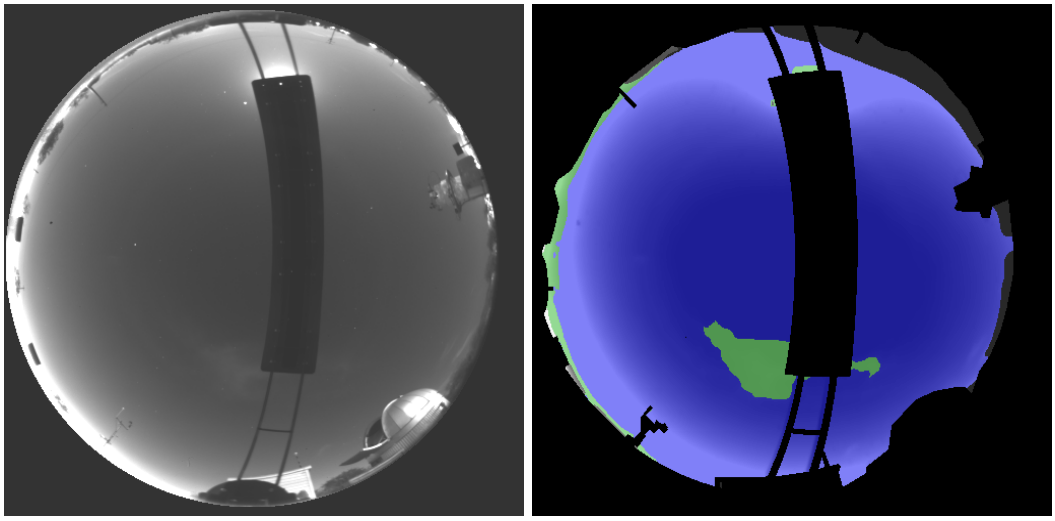

Fig. 39. Raw Image and Cloud Algorithm Results for Site 5, 2 June 2007, 0750 GMT

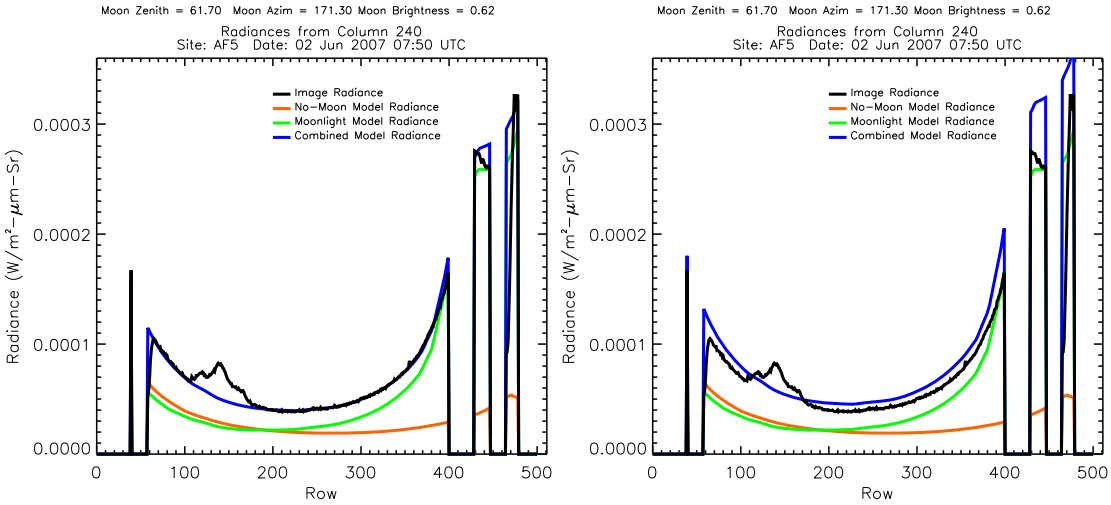

Fig. 40. Model and Measured Radiances, with Adaptive Corr 0.94 (left) and additional 15% threshold correction (right), for Site 5, 2 June 2007, 0750 GMT

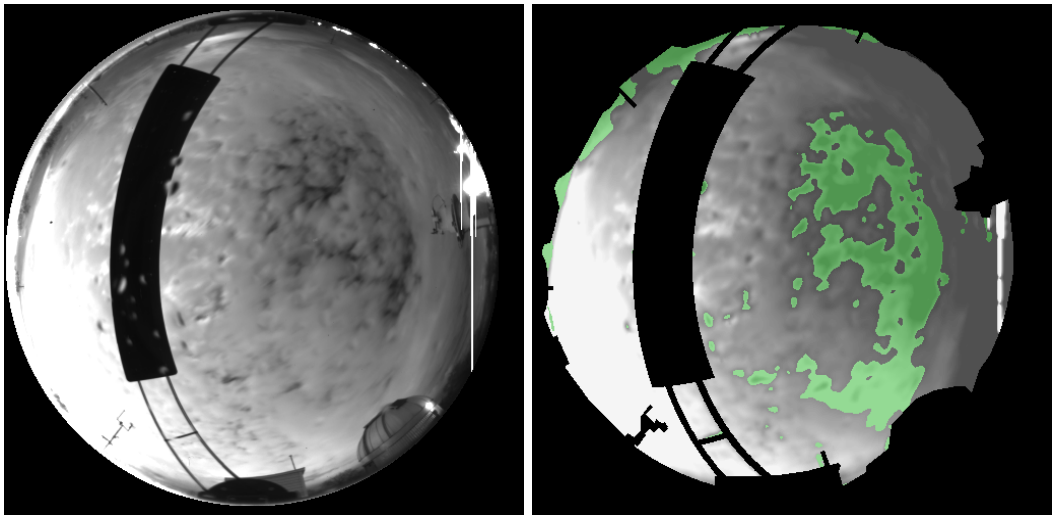

Fig. 41. Raw Image and Cloud Algorithm Results for Site 5, 1 Feb 2007, 1000 GMT

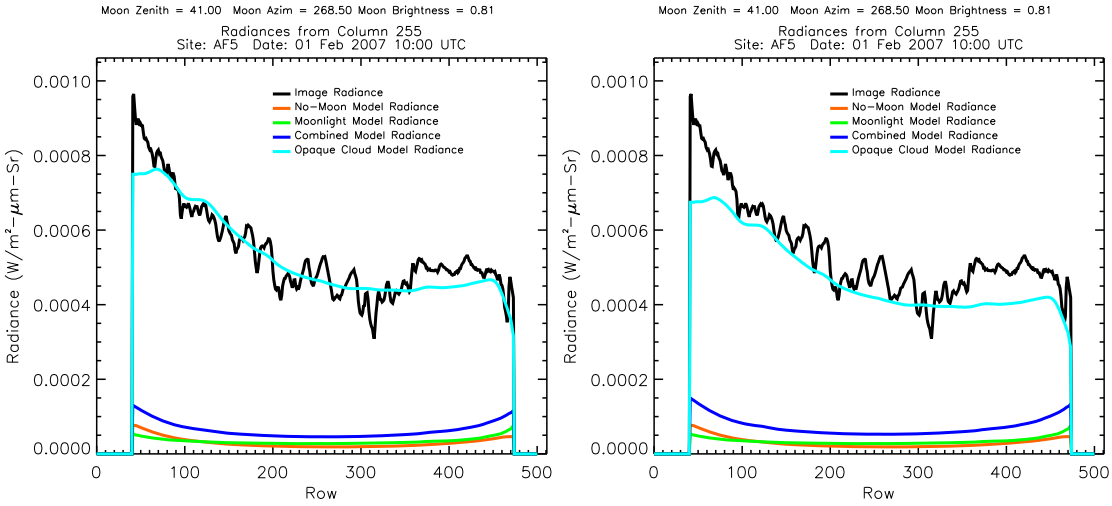

Fig. 42. Model and Measured Radiances, with Adaptive Corr 0.98 for the clear shell and 1.32 for the cloud shell (left); and additional 15% threshold correction on the clear shell and .90 correction on the cloud shell (right), for Site 5, 1 Feb 2007, 1000 GMT. Thus the net corrections are 1.13 and 1.19 for the clear and cloud shells respectively.

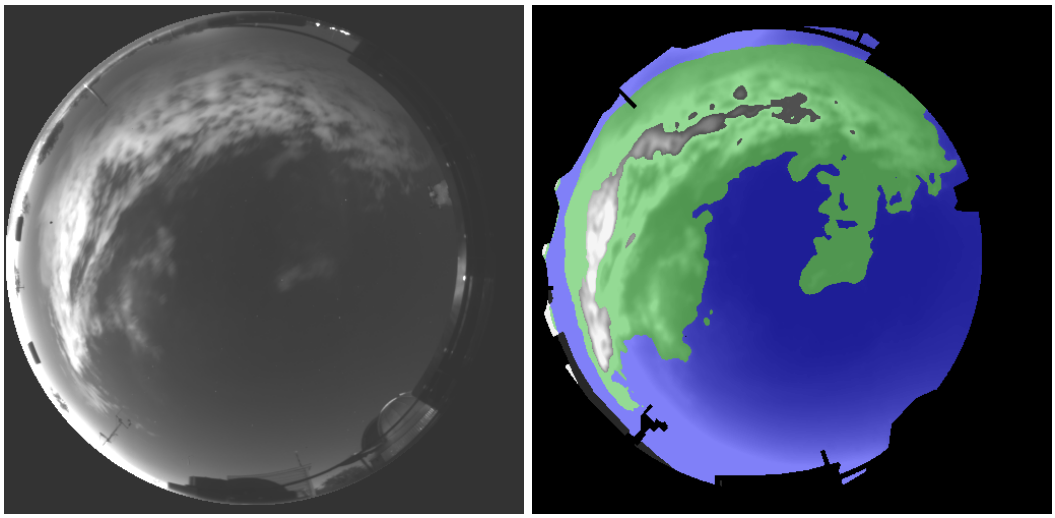

Fig. 43. Raw Image and Cloud Algorithm Results for a case with no moon, Site 5, 20 June 2007, 0716 GMT

Several more examples from other time periods are shown in the May 08 power point talk, which illustrates the results of the Oct 07 interim moonlight algorithm in comparison with the May 08 version that was fielded. This talk also includes movies that are perhaps the most persuasive tool to convince us that the results are quite good nearly all the time (or alternatively, the movies are the best tool to alert us if there are problems).

As will be discussed in the report for the follow-on contract, the threshold for optical fade for the thin clouds appears to be about a loss of 0.7 to 1.0 dB. The threshold for optical fade for the opaque clouds appears to be about a loss of about 8 dB. Our sponsors felt that both of these thresholds were very reasonable, and they were pleased with the results of the new algorithm.

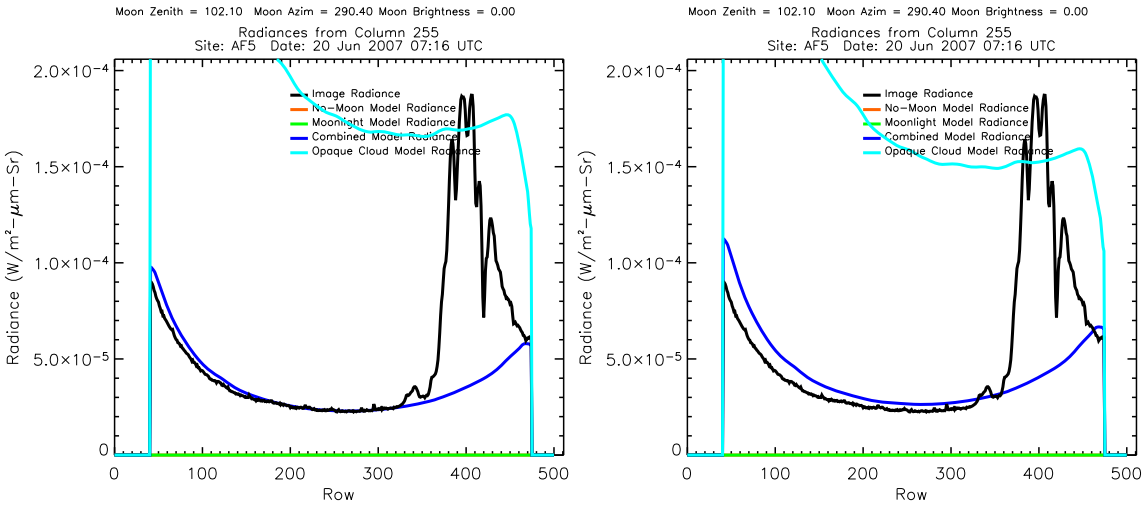

Fig. 44. Model and Measured Radiances, with Adaptive Corr 1.24 for the clear shell and 0.50 for the opaque cloud shell (left) and additional 15% threshold correction on clear shell and .90 correction on cloud shell (right), for Site 5, 20 June 2007, 0716 GMT

9.4. Site 5 Nighttime Processing and Real Time Algorithm

Site 5 had been fielded prior to the start of this contract, during Jan 31 – Feb 2 2007. One of the requirements of this contract was to get the real time algorithm running in the field. Unfortunately, right at the start of the contract, the instrument was struck by lightning in July 2007. The repair was completed January 16, 2008. The instrument ran well until May 22 2008, when the occultor failed. It was replaced on June 30, and also a ring shade was added at that time, to shade the system from lights on the horizon.

In order to field the real time algorithm, it was necessary to extract the algorithm inputs from the archival data. During the interval of the contract period, we also went ahead and processed the archival data that we had available to us at the time, although much of this work was funded by the follow-on contract. We also extracted the inputs for the 2007 data at the same time and went ahead and processed it.

Processing of the archival data from Feb 1 – July 12 2007 is documented in Memo AV09-051t. Several examples are shown in Section 9.3, and more are shown in the memo. The processing of data from Jan 17 – Jun 30 3008 is documented in Memo AV09-052t. The biggest change in the inputs was required because two quite bright lights appeared on the horizon, so the inputs had to be modified to adjust for the stray light on the dome. This adjustment worked quite well, as can be seen in Fig. 45.

Following the repair of the occultor on 30 June, the algorithm was adjusted using data from 30 Jun – 4 Aug 2008. The processing of these data, as well as the inputs used for the fielded version of the algorithm, is documented in Memo AV09-053t. A sample result is shown in Fig. 46.

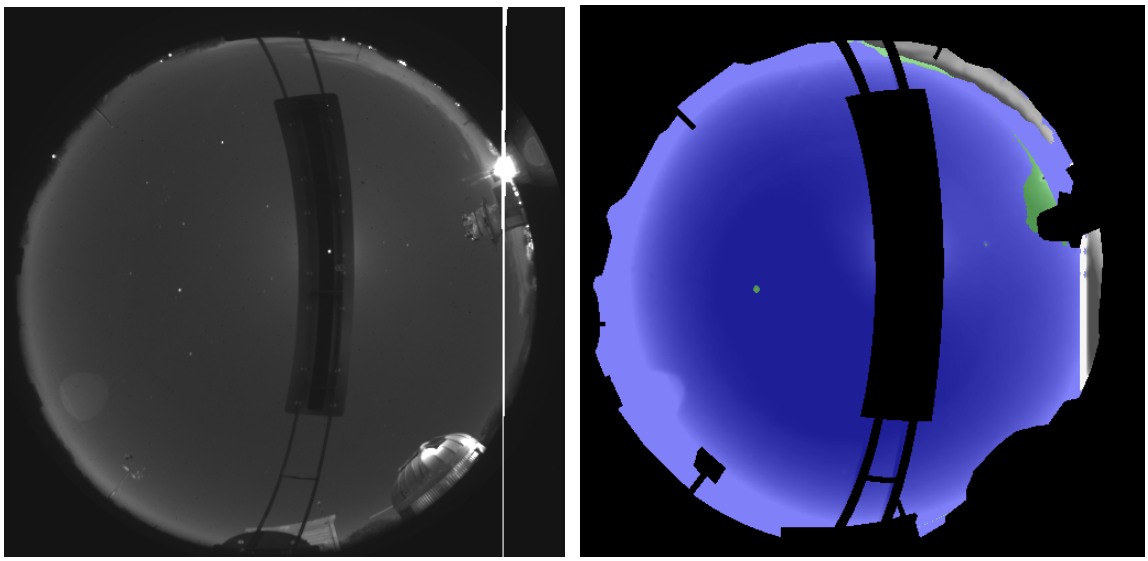

Fig. 45. Raw Image and Cloud Algorithm Results for Site 5, 23 January 2008, 0702 GMT

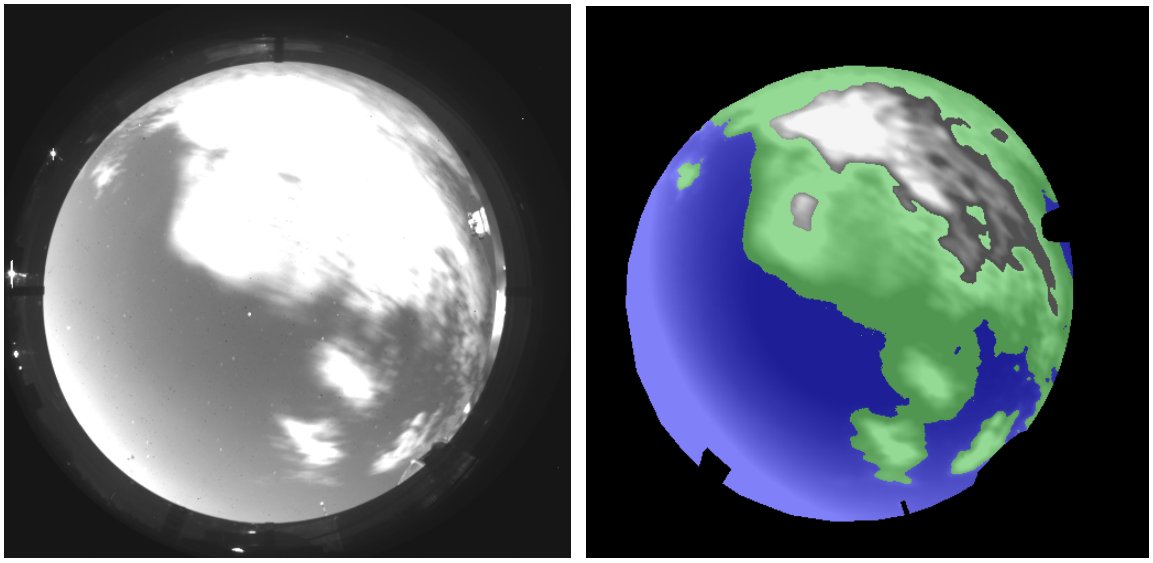

Fig. 46. Raw Image and Cloud Algorithm Results for Site 5, 1 July 2008, 0800 GMT

The data set documented in this section has been delivered to the sponsor, except for data from Jan 16 - Feb 21 2008, which was left out due to an oversight, and delivered under the next contract. The delivery is documented in Memo AV08-038t, and the format of the delivery is documented in Memo AV08-037t. The field version of the night algorithm that handles both starlight and moonlight was installed on August 26 2008, and further updated on September 23 2008. Data prior to September 23 2008 will be processed and delivered as archival data. Data starting on this date may be considered valid, until further updated. The real time algorithm delivery is documented in AV09-024t. These three memos are repeated in Appendices 1, 2, and 3 of this report.

We later discovered that the cloud amounts given in the headers are not correct for the night algorithm, although the imagery is correct. We plan to correct and redeliver this

archival data with correct headers in the future, and update the real time code. The image data that was delivered to the sponsor should be good.

9.5. Site 3 Nighttime Processing and Real Time Algorithm

Site 3 was fielded under this contract during April 9 2008. We had problems with heat at this site, until a different brand of cooler was installed on July 28 2008. There were also intermittent problems with the occultor during the period of the contract. However, we managed to sort the archival data appropriately, so that any bad data are identified as "uncertain". The sponsor was alerted not to use data in this category.

As with Site 3, we were only required to deliver the field code to run the algorithm in real time, however much of the work required to process the archival data is the same. Although we were able to complete the analysis, and get the real time algorithm in the field under this contract, the archival data were not processed until shortly after the time of the contract. For convenience, we have documented all of this archival data in this section.

When we tested the algorithm software from Site 5 on Site 3, we found that the site was somewhat darker, and the Milky Way caused false identification of thin cloud in the images. As a result, we had to add a "Milky Way" feature to the algorithm. We also made sure that this updated version would work well at Site 5.

Processing of the archival data from Apr 9 – July 31 2008 is documented in Memo AV09-048t. The inputs changed after this, primarily because the installation of the new cooler changed the alignment slightly. The processing of data from Aug 1 – Sep 1 2008 is documented in Memo AV09-049t. Processing of the Sep 2 – Oct 28 data is documented in Memo AV09-050t. These inputs were changed, because there had been a smudge on the dome during the Aug 1 – Sep 1 period, and it was cleaned up about Sep 2. This memo also documents the inputs to the field code.

Sample results for Site 3 are shown in Figs. 47 and 48.

The archival data set documented in this section were delivered under the follow-on contract. However, the field code was delivered under this contract. The night algorithm that handles both starlight and moonlight was installed on October 23 2008, and further updated on December 15 2008. Data prior to this date will be processed and delivered as archival data. Data starting on this date may be considered valid, until further updated. The real time algorithm delivery is documented in AV09-024t, which is repeated in Appendix 3 of this report.

We later discovered that the cloud amounts given in the headers are not correct for the night algorithm, although the imagery is correct. We plan to correct and redeliver this archival data with correct headers in the future, and update the real time code. The image data that was delivered to the sponsor should be good.

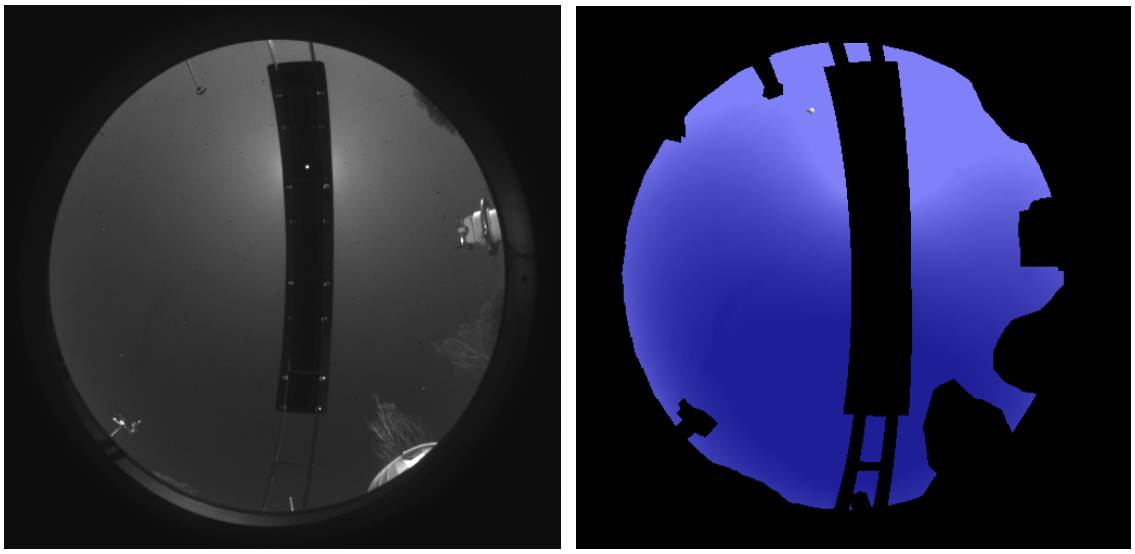

Fig. 47. Raw Image and Cloud Algorithm Results for Site 3, 16 September 2008, 0800 GMT

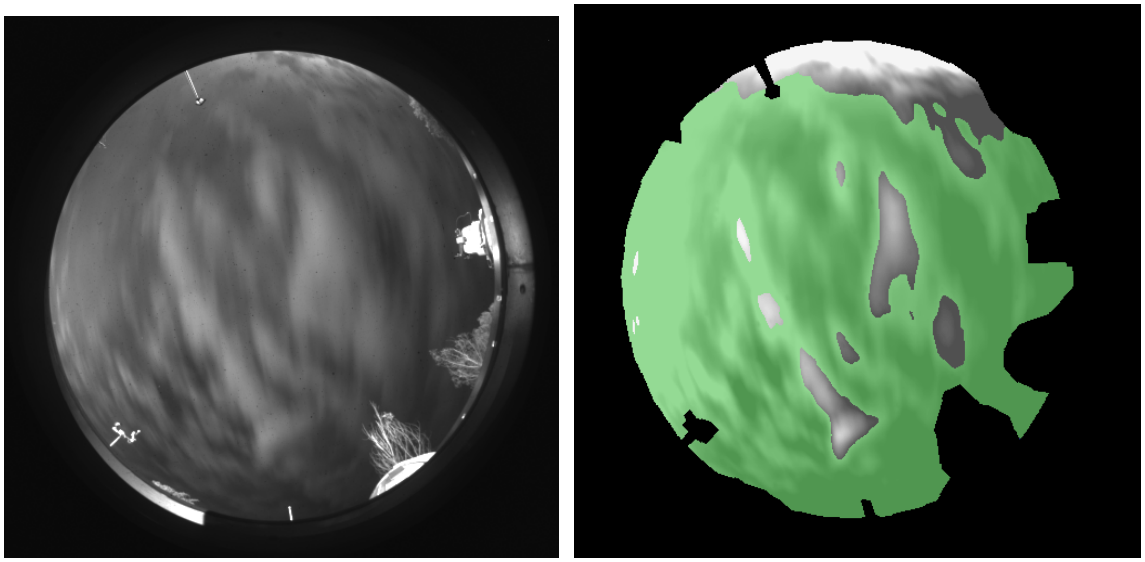

Fig. 48. Raw Image and Cloud Algorithm Results for Site 3, 2 October 2008, 0600 GMT

9.6. Summary of Night Algorithm Results

Under this contract, we made another major step forward with the night algorithm, and completed the moonlight portion of the high resolution night algorithm. This required developing a large amount of theory and software, in order to extract the shape of the night radiance distribution under moonlight, and then use this information in the algorithm. Visual evaluation of the results show them to be very good. Under the follow-on contract we did more systematic evaluation of the accuracy, and that also substantiated this initial impression.

We were able to set up the algorithm inputs for both Sites 3 and 5, and install them both in the field running in real time. In addition, we processed the Site 5 night data archive.

Much of the work of setting up the algorithm inputs and processing the night data was partially funded by the follow-on contract.

10. Summary

Under this contract, we finished refurbishment of WSI Unit #8, and fielded it at Site 3. The WSI Unit #4 at Site 5 had been struck by lighting, and we received permission to repair this instrument. As a result, Unit #4 was repaired, and reinstalled at Site 5. This meant that we had WSI system running at all 3 main sites, Sites 2, 3, and 5. Site 7, the SOR site, was also repaired.

At the start of this contract, Site 2 was running a real time algorithm in the field that was reasonably up to date, although it did not handle haze in the daytime well, nor did it handle moonlight well at night. During this contract, we completed development of the adaptive feature of the day algorithm, and it works very well to handle variable haze. We completed the moonlight version of the night high resolution algorithm. It is also working very well. We consider both of these algorithms to be mature at this point. We recognize that there are minor changes we might consider, but the major changes that we have wanted to do for some time are complete.

We put the new algorithms running real time in the field at Sites 3 and 5, for both day and night. We also processed the archival data that we had available to us for Site 3 2008 day, Site 5 2008 day, and Site 5 2007 and 2008 night and delivered the processed archival data to the SOR.

The work was documented in detail in memos, and in somewhat less detail in this report. Much of this is very detailed work, and requires detailed documentation. We apologize for the volume of documentation, but this is information we needed for the future.

We were very pleased to have all 3 sites with operational WSI systems with algorithms running in real time, and to have begun on the task of processing archival data.

11. Acknowledgements

We would like to express our appreciation to Dr. Don Walters of NPS for working so hard with us getting this grant in place, so that we could continue the work with SOR that both he and we were participating in. We would also like to thank the personnel of Starfire Optical Range and their contractors from Boeing. We would like to thank Dr. Earl Spillar, Ann Slavin, Capt Douglas MacPherson, Lt. Kevin Pastorello, Marjorie Shoemake and Darielle Dexheimer, all of whom have been vey helpful during the interval of this contract. The SOR team is always a pleasure to work with. We feel this WSI work is valuable, and very much appreciate having had the chance to advance the state of the art, as well as meet our sponsor's specific needs.

12. References

12.1. In-house Technical Memoranda, in order by memo number; available to sponsor on request.

This section includes memos written with funding from this contract, as well as memos written under other contracts that are referenced in this memos. Other memos written prior to the period of this contract but during the period of the previous contract are listed in Section 12.1 of Technical Note 273 and in previous Technical Notes.

Shields, J., "Research Approach for High Resolution Night Cloud Algorithms", Atmospheric Optics Group Technical Memorandum AV01-069t, 3 July 2001

Shields, J., "Data Development of the NIR Day Cloud Algorithm for the German Day WSI", Atmospheric Optics Group Technical Memorandum AV04-012t, 9 April 2004

Burden, A., "Cloud-free Background Imagery for Version 3 Night Cloud Algorithm", Atmospheric Optics Group Technical Memorandum AV05-012t, 10 March 2005

Shields, J., "Processing of the VA Apr 05 Data Set", Atmospheric Optics Group Technical Memorandum AV06-018t, 18 September 2006

Shields, J., "Processing of the Site 2 May – June 06 Daytime Data Set", Atmospheric Optics Group Technical Memorandum AV06-020t, 19 September 2006

Burden, A., "WSI Full Resolution Nighttime Cloud Algorithm Progress", Atmospheric Optics Group Technical Memorandum AV06-029t, 10 October 2006

Shields, J., "WSI Run Time Hours", Atmospheric Optics Group Technical Memorandum AV06-034t, 31 October 2006

Karr, M., "Unit 7 Maxtor Drive Replacement", Atmospheric Optics Group Technical Memorandum AV07-017t, 17 April 2007

Burden, A., "Earth-to-Space Beam Transmittance from Nighttime WSI Imagery: Additional Results", Atmospheric Optics Group Technical Memorandum AV07-037t, 24 July 2007

Karr, M., "Unit 7 Site 2 Trip report, 27 – 28 Feb 2007", Atmospheric Optics Group Technical Memorandum AV07-038t, 16 July 2007

Karr, M., "Unit 4 Site 5 Trip report, 27 – 28 June 2007", Atmospheric Optics Group Technical Memorandum AV07-039t, 16 July 2007

Burden, A., "Unit 7v3 Effective Lamp Radiances for Field Calibration", Atmospheric Optics Group Technical Memorandum AV07-040t, 2 July 2007

Burden, A., “Unit 7v3 Field Calibration Results for Site 2”, Atmospheric Optics Group Technical Memorandum AV07-041t, 2 July 2007

Shields, J., “Data Processing of SGP Data for Aerosol Analysis”, Atmospheric Optics Group Technical Memorandum AV07-042t, 24 July 2007

Burden, A., “Unit 4v5b Star-Based Geometric Calibration for Data Collected During Two Time Frames: 1 Feb 2007 (Deployment Date) to 27 June 2007 and 28 June 2007 to 23 July 2007”, Atmospheric Optics Group Technical Memorandum AV07-043t, 23 August 2007

Burden, A., “Unit 4v5b Effective Lamp Radiances for Field Calibration”, Atmospheric Optics Group Technical Memorandum AV07-044t, 10 August 2007

Burden, A., “Unit 4v5b Field Calibration Results for Site 2”, Atmospheric Optics Group Technical Memorandum AV07-045t, 13 August 2007

Shields, J., “SOR Trip Report, 26 September 2007”, Atmospheric Optics Group Technical Memorandum AV07-047t, 25 October 2007

Shields, J., “Unit 12 Trolley Calibration and Alignment Procedure Update”, Atmospheric Optics Group Technical Memorandum AV07-048t, 25 October 2007

Mikuls, V., “Installation of Thermostatic Control in Dome Heater”, Atmospheric Optics Group Technical Memorandum AV07-049t, 31 October 2007

Karr, M., “October 18 – 19 2007 Site 5 Trip report”, Atmospheric Optics Group Technical Memorandum AV07-050t, 9 November 2007

Karr, M., “QCStat program Version 1.0”, Atmospheric Optics Group Technical Memorandum AV07-051t, 14 November 2007

Karr, M., “Nov. 1-2 2007 Photometrics trip report”, Atmospheric Optics Group Technical Memorandum AV07-052t, 20 November 2007

Mikuls, V., “Unit 13 Repair”, Atmospheric Optics Group Technical Memorandum AV07-053t, 21 November 2007

Karr, M., “Red and Yellow Flags in Day/Night WSI Acquisition Programs”, Atmospheric Optics Group Technical Memorandum AV07-054t, 7 November 2007

Karr, M., “Field Unit Summary of Day/Night WSIs”, Atmospheric Optics Group Technical Memorandum AV07-055t, 27 November 2007

Shields, J., “Procedure for Drying Camera Housing”, Atmospheric Optics Group Technical Memorandum AV07-056t, 6 December 2007

Shields, J., “SOR Trip Report, 29 November 2007”, Atmospheric Optics Group Technical Memorandum AV07-057t, 6 December 2007

Shields, J., “Unit 4 Camera Repair, Focus, and Field Cal for Site 5”, Atmospheric Optics Group Technical Memorandum AV08-001t, 3 January 2008

Karr, M., “15 – 17 Jan. 08 Site 5, Unit 4 Trip Report”, Atmospheric Optics Group Technical Memorandum AV08-002t, 13 March 2008

Karr, M., “WSI Quick Checklist, Emergency Shutdown/Startup Procedures and Reboot Instructions – Unit 8, Site 3”, Atmospheric Optics Group Technical Memorandum AV08-004t, 19 March 2008

Karr, M., “WSI Field Check List for Unit 8”, Atmospheric Optics Group Technical Memorandum AV08-005t, 26 March 2008

Karr, M., “Control Computer operations overview for WSI Unit 8, Site3”, Atmospheric Optics Group Technical Memorandum AV08-006t, 18 March 2008

Karr, M., “Processing Computer operations overview for WSI Unit 8, Site 3”, Atmospheric Optics Group Technical Memorandum AV08-007t, 18 March 2008

Shields, J. and M. Karr, “Set-Up Instructions for WSI Unit 8, Site 3”, Atmospheric Optics Group Technical Memorandum AV08-008t, 31 March 2008

Shields, J., “Unit 8 System Focus and Calibration, Site 3”, Atmospheric Optics Group Technical Memorandum AV08-009t, 4 April 2008

Shields, J. and M. Karr, “Unit 8 System Overview and Parts List, Site 3”, Atmospheric Optics Group Technical Memorandum AV08-010t, 31 March 2008

Shields, J., “Camera Drawing and O-rings”, Atmospheric Optics Group Technical Memorandum AV08-011t, 4 April 2008

Shields, J., “Field Calibration Update”, Atmospheric Optics Group Technical Memorandum AV08-012t, 16 April 2008

Karr, M., “8 – 10 April 2008 Unit 8, Site 3 Installation Report”, Atmospheric Optics Group Technical Memorandum AV08-013t, 2 May 2008

Karr, M., “13-16 April 2008 Unit 7, Site 2 Repair Trip”, Atmospheric Optics Group Technical Memorandum AV08-014t, 5 May 2008

Shields, J., “Return of D/N WSI Unit 10 from SGP Site on Loan to MPL”, Atmospheric Optics Group Technical Memorandum AV08-017t, 13 June 2008

Shields, J., “Unit 3 and 9 CEU’s (Camera Electronics Unit)”, Atmospheric Optics Group Technical Memorandum AV08-018t, 12 June 2008

Shields, J., “Unit 9 Camera Housing Status”, Atmospheric Optics Group Technical Memorandum AV08-019t, 13 June 2008

Mikuls, V., “3 -5 June 08 Site 3, Unit 8 Trip Report”, Atmospheric Optics Group Technical Memorandum AV08-020t, 13 June 2008

Shields, J. “WSI and MSI Coolers”, Atmospheric Optics Group Technical Memorandum AV08-021t, 17 June 2008

Shields, J., “Photometrics Camera Components Status”, Atmospheric Optics Group Technical Memorandum AV08-022t, 17 June 2008

Shields, J., “WSI Main Components Status”, Atmospheric Optics Group Technical Memorandum AV08-023t, 17 June 2008

Karr, M., “3-5 June 08 Site 2 Trip report”, Atmospheric Optics Group Technical Memorandum AV08-024t, 11 July 2008

Karr, M., “16-18 June 08 Unit 12, SOR Trip Report”, Atmospheric Optics Group Technical Memorandum AV08-025t, 14 July 2008

Mikuls, V., “30 June to 2 July 2008 Site 5, Unit 4 Trip Report”, Atmospheric Optics Group Technical Memorandum AV08-026t, 8 July 2008

Mikuls, V., “Site 5, Unit 4 Occultor ACP Power Supply Adjustment Procedure”, Atmospheric Optics Group Technical Memorandum AV08-027t, 8 July 2008

Shields, J., “Photometrics Schematics”, Atmospheric Optics Group Technical Memorandum AV08-028t, 14 July 2008 [subject to Non-disclosure agreement, not available to others]

Cameron, J., “Software Update: SortWSIFiles Version 1.2”, Atmospheric Optics Group Technical Memorandum AV08-029t, 25 July 2008

Karr, M., “28 - 30 July 2008 Site 3, Unit 8 Trip Report”, Atmospheric Optics Group Technical Memorandum AV08-030t, 15 August 2008

Cameron, J., “Software Update: ClearBackgroundUnit7.v Version 1.2”, Atmospheric Optics Group Technical Memorandum AV08-031t, 28 August 2008

Cameron, J., “Software Update: SortWSIFiles Version 1.3”, Atmospheric Optics Group Technical Memorandum AV08-032t, 3 September 2008

Cameron, J., “Software Update: AutoProcWSI Version 2.1”, Atmospheric Optics Group Technical Memorandum AV08-033t, 18 September 2008

Cameron, J., “Software Update: ClearBackgroundUnit7.v Version 1.3”, Atmospheric Optics Group Technical Memorandum AV08-034t, 22 September 2008

Cameron, J., “Software Update: AutoProcWSI Version 2.2-20 and AutoProcWSI Version 2.4-20”, Atmospheric Optics Group Technical Memorandum AV08-035t, 23 September 2008

Cameron, J., “Software Update: CombNorm Version 1.2”, Atmospheric Optics Group Technical Memorandum AV08-036t, 31 December 2008 (the work was done earlier)

Shields, J., M. Karr, and A. Burden, “WSI Cloud Product Data Archive Format Overview”, Atmospheric Optics Group Technical Memorandum AV08-037t, 21 October 2008

Shields, J., M. Karr, A. Burden, and J. Streeter “Delivery of WSI Cloud Data Archival External Drive Serial Number L80QDGFG”, Atmospheric Optics Group Technical Memorandum AV08-038t, 21 October 2008

Cameron, J., “Software Update: WSIImageLoop Version 1.2”, Atmospheric Optics Group Technical Memorandum AV08-039t, 27 October 2008

Shields, J., “Return of D/N WSI Unit 11 from SGP Site on Loan to MPL”, Atmospheric Optics Group Technical Memorandum AV08-040t, 31 October 2008

Shields, J., “Refurbishment of D/N WSI Unit 11”, Atmospheric Optics Group Technical Memorandum AV08-041t, 31 October 2008

Karr, M., “11- 14 November 2008 Site 2, Unit 7 Trip Report”, Atmospheric Optics Group Technical Memorandum AV08-046t, 26 November 2008

Karr, M., “Software updates ProcWSID Version 3.0 – 3.4”, Atmospheric Optics Group Technical Memorandum AV08-051t, 31 December 2008

Shields, J., “Optical Density Techniques for Daytime”, Atmospheric Optics Group Technical Memorandum AV08-053t, 31 December 2008

Karr, M., “Software Summary for fielded D/N WSI Units”, Atmospheric Optics Group Technical Memorandum AV09-005t, 29 January 2009

Streeter, J. “Processing of the Site 3 April – August 08 Daytime Data Set”, Atmospheric Optics Group Technical Memorandum AV09-008t, 9 February 2009

Burden, A., “Unit 4v5b Star-Based Geometric Calibration Summary”, Atmospheric Optics Group Technical Memorandum AV09-022t, 25 February 2009

Shields, J., M. Karr, A. Burden, and J. Streeter “Delivery of Real Time Cloud Algorithms”, Atmospheric Optics Group Technical Memorandum AV09-024t, 9 March 2009

Burden, A., “Unit 8 Star-Based Geometric Calibration Summary”, Atmospheric Optics Group Technical Memorandum AV09-027t, 12 March 2009

Burden, A., “Unit 8v3 Effective Lamp Radiances for Field Calibration”, Atmospheric Optics Group Technical Memorandum AV09-028t, 18 March 2008

Burden, A., “Unit 8v3 Field Calibration Results For Site 3”, Atmospheric Optics Group Technical Memorandum AV09-029t, 18 March 2009

Burden, A., “Unit 4v6 Field Calibration Results For Site 5”, Atmospheric Optics Group Technical Memorandum AV09-039t, 22 April 2009

Shields, J., “WSI Daytime Cloud Decision Adaptive Algorithm Overview”, Atmospheric Optics Group Technical Memorandum AV09-040t, 30 April 2009

Shields, J., “WSI Daytime Cloud Decision Adaptive Algorithm Development Details”, Atmospheric Optics Group Technical Memorandum AV09-041t, 30 April 2009

Shields, J., “Processing of the Site 5 January – May 2008 Daytime Data Set”, Atmospheric Optics Group Technical Memorandum AV09-042t, 30 April 2009

Shields, J., “Processing of the Site 5 July – October 2008 Daytime Data Set, and Realtime Algorithm Inputs starting October 2008”, Atmospheric Optics Group Technical Memorandum AV09-043t, 30 April 2009

Streeter, J., “Processing of the Site 3 August - December 08 Daytime Data Set”, Atmospheric Optics Group Technical Memorandum AV09-046t, 2 June 2009

Karr, M., A. Burden, and J. Shields “Processing of Site 3 April 9 – July 31 2008 Night Data Set”, Atmospheric Optics Group Technical Memorandum AV09-048t, 12 June 2009

Karr, M., A. Burden, and J. Shields “Processing of Site 3 August 1 – September 1 2008 Night Data Set”, Atmospheric Optics Group Technical Memorandum AV09-049t, 12 June 2009

Karr, M., A. Burden, and J. Shields "Processing of Site 3 September 2 – October 28, 2008 Night Data Set and Real Time Algorithm Inputs starting December 2008", Atmospheric Optics Group Technical Memorandum AV09-050t, 12 June 2009

Karr, M., A. Burden, and J. Shields "Processing of Site 5 February 1 – July 12, 2007 Night Data Set", Atmospheric Optics Group Technical Memorandum AV09-051t, 12 June 2009

Karr, M., A. Burden, and J. Shields "Processing of Site 5 January 17 – June 30, 2008 Night Data Set", Atmospheric Optics Group Technical Memorandum AV09-052t, 12 June 2009

Karr, M., A. Burden, and J. Shields "Processing of Site 5 July 1 – August 4, 2008 Night Data Set and Real Time Algorithm Inputs starting October 2008.", Atmospheric Optics Group Technical Memorandum AV09-053t, 12 June 2009

Shields, J., "WSI Ring Shade at Sites 3 and 5", Atmospheric Optics Group Technical Memorandum AV09-054t, 4 June 2009

Shields, J. and A. Burden, "Night moonlight algorithm concepts", Atmospheric Optics Group Technical Memorandum AV09-056t, 12 June 2009

Streeter, J., "Fielded Site 3 Daytime 2008 Inputs", Atmospheric Optics Group Technical Memorandum AV09-057t, 15 June 2009

12.2. Power Point Files from Presentations to SOR

Note: Some of this work was funded under the follow-on contract that started in Feb 08, and some was funded under the contract that is the subject of this report. We have listed all the talks given during the interval of this contract, and given a cryptic description of the contents of the talks.

October 07: This trip was cancelled due to a wildfire near my home, but the talk was sent to SOR.

"Whole Sky Imager Update" provided hardware status and overview of algorithm status. Site 2 was operating well, Site 3 deployment was delayed due to camera repair, Site 5 was hit by lightning and under repair, Site 7 was brought back on-line, VA site was not funded. Provided overview of concepts behind new moonlight algorithm, and examples from Site 5, as well as Site 5 starlight algorithm results.

November 07:

a) "Whole Sky Imager Current Cloud Algorithm Sample Results Developed at MPL". Reviewed night algorithm for starlight, and new results for moonlight with partially

completed algorithm, for Site 5, and past transmittance results. Reviewed day alg results for clear (SOR) and hazy (VA) site.

b) "Using the WSI for aerosol characterization" presented Alberto Cazorla's results for extracting aerosol amount.

January 08:

a) "Whole Sky Imager and Night Algorithm Update". Updated hardware status: Site 2 operating well, Site 5 repaired and operating well, Site 3 nearing deployment, SOR and VA sites not funded. Updated moonlight algorithm, examples for Site 5, presented blind test and cloud assess results.

b) "An Update of Wavelength Analysis for Cloud Imaging" analyzed current IR systems, SWIR options, pros and cons.

c) "Using the WSI for aerosol characterization" presented Alberto Cazorla's results for extracting aerosol amount. This was a slightly updated version, presented to a wider audience.

d) "Whole Sky Imager and Night Algorithm Update Summary". The above 3 talks were detailed talks for the working group. This was the summary of all of the above for the TIM group.

May 08:

a) "Whole Sky Imager and Night Algorithm Status Update". Discussed Site 3 deployment. All 3 sites are operational. Provided operational statistics. Site 5 nt alg almost ready to go, also working on Site 3 nt alg. Presented updated results and stats. Showed transmittance, and determined threshold optical fade.

b) "Whole Sky Imager Capabilities related to SWIR Optical Fades". Reviewed extinction mechanisms, visible vs. SWIR relationships, methods to extract optical fade at night, several current transmittance results, range of fades we can detect and thresholds. Presented method to determine fade in daytime.

c) "Whole Sky Imager SWIR Optical Fades and Status Updates". The above 2 talks were detailed talks for the working group. This was the summary of all of the above for the TIM group.

September 08:

"Whole Sky Imager Status Update": Overview of purpose of WSI, and site status. Site 2 down due to power surge, other sites operational. Site 5 night archival data has been processed, real time algs installed both day and night, updated transmittance results, also completed adaptive alg for day. Discussed adaptive alg and how it works.

October 08:

"Whole Sky Imager Status Update": Hardware overview. Sites 3, 5, 7 running well, 2 scheduled for repair in Nov. Site 5 day and night running real time in field; day 2008 archival data processed and delivered, Site 5 night 2007 and 2008 archival data processed and delivered. Site 3 day and night running real time in field; day archival data processed and delivered. Evaluated available data remaining to be processed.

12.3. Selected Published References and Technical Notes in order by date

Johnson, R. W., W. S. Hering and J. E. Shields (1989), "Automated Visibility and Cloud Cover Measurements with a Solid-State Imaging System", Marine Physical Laboratory, Scripps Institution of Oceanography, University of California San Diego, SIO 89-7, GL-TR-89-0061, NTIS No. ADA216906

Johnson, R. W., J. E. Shields, and T. L. Koehler (1991), "Analysis and Interpretation of Simultaneous Multi-Station Whole Sky Imagery", Marine Physical Laboratory, Scripps Institution of Oceanography, University of California San Diego, SIO 91-3, PL-TR-91-2214

Shields, J. E., R. W. Johnson, and T. L. Koehler, (1993), "Automated Whole Sky Imaging Systems for Cloud Field Assessment", Fourth Symposium on Global Change Studies, 17 – 22 January 1993, American Meteorological Society, Boston, MA

Shields, J. E., R. W. Johnson, and M. E. Karr, (1994), "Upgrading the Day/Night Whole Sky Imager from Manual/Interactive to Full Automatic Control, Marine Physical Laboratory, Scripps Institution of Oceanography, University of California San Diego, Report MPL-U-140/94

Shields, J. E., R. W. Johnson, M. E. Karr, R. A. Weymouth, and D. S. Sauer, (1997a), "Delivery and Development of a Day/Night Whole Sky Imager with Enhanced Angular Alignment for Full 24 Hour Cloud Distribution Assessment", Marine Physical Laboratory, Scripps Institution of Oceanography, University of California San Diego, Report MPL-U-8/97

Shields, J. E., M. E. Karr, and R. W. Johnson, (1997b), "Service Support for the Phillips Laboratory Whole Sky Imager", Marine Physical Laboratory, Scripps Institution of Oceanography, University of California San Diego, Report MPL-U-10/97

Shields, J. E., R. W. Johnson, M. E. Karr, and J. L. Wertz, (1998), "Automated Day/Night Whole Sky Imagers for Field Assessment of Cloud Cover Distributions and Radiance Distributions", Tenth Symposium on Meteorological Observations and Instrumentation, 11 – 16 January 1998, American Meteorological Society, Boston, MA

Feister, U., Shields, J., Karr, M., Johnson, R., Dehne, K. and Woldt, M, (2000), "Ground-Based Cloud Images and Sky Radiances in the Visible and Near Infrared Region from Whole Sky Imager Measurements", Proceedings of Climate Monitoring – Satellite Application Facility Training Workshop sponsored by DWD, EUMETSAT and WMO, Dresden 2000.

Shields, J. E., M. E. Karr, A.R. Burden, R.W. Johnson, and J. G. Baker, (2002), "Analytic Support for the Phillips Laboratory Whole Sky Imager, 1997 - 2001", Marine Physical Laboratory, Scripps Institution of Oceanography, University of California San Diego.

Shields, J. E., R.W. Johnson, M. E. Karr, A.R. Burden, and J. G. Baker, (2003a), "WSI Field Calibration System Operations Manual", Marine Physical Laboratory, Scripps Institution of Oceanography, University of California San Diego, Technical Note 252, February 2003.

Shields, J. E., M. E. Karr, A.R. Burden, R.W. Johnson, and J. G. Baker, (2003b), "Analysis and Measurement of Cloud Free Line of Sight and Related Cloud Statistical Behavior – Published as Final Report for ONR Contract N00014-97-D-0350 DO #2", Marine Physical Laboratory, Scripps Institution of Oceanography, University of California San Diego, Technical Note 262, June 2003.

Shields, J. E., R. W. Johnson, M. E. Karr, A. R. Burden, and J. G. Baker (2003c), Calibrated Fisheye Imaging Systems for Determination of Cloud Top Radiances from a UAV, International Symposium on Optical Science and Technology, SPIE the International Society for Optical Engineering, 2003.

Shields J. E., R. W. Johnson, M. E. Karr, A. R. Burden, and J. G. Baker, (2003d), Daylight Visible/NIR Whole Sky Imagers for Cloud and Radiance Monitoring in Support of UV Research Programs, International Symposium on Optical Science and Technology, SPIE the International Society for Optical Engineering, 2003.

Shields, J. E., R. W. Johnson, M. E. Karr, A. R. Burden, and J. G. Baker (2003e), Whole Sky Imagers for Real-time Cloud Assessment, Cloud Free Line of Sight Determinations and Potential Tactical Applications, The Battlespace Atmospheric and Cloud Impacts on Military Operations (BACIMO) Conference, Monterey, CA. http://www.nrlmry.navy.mil/bacimo.html, 2003.

Shields, J. E., A.R. Burden, M. E. Karr, R.W. Johnson, and J. G. Baker, (2004a), "Development of Techniques for Determination of Nighttime Atmospheric Transmittance and Related Analytic Support for the Whole Sky Imager – Published as Final Report for ONR Contract N00014-01-D-0043 DO #5", Marine Physical Laboratory, Scripps Institution of Oceanography, University of California San Diego, Technical Note 263, April 2004.

Shields, J. E., M. E. Karr, A.R. Burden, R.W. Johnson, and J. G. Baker, (2004b), "Project Report for Providing Two Day/Night Whole Sky Imagers and Related Development

Work for Starfire Optical Range – Published as Final Report for ONR Contract N00014-97-D-0350 DO #6", Marine Physical Laboratory, Scripps Institution of Oceanography, University of California San Diego, Technical Note 265, May 2004.

Shields, J. E., J. G. Baker, M. E. Karr, R. W. Johnson, and A. R. Burden, (2005a), Visibility measurements along extended paths over the ocean surface, International Symposium on Optical Science and Technology, SPIE the International Society for Optical Engineering, August 2005.

Shields, J. E., A.R. Burden, R.W. Johnson, M. E. Karr, and J. G. Baker, (2005b), "Cloud Free Line of Sight Probabilities and persistence Probabilities from Whole Sky Imager Data", Marine Physical Laboratory, Scripps Institution of Oceanography, University of California San Diego, Technical Note 266, August 2005.

Shields, J. E., A. R. Burden, R. W. Johnson, M. E. Karr, and J. G. Baker (2005c), "Measurement and Evaluation of Cloud Free Line of Sight with Digital Whole Sky Imagers", The Battlespace Atmospheric and Cloud Impacts on Military Operations (BACIMO) Conference, Monterey, CA. http://www.nrlmry.navy.mil/bacimo.html, 2005.

Shields, J. E., R. W. Johnson, J. G. Baker, M. E. Karr, and A. R. Burden, (2006), "Multispectral scattering measurements along extended paths using an imaging system", International Symposium on Optical Science and Technology, SPIE the International Society for Optical Engineering, August 2006.

Shields, J. E., M. E. Karr, A.R. Burden, R.W. Johnson, and W. S. Hodgkiss, (2007a), "Enhancement of Near-Real-Time Cloud Analysis and Related Analytic Support for Whole Sky Imagers, Final Report for ONR Contract N00014-01-D-0043 DO #4", Marine Physical Laboratory, Scripps Institution of Oceanography, University of California San Diego, Technical Note 271, May 2007.

Shields, J. E., M. E. Karr, A.R. Burden, R.W. Johnson, and W. S. Hodgkiss, (2007b), "Whole Sky Imaging of Clouds in the Visible and IR for Starfire Optical Range, Final Report for ONR Contract N00014-01-D-0043 DO #11", Marine Physical Laboratory, Scripps Institution of Oceanography, University of California San Diego, Technical Note 272, July 2007.

Shields, J. E., M. E. Karr, A.R. Burden, R.W. Johnson, and W. S. Hodgkiss, (2007c), "Continuing Support of Cloud Free Line of Sight Determination Including Whole Sky Imaging of Clouds, Final Report for ONR Contract N00014-01-D-0043 DO #13", Marine Physical Laboratory, Scripps Institution of Oceanography, University of California San Diego, Technical Note 273, November 2007.

Appendix 1: Contents of Memo AV08-037, documenting the format of the delivered data archive.

Note: In order to be reasonably clear within the context of this report, all of the technical memo section numbers have had "A1." added to them, so that Section 1 because Section A1.1. If the memo refers to a given section X, then it should be understood that in the context of this report, this becomes Section A1.X.

Subject: WSI Cloud Product Data Archive Format Overview

Having recently completed the night cloud algorithm with high resolution for both starlight and moonlight, as well as the day cloud algorithm with an adaptive algorithm that corrects for haze, we are in the process of getting the required inputs for all sites, and processing (or reprocessing) the archival data. This memo is intended to enable users to extract the cloud decision results from the archival drives that we are generating. The memo will document the directory structure, file format, header format, how to sort the data using the headers, the meaning of the data levels, how to display them, and the approximate geometry of the image. The specific site, dates, geometric equations, and comments, will be provided in separate memoranda that are associated with each drive delivered to the sponsors. Memo AV08-038t documents the first archive drive.

A1.1. Directory Structure

The directory structure is based on the one that the SOR team uses when they download data from the field. The data will have a directory name such as "Site 5". The next subdirectory down will be something descriptive, such as "Archival2008DaySet1Proc13Oct08". Under this will be the standard format used by SOR, i.e. the next subdirectory will be the year, such as "2008". Below that will be the month in the format "01", and below that will be the day in the format "01". Within this directory will be the cloud decision images and a single additional file for each day indicating the confidence level for each cloud decision image in the directory. In the near future, for night images, we will add transmittance or optical fade data files as soon as feasible, although we are putting priority on the cloud results for the moment. Similarly, we anticipate adding an optical fade product for the daytime in the longer term.

A1.2. File Format

The files are named WSIUUUDDDDYYYYTTTT.cld, where UUU is unit number, DDDD is calendar day (month and day), YYYY is year, and TTTT is time in GMT.

The images are 512 x 512, 8 bits deep. Although the raw data are 16 bits deep, the algorithm results are mapped into an 8-bit image, as discussed in section 5. Most of the pixels represent algorithm results, as documented in Section 5, although some near the top represent header values, as documented in Section 3.

A1.3. Header Format

There are 9 header lines in the cloud decision images. The headers include information that enables us to trace back to the measurement conditions, as well as processing parameters. Most of the items in the headers are for internal use, however some may be useful to the data users. We have documented those parameters we feel may be useful. In some cases, header parameters are obsolete and not updated, so please do not attempt to use parameters that are not documented here.

This section documents the headers for Units 4, 7, and 8, which are at Air Force Sites 5, 2, and 3 respectively. Other systems may have other formats, and will be documented when we begin archival processing.

Line 1: Line 1 documents the site, date and time, as well as various hardware readings. The parameters relevant to data users are the Site, date, time, and file (type). The other parameters are for internal use. For Site, we have used "AFT" for Site 2, and "AF3" and "AF5" for Sites 3 and 5. The SOR site currently has a different header format. If funds permit, we hope to update this in the future. The file type is given as CldNR or CldRD for the day cloud decision, depending on whether it was derived with Near Infrared (NIR) or red images. The night cloud decision images are identified as "CLR", because the data were derived from the Clear, or Open hole, data. A sample of Line 1 is shown below.

```
Site:AFT Bd=   27.9Cew=   82.48 File:CldNR mage    Day=14
Month= 9 Year=2006  Time=1615Z G Exposure=    100ms  ND=3
SP=9 Occultor Destination:  Arc= 70.8   Trle=113.2  Housing
Temp=26  Hware Ver:  7.30 Sware Ver:  1.20 Time Stat: 4  N2
pressure= 5   Flow rate= 0.39   Env. Housing Temp= 23   CCD
Chip Temp=-29   Occultor Position:  Arc= 70.6 Trolley=999.0
Rel. Humidity= 68   Red flags:   00000000000  Yellow flags
0000000000000000
```

Line 2: Line 2 includes the sun and moon position, that the user may wish to use. The user should not use the image position values shown in the header; these values are estimated values before fielding, used in the field acquisition code, but should not be used for the precise image geometry. (The image geometry will be provided with each archival drive.) The remainder of the line contains obsolete parameters that should not be used. A sample of Line 2 is shown below.

```
Sun Position: Azimuth=142.5 Zenith= 29.8   Moon Position:
Azimuth=289.3 Zenith= 62.6   Source=Sun    Azimuth Offsets:
Camera=  0.0 Field=  0.0  Occultor Offsets: Azimuth=  0.0
Zenith=   0.0   Image Center: Col=254 Row=254 Radius=244
Field Azm. update time: 0909:09
```

Line 3, 4, and 5: Lines 3, 4, and 5 provide details of the data acquisition and processing that are used internally by MPL.

Line 6: Parts of Line 6 pertain to the processing, and other parts are obsolete, as they refer to features not used by the SOR program. The obsolete portions are not checked for accuracy. However, the parameters starting at pixel 418 may be useful to the data user. These parameters list the percent of the full image identified as clear, thin, opaque, no decision, indeterminate, and offscale bright. To determine clear fraction, divide the clear by the sum of clear, thin, and opaque. To determine cloud fraction, divide the sum of thin and opaque by the sum of clear, thin, and opaque. The no decision value is very high, because at the time these instruments were fielded, the funding levels were very low, and we had to use fixed occultor shades. New occultor shades that are much smaller are in design.

A sample of Line 6 starting at Pixel 418 is given below.

```
Clear=  4%  Thin=  3%  Opaque= 68%  No Dec= 24%  Indeter=
0%  Off Brt=  0%
```

Line 7: Line 7 is used internally by MPL.

Line 8: Line 8 contains the error strings, and bit 18 is very important to the user. Bits 0 through 11 are used to annotate abnormalities in data acquisition. Bits 12 and 13 are saved positions, in case we wish to add additional parameters in the future. Bits 14 – 17 are blank. Bit 18 is the most important to the user, as it identifies images that we feel should not be used. The decision was made to go ahead and provide a cloud decision even when there is a known error in the raw data, but to identify it in the header as an image that is probably bad.

If bits 0-11 are all 0's, the quality value in bit 19 will be set to 1. This indicates a high level of confidence in the cloud decision image. If any of the flags in the table above are set, the quality bit value will be set to 2. This indicates that the cloud decision image should be examined because it may be compromised due to a system error. If bits 0 or 5 are set to 1, the quality bit value will be set to 3. This indicates that the cloud decision image results are not valid and should not be included in routine data analysis.

The data bits are listed below.

```
Bit 0 Spectral filter error
Bit 1 Neutral density filter error
Bit 2 Arc position off by >= 8 deg.
Bit 3 Trolley position off by >= 8 deg.
Bit 4 Flux level – 5% of pixels offscale bright
Bit 5 Flux level – offscale dark
Bit 6 Flux level – 1% of pixels offscale bright
Bit 7 Flux level – Possible shutter malfunction
Bit 8 Flow < .09
Bit 9 Env. Housing temp > 49
Bit 10 Cam. Housing temp. > 49
```

```
Bit 11 CCD chip temp. > -1
Bit 12 Not used (always 0)
Bit 13 Not used (always 0)
Bits 14 – 17 are blank
Bit 18 Cloud Decision QC bit
```

A sample of Line 8 is given below.

```
00000000000000    1
```

Line 9: Line 9 is for internal use. It exists in images created after Sept.6, 2006

The remainder of the image is non-header data, as described in Section 5.

A1.4. Sorting the Data for cases expected to be valid

As noted earlier, the decision was made at SOR that we should include cloud decision images that may not be valid due to instrumental problems, but should identify them in the headers as being not valid. An example might be if the occultor hangs, and there is stray light present in the image.

There are two ways for the user to identify and remove these images. The user can read the header, line 8 pixel 18. If the value is 3, this image should not be used. If the value is 2, we will try to advise you in the specific memos. For example, if the "2" is caused by an arc error, as in bit 2, then the images should not be used. On the other hand, if the "2' is caused by too many offscale bright pixels, as in bit 6, that doesn't matter because the algorithm will handle the bad pixels and reject them. As we have more opportunity to evaluate the processed data, we will try to update the criteria to make them more definitive.

The second way the user can remove the images is by use of the CloudDecQCReport.txt files. There is a file for each day, provided in the subdirectory for each day, that provides the result of sorting the QC pixel discussed above. A portion of a sample output file is shown in Figure 1.

Figure 1
A portion of File CloudDecQCReport.txt

```
CloudDecQC v1.0          Cloud Decision Confidence Level Report          Page: 1
                              Sort By: Name                    Date: 10/16/08
Atmospheric Optics Group (UCSD)                                    Time: 15:35:20
================================================================================
=====================================
Directory: G:\Site 5\Archival 2008 Day Set 1 Proc 13 Oct 08\2008\01\17\
================================================================================
=====================================
Cloud File Name        Confidence Level
```

---------- ----------
WSI004011720080000.CLD 1 - Valid
WSI004011720080001.CLD 1 - Valid
WSI004011720080002.CLD 1 - Valid
WSI004011720080003.CLD 1 - Valid
WSI004011720080004.CLD 1 - Valid
WSI004011720080005.CLD 1 - Valid
WSI004011720080006.CLD 1 - Valid
WSI004011720080007.CLD 1 - Valid

At the present time, times that are not expected to be valid due to sunrise or sunset are not processed. Typically, the day is processed for all Solar Zenith angles (SZA) of 85 degrees or less. The night data are processed for all SZA values of 104 or higher. We will indicate what angles were used in the memos that go with specific data.

It should be noted that the QC checks are continuing to mature. If we find problems that we feel will significantly affect the statistics, but that are not identified by the QC parameters, we reserve the right to remove these data from the archival directory. In such a case, we will document this decision in the memo that goes along with the delivery.

A1.5. Data format

The raw data have been processed to yield cloud decisions, and the results of the decisions are coded into 8 bits in the following way. The color code refers to the colors used in the displays that MPL produces.

For the day algorithm:

Numeric Range	Decision	Color Code
0	No data	Black
1 – 99	Clear or Haze	Blue
100 – 139	Thin cloud	Yellow
140 – 200	Opaque cloud	Grey to White
201	Offscale bright	Bright White
202	Indeterminate	Dark Grey

For the night algorithm:

Numeric Range	Decision	Color Code
0 - 49	No data	Black
50 – 119	Clear or Haze	Blue
120 – 179	Thin cloud	Green
180 – 249	Opaque cloud	Grey to White

A range of values is used for each category such as "opaque", such that we can retain characteristics of the original image for ease in viewing. For example, once a pixel is identified as day opaque cloud, its value is assigned within the range of 140 – 200 based on the relationship between the pixel's actual ratio and the threshold ratio. At the present time, variations within each category are not technically meaningful, but are only used in

creating the display image. The color look-up tables for displaying the images are given in Appendices 1 and 2. These color tables are for the version that shows solid blue in the "clear or haze" category.

For night, the threshold between "clear or haze" and "thin cloud" is approximately 0.8 dB. The threshold between "thin cloud" and "opaque cloud" is approximately 8 dB. For daytime, we have not yet extracted these thresholds; however the same values are good working numbers. That is, we expect the thresholds to be similar, because the appearance of the thin clouds that are missed by the night and the day algorithms are similar. As mentioned earlier, we plan to add the transmittance or optical fade table data product at night as soon as feasible, and plan to follow up with work to provide optical fade for the daytime.

A1.6. Image Geometry

Because the images are acquired looking up, they do not have the same directions as looking down on a map. Specifically, North is at the bottom of the image, South at the top, East on the right edge, and West on the left. The image typically has about a 181.5 degree field of view, and each pixel is about 1/3 degree. The specific equations relating pixel location to angular location and visa versa will be documented with each data set.

A1.7. Upgrades

There may be additional upgrades to the algorithms in the future. As an example, occasionally a very small rim of opaque cloud is identified near the aureole. We chose to get this data out now, rather than take the time to fix it. But if it causes problems with the data analysis, we would plan to fix it and reissue the archival data. For this reason, if the users find problems with these data sets, we appreciate being politely alerted so that we can make the necessary upgrades.

Sub-Appendix 1.1: Code for Color Table for Day Algorithm Colors

```
/* ---------------------- DECIDE function VgaViewDecision --
-------------- */

void SetCldPalette (imgdes *image)


{ int j,jt3;

/*  Set the cloud decision color palette - First set up gray
scale  */
  image->palette[0].rgbRed = 0;              /*  Set no data
(0) to black {0,0,0}*/
  image->palette[0].rgbGreen = 0;
  image->palette[0].rgbBlue = 0;


/*  Set the clear sky range, Make it solid blue */
```

```
  for (j = 1 ; j < 100 ; j++)
  {
    image->palette[j].rgbRed = 90;
    image->palette[j].rgbGreen = 90;
    image->palette[j].rgbBlue = 194;
  }


/*  Set the thin cloud range */
  for (j = 100 ; j < 140 ; j++)  /* make it yellow */
  { jt3 = j * 3;
    image->palette[j].rgbRed = (UCHAR) 20 + (UCHAR) ( (float
) 1.3 * (float ) j
                              + (float ) .5);          /*  Red
value   */
    image->palette[j].rgbGreen = image-
>palette[j].rgbRed;        /*  Green value */
    image->palette[j].rgbBlue = 0;          /*  Blue value
*/
  }

/*  Set the opaque cloud range */
  for (j = 140 ; j < 201 ; j++)
  { jt3 = j * 3;
    image->palette[j].rgbRed = (UCHAR) 68 + (UCHAR) ( (float
) .8 * (float ) j
                              + (float ) .5);
/*  Red value   */
    image->palette[j].rgbGreen = image-
>palette[j].rgbRed;        /*  Green value */
    image->palette[j].rgbBlue = image-
>palette[j].rgbRed;        /*  Blue value  */
  }

  image->palette[201].rgbRed = 240;  /*  Set off scale (201)
to {240,240,240}    */
  image->palette[201].rgbGreen = 240;
  image->palette[201].rgbBlue = 240;

  image->palette[202].rgbRed = 40;  /*  Set indeterminate
(202) to {40,40,40}    */
  image->palette[202].rgbGreen = 40;
  image->palette[202].rgbBlue = 40;

  for (j = 203 ; j < 256 ; j++) image->palette[j].rgbRed =
(UCHAR) (j);
  for (j = 203 ; j < 256 ; j++) image->palette[j].rgbGreen =
(UCHAR) (j);
  for (j = 203 ; j < 256 ; j++) image->palette[j].rgbBlue =
(UCHAR) (j);
```

```
} /*  End function SetCldPalette  */
```

Sub-Appendix 1.2: Code for Color Table for Night Algorithm Colors

```
void SetNightCldPalette (imgdes *image)


{ int j,jt3;

/*  Set the cloud decision color palette - First set up gray
scale  */
  for (j = 0; j < 50; j++)
  {
         image->palette[j].rgbRed = 0;              /*  Set
no data (0) to black {0,0,0}*/
         image->palette[j].rgbGreen = 0;
         image->palette[j].rgbBlue = 0;
  }


/*  Set the clear sky range */
  for (j = 50 ; j < 120 ; j++)
  {
    //Below is for varying shades of blue
    //jt3 = j * 3;
    //image->palette[j].rgbRed = (unsigned int) ((j-50) *
100./70.) + 60;                /*  Red value   */
    //image->palette[j].rgbGreen = image-
>palette[j].rgbRed;         /*  Green value */
    //image->palette[j].rgbBlue = (unsigned int) ((j - 50) *
100./70.) + 150;           /*  Blue value  */
    //Version with solid blue
    image->palette[j].rgbRed = ( unsigned int )
60;                 /*  Red value   */
    image->palette[j].rgbGreen = image-
>palette[j].rgbRed;         /*  Green value */
    image->palette[j].rgbBlue = 150;          /*  Blue
value  */
  }


/*  Set the thin cloud range, Make it green*/
  for (j = 120 ; j < 180 ; j++)
  { jt3 = j * 3;
    image->palette[j].rgbRed = ( unsigned int ) ((j - 120) *
70./60.) + 80;                /*  Red value   */
    image->palette[j].rgbGreen = ( unsigned int ) ((j - 120)
* 70./60.) + 150;;         /*  Green value */
    image->palette[j].rgbBlue = image-
>palette[j].rgbRed;         /*  Blue value  */
  }
```

```
/*  Set the opaque cloud range */
  for (j = 180 ; j < 250 ; j++)
  { jt3 = j * 3;
    //Oldimage->palette[j].rgbRed = (unsigned int) ((j -
180) * 170./70.) + 80;
    image->palette[j].rgbRed = ( unsigned int ) ((j - 180) *
50./70.) + 180;                //New per JS 22Sep06 Red
value   */
    image->palette[j].rgbGreen = image-
>palette[j].rgbRed;         /*  Green value */
    image->palette[j].rgbBlue = image-
>palette[j].rgbRed;         /*  Blue value  */
  }



} /*  End function SetNightCldPalette  */
```

Appendix 2: Contents of Memo AV08-038, documenting the delivered data archive.

Note: In order to be reasonably clear within the context of this report, all of the technical memo section numbers have had "A2." added to them, so that Section 1 because Section A2.1. If the memo refers to a given section X, then it should be understood that in the context of this report, this becomes Section A2.X.

Subject: Delivery of WSI Cloud Data Archival External Drive Serial Number L80QDGFG

We have prepared a drive with archival cloud algorithm data, for hand delivery to SOR on 23 October 2008. Memo AV08-037t provides an overview of the data format. It is important to either sort the data as noted in Section 4 of that memo, or use the CloudDecQCReport.txt file that is included in each subdirectory and documented in Section 4 of that memo. This file provides a summary for each day of the cases in which the raw data are abnormal and the cloud decision data are not expected to be valid. As stated in Section 4 of Memo AV08-037t, the cloud decision images in the file CloudDecQCReport.txt are labeled as 'Valid', 'Uncertain' or 'Invalid'. The invalid cases should not be used. The uncertain cases also should normally not be used. In the future, we plan to evaluate the data in more detail and can reassess this, as in some cases it may be Ok to use the uncertain cases.

This memo documents the specifics of what is included in this delivery. The External Drive has serial number L80QDGFG. Because our sponsors are asking for data as quickly as possible, we opted to send what we could readily process. In each section, we discuss what was and was not processed, and why. The additional data that has not been processed will be sent as quickly as we can.

I would also like to note that we have visually reviewed the hourly images, but we have not run a program such as a blind test to assess the overall accuracy. We believe the day data are coming out better than the sites we assessed before, which had an overall accuracy of over 97%. Similarly, the night data appear to be coming out better than the data we assessed before, which had an overall accuracy of about 90 – 95%. Of this error, we believe most of it was actually thin cloud that fell below the thin cloud threshold of about 0.8 dB, and not actual error. We plan to assess the accuracy of the data sets on this drive in the future.

A2.1. Site 5 Day 2008 Set 1 Archive

This section documents the Site 5 Day 2008 Set 1 data.

A2.1.1 Directory Name on Archival Drive: Site5\Archival2008DaySet1Proc13Oct08. The date indicates the date that processing started.

A2.1.2 Dates Processed: Jan 16 2008 – May 20 2008

A2.1.3 Solar Zenith Angles Processed: 0 - 85

A2.1.4 Algorithm Used: These data used the first version of the adaptive algorithm, Program AutoProc2.4-20.

A2.1.5 General Comments:

The data in general look quite good. In some instances, the solar aureole has edges identified as opaque. We know how to fix this, but did not want to slow down to do this at this time. Also, we may make further upgrades to the adaptive algorithm in the future, as there are occasional times when it misses more cirrus than we would like. If it does miss cirrus, it normally identifies some of the cirrus in the image, and we believe the problem occurs in about 2% of the images. We feel that the clear cases and the opaque cases are normally identified correctly.

A2.1.6 Processing of Day Site 5 Data:

A record of the data availability and data processed for Site 5 is shown in the Appendix.

The instrument was deployed during 31 Jan – 1 Feb 07. It ran until struck by lightning in July 07. The repair was completed Jan 16 2008. The occultor ACP failed May 22 2008, and was repaired June 30 – July 2 2008. The 2007 daytime data have not yet been processed, because we will have to probably pull a new clear sky background for that set.

The daytime data for Set 1 2008, 16 Jan – 20 May 08, are processed and delivered with this delivery. The processing computer stopped during the run (perhaps due to a power outage), so we will have to separately run the 21 – 22 May 08 data. The daytime data for Set 2 2008 are the data since July 2. We received Set 2 test data August 12, and the real time algorithm, tested with Set 2 data, was installed August 26. An upgrade to the algorithm was installed 14 October. The data since August 26 should be valid, but we will process all data from July 2 through October 14 after we receive the data. The night data for Site 5 has been processed, and will be discussed below.

A2.1.7 Equations to relate Pixel Position to Angle:

The following equations may be used to convert between image coordinates and spherical coordinates. The zenith and azimuth are in degrees, and azimuth is clockwise with respect to True North in real space (not in image space). That is, the bottom of the image is North, and the right side is East, as explained in Memo AV08-037t.

The equations for azimuth, ϕ, and zenith, θ in degrees, given pixel location x,y are:

$$\phi = 0.05787 + \phi_0 - 0.004426\ \rho \mathrm{Cos}(\pi \phi_0 / 90) + 0.0002416\ \rho \mathrm{Sin}(\pi \phi_0 / 90) \qquad (1)$$

$$\theta = 0.3436\,\rho - 0.00004412\,\rho^2 + 7.145\times10^{-7}\,\rho^3 + 0.0006305\,\rho\,\mathrm{Cos}(\pi\phi/90) - 0.004436\rho\,\mathrm{Sin}(\pi\phi/90) \quad (2)$$

where $\phi_0 = \arctan\left[\frac{(x - x_{center})}{(y - y_{center})}\right]$ and $\rho = \sqrt{(x - x_{center})^2 + (y - y_{center})^2}$.

The geometric calibration is affected when the instrument is moved, such as during repairs. In this case, the image center changed, but camera rotation was minimal. Therefore, three different sets of image center values are valid for the above equations. For data through July 2007, x_{center} = 244.3 and y_{center} = 250.5. For data from Jan-Jun 2008, x_{center} = 246.3 and y_{center} = 239.5. Finally, for data from July 2008 and later, x_{center} = 243.8 and y_{center} = 240.5.

To derive the x,y pixel position corresponding to a given angular position θ, ϕ, in degrees, the equations are:

$$X = X_C + P \times Sin(\pi\phi_P/180) \quad (3)$$

$$Y = Y_C + P \times Cos(\pi\phi_P/180) \quad (4)$$

where P and ϕ_p are defined by

$$\mathrm{P} = 2.932\,\theta - 0.0002749\,\theta^2 - 0.00003042\,\theta^3 - 0.004269\,\theta\,\mathrm{Cos}(\pi\phi/90) + 0.03171\,\theta\,\mathrm{Sin}(\pi\phi/90) \quad (5)$$

$$\phi_\mathrm{p} = \phi - (0.05787 - 0.004426\,\mathrm{P}\,\mathrm{Cos}(\pi\phi/90) + 0.0002416\,\mathrm{P}\,\mathrm{Sin}(\pi\phi/90)) \quad (6)$$

A2.2. Site 3 Day 2008 Archive

This section documents the Site 3 Day 2008 Set 1 data.

A2.2.1 Directory Name on Archival Drive: Site3\Archival2008DaySet1Proc10Oct08. The date indicates the date that processing started.

A2.2.2 Dates Processed: Apr. 9 2008 – Aug. 4 2008

A2.2.3 Solar Zenith Angles Processed: 0 - 85

A2.2.4 Algorithm Used: These data used the first version of the adaptive algorithm, Program AutoProc2.2-20.

A2.2.5 General Comments:

This site had more start-up hardware problems than normal due to the extreme heat. At times the outside temperature was over 120 F, and under these conditions both the camera electronics unit and the occultor brake had difficulties. Although the QC indicators are able to catch some of the bad cases, it was not sophisticated enough to catch others. For this reason, we have deleted those days that we feel are adversely impacted. It is possible that we may be able to develop more sophistication in either the algorithm (to identify the bad pixels) or the QC (to identify the bad images) in the future, in which case we would issue the data at that time.

The cooler was replaced on July 29 2008, and this solved the camera problems. The dates that have been deleted are April 17 – 22 and 25, May 10 – 12, 16, and 18 – 21, June 24 – 30, and July 1 – 28. In addition, the raw data from April 26 through May 8 was lost due to a combination of failed ftp, and an external drive damaged in transit. The WSI will save the data if ftp is down and send it later, but if the WSI sends the data and it is damaged, the external drive is normally used to recover the lost data. May 9 was also deleted, because there were people working on the WSI. At this site, the "uncertain" cases are due to the occultor being off, and should not be used. (Removing the data as noted above may have removed all these cases.)

For those data that were not affected by the heat, the cloud results look very good. Most clear days are determined correctly and when they are not, it is only at sunset where there is a slight undefined region. Most opaque and thin clouds are identified correctly. On some partly cloudy days, there are regions near the clouds that probably have too much thin cloud identified, although these regions may also be caused by cloud debris.

A2.2.6 Processing of Day Site 3 Data:

A record of the data availability and data processed for Site 3 is shown in the Appendix.

The instrument was deployed during 8 – 10 Apr 2008. As noted above, some periods have problems due to the heat, and a short period of data was lost during Apr 26 – May 8 due to a problem with the ftp and external drive. Those dates strongly affected by the heat problems were deleted from the archive. The real time algorithm was installed October 14. At the present time, we have processed all the data we have received, which is the data from April 9 through August 4 2008. We will process the data between August 4 and October 14 after we receive the data from the field, and will deliver it in a later delivery. Similarly, the night data for site 3 will be processed in a later delivery.

A2.2.7 Equations to relate Pixel Position to Angle:

The instrument was moved slightly during replacement of the environmental housing that was completed on 30 July 2008. The first set of equations is used for data collected through July 2008.

The equations for azimuth, ϕ, and zenith, θ in degrees, given pixel location x,y are:

$$\phi = -0.8812 + \phi_0 + 0.0004301\rho\,\mathrm{Cos}(\pi\phi_0/90) + 0.007124\rho\,\mathrm{Sin}(\pi\phi_0/90) \quad (7)$$

$$\theta = 0.3365\rho + 2.322\times10^{-5}\rho^2 + 3.818\times10^{-7}\rho^3 - 0.006826\rho\,\mathrm{Cos}(\pi\phi/90) - 0.0001109\rho\,\mathrm{Sin}(\pi\phi/90) \quad (8)$$

where $\phi_0 = \arctan\left[\frac{(x - x_{center})}{(y - y_{center})}\right]$ and $\rho = \sqrt{(x - x_{center})^2 + (y - y_{center})^2}$. For these equations, $x_{center} = 249.7$ and $y_{center} = 251.7$.

To derive the x,y pixel position corresponding to a given angular position θ, ϕ, in degrees, the equations are:

$$X = X_C + P \times Sin(\pi\phi_P/180) \quad (9)$$

$$Y = Y_C + P \times Cos(\pi\phi_P/180) \quad (10)$$

where P and ϕ_p are defined by

$$\mathrm{P} = 2.980\theta - 0.001206\theta^2 - 0.00001754\theta^3 + 0.05211\theta\,\mathrm{Cos}(\pi\phi/90) + 0.0008375\theta\,\mathrm{Sin}(\pi\phi/90) \quad (11)$$

$$\phi_\mathrm{p} = \phi + 0.8812 - 0.0004301\,\mathrm{P}\,\mathrm{Cos}(\pi\phi/90) - 0.007124\,\mathrm{P}\,\mathrm{Sin}(\pi\phi/90)) \quad (12)$$

The following set of equations is used for data collected after July 2008.

The equations for azimuth, ϕ, and zenith, θ in degrees, given pixel location x,y are:

$$\phi = 0.6730 + \phi_0 - 0.0005058\,\rho\,\mathrm{Cos}(\pi\phi_0/90) + 0.007731\,\rho\,\mathrm{Sin}(\pi\phi_0/90) \quad (13)$$

$$\theta = 0.3366\rho + 1.179\times10^{-5}\rho^2 + 4.242\times10^{-7}\rho^3 - 0.006667\rho\,\mathrm{Cos}(\pi\phi/90) - 0.0005109\rho\,\mathrm{Sin}(\pi\phi/90) \quad (14)$$

where $\phi_0 = \arctan\left[\frac{(x - x_{center})}{(y - y_{center})}\right]$ and $\rho = \sqrt{(x - x_{center})^2 + (y - y_{center})^2}$. For these equations, $x_{center} = 249.9$ and $y_{center} = 250.5$.

To derive the x,y pixel position corresponding to a given angular position θ, ϕ, in degrees, the equations are:

$$X = X_C + P \times Sin(\pi\phi_P/180) \quad (15)$$

$$Y = Y_C + P \times Cos(\pi\phi_P/180) \quad (16)$$

where P and ϕ_p are defined by

$$P = 2.980\,\theta - 0.0009243\,\theta^2 - 0.00002075\,\theta^3 + 0.05119\,\theta\,\mathrm{Cos}(\pi\phi/90) + 0.003791\,\theta\,\mathrm{Sin}(\pi\phi/90) \quad (17)$$

$$\phi_p = \phi - 0.6730 + 0.0005058\,P\,\mathrm{Cos}(\pi\phi/90) - 0.007731\,P\,\mathrm{Sin}(\pi\phi/90)) \quad (18)$$

A2.3. Site 5 Night 2007 Archive

This section documents the Site 5 Night 2007 data.

A2.3.1 Directory Name on Archival Drive: Site5\Archival2007NightSetProc8Jul08. The date indicates the date that processing started.

A2.3.2 Dates Processed: Feb. 1 2007 – Jul. 12 2007

A2.3.3 Solar Zenith Angles Processed: 104 and greater

A2.3.4 Moon Zenith Angles Processed: 0 and greater.

A2.3.5 Algorithm Used: These data used the new moonlight night cloud decision algorithm with ProcWSID Version 2.4. This version is the first one that is good for both starlight and moonlight.

A2.3.6 General Comments:

The night cloud detection software performed well for no-moon and moonlight conditions. Tests based on earlier runs that were not yet quite optimized showed 90 - 95% accuracy for zenith angles < 60°. Very thin cloud gets missed in some cases (identified as cloud-free), but this issue may be reduced with future updates to nominal background imagery.

A2.3.7 Processing of Night Site 5 2007 Data:

A record of the data availability and data processed for Site 5 is shown in the Appendix.

The instrument was deployed during 31 Jan – 1 Feb 07. It ran until struck by lightning in July 07. All of this 2007 data have been processed through the night algorithm and are included on the drive.

A2.3.8 Equations to relate Pixel Position to Angle:

The same equations given in Section 1 of this memo may be used for the night data, being careful to use the image center for the correct period.

A2.4. Site 5 Night 2008 Set 1 Archive (data through Jun. 30, 2008)

This section documents the Site 5 Night 2008 Set 1 data.

A2.4.1 Directory Name on Archival Drive: Site5\Archival2008NightSet1Proc31Jul08. The date indicates the date that processing started.

A2.4.2 Dates Processed: Feb. 21 2008 – Jun. 30 2008

A2.4.3 Solar Zenith Angles Processed: 104 and greater

A2.4.4 Moon Zenith Angles Processed: 0 and greater.

A2.4.5 Algorithm Used: These data used the new moonlight cloud decision algorithm with ProcWSID Version 2.4

A2.4.6 General Comments:

Nighttime data collected during this period were occasionally affected by image artifacts and offscale pixels caused by multiple light sources added to the site prior to camera repairs. New inputs were created to account for a shift in camera position, re-calibration of the camera, and to account for stray light effects. Though no test has been performed, results appear to be comparable to 2007 results. Also, during May 23 – June 30, some data are marked with a QC level of 2, or "uncertain", during the May 23 – June 30 period. This is because the occultor had failed, so starlight data are good, but some moonlight data are not valid because the occultor was not in place. These flagged data should not be used.

A2.4.7 Processing of Night Site 5 2008 Set 1 Data:

A record of the data availability and data processed for Site 5 is shown in the Appendix.

In 2008, the repaired instrument was installed Jan 16 2008. The occultor ACP failed May 22 2008, and was repaired and a new shade was installed June 30 – July 2 2008. Set 1 consists of the data from Jan 16 – June 30 2008. During May 23 – June 30, only the starlight data are valid, but the moonlight data are flagged as "uncertain" and should be removed. Of this period, all but Jan 16 – Feb 20 have been processed. This residual data will be processed and delivered with the next delivery.

A2.4.8 Equations to relate Pixel Position to Angle:

The same equations given in Section 1 of this memo may be used for the night data, being careful to use the image center for the correct period.

A2.5. Site 5 Night 2008 Set 2 Archive (data from Jun. 30, 2008 – Aug. 4, 2008)

This section documents the Site 5 Night 2008 Set 2 data.

A2.5.1 Directory Name on Archival Drive:
Site5\Archival2008NightSet2Proc16Oct08. The date indicates the date that processing started.

A2.5.2 Dates Processed: Jul. 1 2008 – Aug. 4 2008

A2.5.3 Solar Zenith Angles Processed: 104 and greater

A2.5.4 Moon Zenith Angles Processed: 0 and greater.

A2.5.5 Algorithm Used: These data used the new moonlight cloud decision algorithm with ProcWSID Version 3.1.

A2.5.6 General Comments:

A light shade was added to the camera, which eliminated most of the stray light artifacts found in the earlier 2008 nighttime data. New inputs were created to account for the shade, shift in camera position, and elimination of the stray light issue. As with earlier 2008 nighttime data, initial assessment of the results indicate accuracy is on par with 2007 test results.

A2.5.7 Processing of Night Site 5 2008 Set 2 Data:

A record of the data availability and data processed for Site 5 is shown in the Appendix.

The instrument was repaired and a new shade was installed June 30 – July 2 2008. We received Set 2 test data August 12, and the real time algorithm, tested with Set 2 data, was installed August 26. An upgrade to the algorithm was installed 23 September. We have processed the data from July 1 through August 4 2008. The data since August 26 should be valid, but we will process all data from August 5 through September 23 after we receive the data.

A2.5.8 Equations to relate Pixel Position to Angle:

The same equations given in Section 1 of this memo may be used for the night data, being careful to use the image center for the correct period.

A2.6. Next Delivery

At the present time, we are working on Site 3 Night data, as well as Site 2 daytime data. The Site 2 data is especially important, because it includes a long data archive starting in 2006. We also plan to include missing pieces from this data set, such as the Site 5 May 21 and 22 2008 daytime data mentioned in Section 1.6.

Sub-Appendix 2.1: Current Data Availability for Site 5 and 3

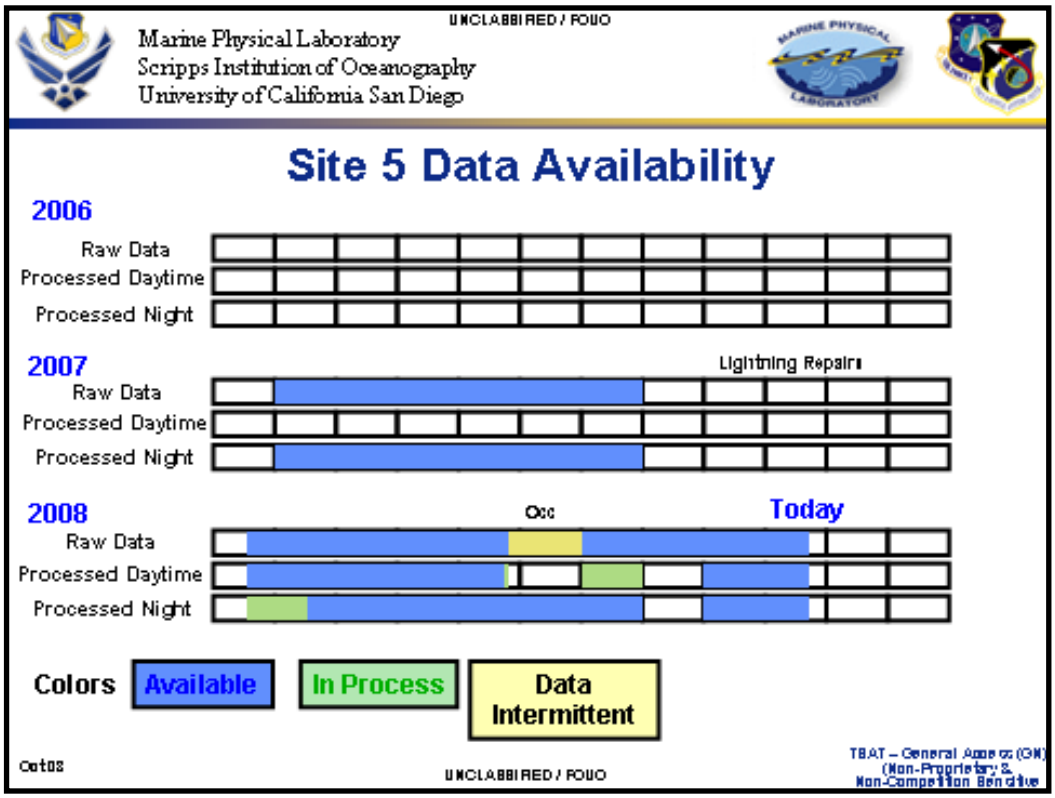

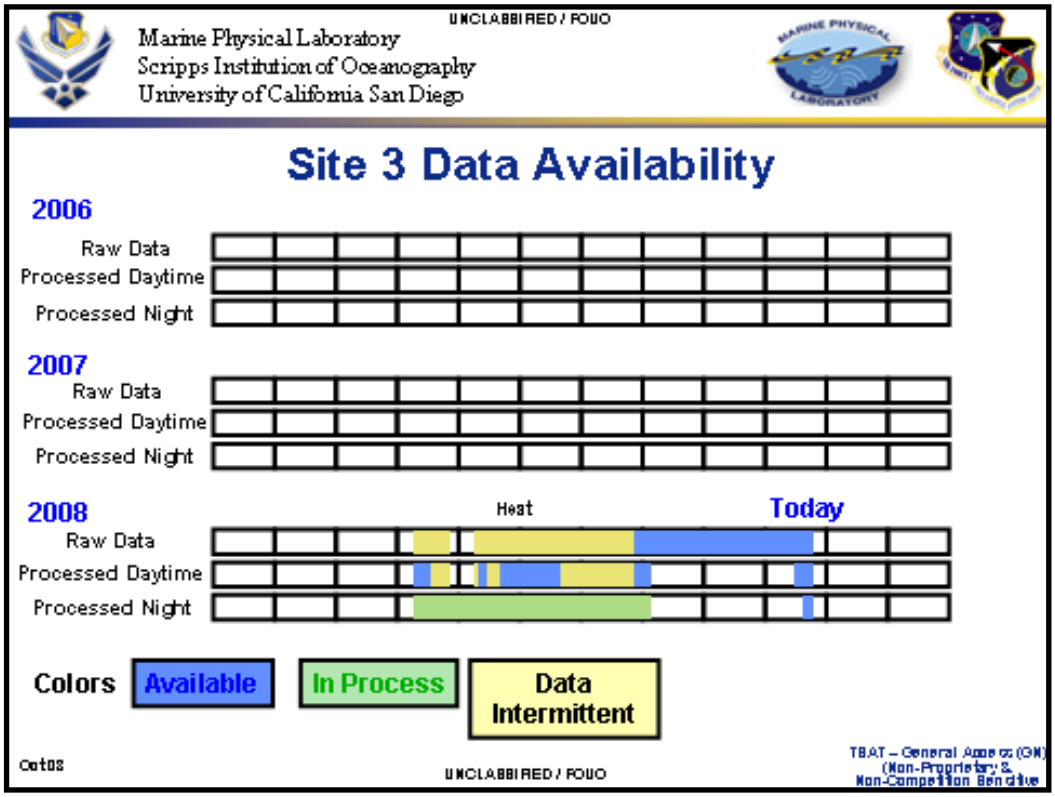

Appendix 3: Contents of Memo AV09-024, documenting the use of the real time algorithms.

Note: In order to be reasonably clear within the context of this report, all of the technical memo section numbers have had "A3." added to them, so that Section 1 because Section A3.1. If the memo refers to a given section X, then it should be understood that in the context of this report, this becomes Section A3.X.

Subject: Delivery of Real Time Cloud Algorithms

At the time that we delivered the first archival cloud algorithm data to SOR, we also delivered Memos AV08-037t that provides an overview of the data format, and Memo AV08-038t, that documents the actual contents of the archival delivery, as well as the specific geometric calibrations for that data. At that time, our sponsors asked if we could create a memo similar to AV08-038t that documents the delivery of the cloud algorithms for real time processing.

Monette recently wrote Memo AV09-005t that documents the actual software versions and when they were fielded, as well as a brief statement on their differences. In this memo, we will document the additional information needed to interpret the cloud data processed in the field. We have also recently completed a second archival of processed data, and that data is documented in Memo AV09-023t.

A3.1. Site 2 Day Real Time Cloud Algorithm

This section documents the Site 2 Day real time cloud algorithm status.

A3.1.1 Overview of Earlier Deliveries: The first version of the day algorithm set up with the inputs extracted for Site 2 was installed on Sep 6 2006. The day algorithm extraction is documented in Memo AV06-020t. More recently, the day algorithm was upgraded to include the adaptive algorithm, to better handle haze, and the inputs have been updated. The rest of this section documents this version of the code.

A3.1.2 Date Installed: The real time algorithm with the new adaptive algorithm was sent to SOR on Feb 12 2009. They will install it on the system as soon as practical. This has been delayed because there is a problem with the link from SOR to the WSI processing computer. Data prior to this date will be processed and delivered as archival data. Data starting on this date may be considered valid, until further updated.

A3.1.3 Solar Zenith Angles Processed: 0 - 85

A3.1.4 Algorithm Used: This algorithm is ProcWSID Version 3.5, which will be documented in a future memo.

A3.1.5 General Comments:

These algorithm inputs are extracted using the data from Jan 1 – Jul 31 2008 documented in Memo AV09-007t. Minor updates to the algorithm are based on the data from November 14, 2008 to January 27, 2009 and are documented in Memo AV09-019t.

A3.1.6 Equations to relate Pixel Position to Angle:

The following equations may be used to convert between image coordinates and spherical coordinates. The zenith and azimuth are in degrees, and azimuth is clockwise with respect to True North in real space (not in image space). That is, the bottom of the image is North, and the right side is East, as explained in Memo AV08-037t.

The following equations are identical to those used in Section 2.7 of Memo AV09-023t, using the center coordinates given in Section 3.7 of that same memo.

$$\phi = -0.8159 + \rho + 0.003908\,\rho\,\mathrm{Cos}(\pi\phi_0/90) - 0.0006394\,\rho\,\mathrm{Sin}(\pi\phi_0/90) \qquad (1)$$

$$\theta = 0.3357\ \rho - 0.00002765\ \rho^2 + 5.861\times10^{-7}\ \rho^3 + 0.0009443\ \rho\,\mathrm{Cos}(\pi\phi/90) + 0.003616\ \rho\,\mathrm{Sin}(\pi\phi/90) \qquad (2)$$

$$\text{where } \phi_0 = \arctan\left[\frac{(x - x_{center})}{(y - y_{center})}\right] \text{ and } \rho = \sqrt{(x - x_{center})^2 + (y - y_{center})^2}\,. \qquad (3)$$

For Site 2 data collected on and after Feb 12 2009, x_{center} = 255.5 and y_{center} = 256.0.

To derive the x,y pixel position corresponding to a given angular position θ, ϕ, in degrees, the equations are:

$$X = X_C + P \times Sin(\pi\phi_P/180) \qquad (4)$$

$$Y = Y_C + P \times Cos(\pi\phi_P/180) \qquad (5)$$

where

$$\mathrm{P} = 3.004\,\theta - 0.0007256\,\theta^2 - 0.00002487\,\theta^3 - 0.006796\,\theta\,\mathrm{Cos}(\pi\phi/90) - 0.02725\,\theta\,\mathrm{Sin}(\pi\phi/90) \qquad (6)$$

$$\phi_\mathrm{p} = \phi - (-0.8158 + 0.003908\,\mathrm{P}\,\mathrm{Cos}(\pi\phi/90) - 0.0006394\,\mathrm{P}\,\mathrm{Sin}(\pi\phi/90) \qquad (7)$$

A3.2. Site 2 Night Real Time Cloud Algorithm

This section documents the Site 2 Night real time cloud algorithm status.

A3.2.1 Overview of Earlier Deliveries: The first version of the night algorithm set up with the inputs extracted for Site 2 was installed on March 5 2007. The night algorithm extraction is documented in Memo AV06-030t. This first version did not handle moonlight well, and only the starlight data were intended for use. More recently, the night algorithm was upgraded to include moonlight, and the inputs have been updated. The rest of this section documents this version of the code.

A3.2.2 Date Installed: The real time algorithm with the moonlight algorithm was sent to SOR on Feb 12 2009. They will install it on the system as soon as practical. This has been delayed because there is a problem with the link from SOR to the WSI processing computer. Data prior to this date will be processed and delivered as archival data. Data starting on this date may be considered valid, until further updated.

A3.2.3 Solar Zenith Angles Processed: 104 and greater

A3.2.4 Moon Zenith Angles Processed: 0 and greater.

A3.2.5 Algorithm Used: This algorithm is ProcWSID Version 3.5. The updates will be documented in a future memo.

A3.2.6 General Comments:

These algorithm inputs are extracted using data from 15 April – 31 July 2008. The data from 1 Jan – 27 Jan, 2009, have been tested to verify that the algorithm inputs apply well to the current data.

A3.2.7 Equations to relate Pixel Position to Angle:

The same equations used for the day algorithm, and provided in Section 1.6, may be used for the night algorithm.

A3.3. Site 3 Day Real Time Cloud Algorithm

This section documents the Site 3 Day real time cloud algorithm status.

A3.3.1 Overview of Earlier Deliveries: There were no earlier deliveries of the day algorithm for this site.

A3.3.2 Date Installed: The real time algorithm with the new adaptive algorithm was installed on 14 October 2008. Data prior to this date will be processed and delivered as archival data. Data starting on this date may be considered valid, until further updated.

A3.3.3 Solar Zenith Angles Processed: 0 - 85

A3.3.4 Algorithm Used: This algorithm is ProcWSID Version 3.2, documented in Memo AV08-051t.

A3.3.5 General Comments:

These algorithm inputs are extracted using the data from April 9 – August 4 2008 documented in Memo AV09-008t. We were able to use the same inputs for the real time algorithm, so these inputs are not documented separately.

A3.3.6 Equations to relate Pixel Position to Angle:

The following equations may be used to convert between image coordinates and spherical coordinates. The zenith and azimuth are in degrees, and azimuth is clockwise with respect to True North in real space (not in image space). That is, the bottom of the image is North, and the right side is East, as explained in Memo AV08-037t. The equations are the same as those presented in Section 6.8 of Memo AV09-023t, and are repeated below.

The equations for azimuth, ϕ, and zenith, θ in degrees, given pixel location x,y are:

$$\phi = 0.6730 + \phi_0 - 0.0005058\ \rho \mathrm{Cos}(\pi\phi_0/90) + 0.007731\ \rho\ \mathrm{Sin}(\pi\phi_0/90) \quad (8)$$

$$\theta = 0.3366\,\rho + 1.179\times10^{-5}\,\rho^2 + 4.242\times10^{-7}\,\rho^3 - 0.006667\,\rho\,\mathrm{Cos}(\pi\phi/90) - 0.0005109\,\rho\,\mathrm{Sin}(\pi\phi/90) \quad (9)$$

$$\text{where } \phi_0 = \arctan\left[\frac{(x - x_{center})}{(y - y_{center})}\right] \text{ and } \rho = \sqrt{(x - x_{center})^2 + (y - y_{center})^2}\ . \quad (10)$$

For these equations, x_{center} = 249.9 and y_{center} = 250.5.

To derive the x,y pixel position corresponding to a given angular position θ, ϕ, in degrees, the equations are:

$$X = X_C + P \times Sin(\pi\phi_P/180) \quad (11)$$

$$Y = Y_C + P \times Cos(\pi\phi_P/180) \quad (12)$$

where P and ϕ_p are defined by

$$\mathrm{P} = 2.980\,\theta - 0.0009243\,\theta^2 - 0.00002075\,\theta^3 + 0.05119\,\theta\,\mathrm{Cos}(\pi\phi/90) + 0.003791\,\theta\,\mathrm{Sin}(\pi\phi/90) \quad (13)$$

$$\phi_\mathrm{p} = \phi - (0.6730 - 0.0005058\,\mathrm{P}\,\mathrm{Cos}(\pi\phi/90) + 0.007731\,\mathrm{P}\,\mathrm{Sin}(\pi\phi/90)) \quad (14)$$

A3.4. Site 3 Night Real Time Cloud Algorithm

This section documents the Site 3 Night real time cloud algorithm status.

A3.4.1 Overview of Earlier Deliveries: There were no earlier deliveries of the night algorithm for this site.

A3.4.2 Date Installed: The night algorithm that handles both starlight and moonlight was installed on October 23 2008, and further updated on December 15 2008. Data prior to this date will be processed and delivered as archival data. Data starting on this date may be considered valid, until further updated.

A3.4.3 Solar Zenith Angles Processed: 104 and greater

A3.4.4 Moon Zenith Angles Processed: 0 and greater.

A3.4.5 Algorithm Used: This algorithm is ProcWSID Version 3.4 documented in AV08-051

A3.4.6 General Comments:

These algorithm inputs are extracted using Data from the period April 9 – September 30 2008.

A3.4.7 Equations to relate Pixel Position to Angle:

The same equations used for the day algorithm, and provided in Section 3.6, may be used for the night algorithm.

A3.5. Site 5 Day Real Time Cloud Algorithm

This section documents the Site 5 Day real time cloud algorithm status.

A3.5.1 Overview of Earlier Deliveries: There were no earlier deliveries of the day algorithm for this site.

A3.5.2 Date Installed: The real time algorithm with the new adaptive algorithm was installed on August 26 2008, and then updated October 14 2008. Data prior to October 14 will be processed and delivered as archival data. Data starting on this date may be considered valid, until further updated. The rest of this section documents the October 14 2008 delivery.

A3.5.3 Solar Zenith Angles Processed: 0 - 85

A3.5.4 Algorithm Used: This algorithm is ProcWSID Version 3.2, documented in AV08-051

A3.5.5 General Comments:

These algorithm inputs are extracted using the data from Jan - May 2008, updated slightly using data from July 2008. The October 14 update also was based on July 2008 data, but used a slightly upgraded version of the adaptive algorithm.

A3.5.6 Equations to relate Pixel Position to Angle:

The following equations may be used to convert between image coordinates and spherical coordinates. The zenith and azimuth are in degrees, and azimuth is clockwise with respect to True North in real space (not in image space). That is, the bottom of the image is North, and the right side is East, as explained in Memo AV08-037t. The equations are the same as those presented in Section 9.7 of Memo AV09-023t, and are repeated below.

The equations for azimuth, ϕ, and zenith, θ in degrees, given pixel location x,y are:

$$\phi = 0.05787 + \phi_0 - 0.004426\ \rho \mathrm{Cos}(\pi\phi_0/90) + 0.0002416\ \rho \mathrm{Sin}(\pi\phi_0/90) \qquad (15)$$

$$\theta = 0.3436\rho - 0.00004412\rho^2 + 7.145\times10^{-7}\ \rho^3 + 0.0006305\rho \mathrm{Cos}(\pi\phi/90) - 0.004436\rho \mathrm{Sin}(\pi\phi/90) \qquad (16)$$

$$\text{where } \phi_0 = \arctan\left[\frac{(x - x_{center})}{(y - y_{center})}\right] \text{ and } \rho = \sqrt{(x - x_{center})^2 + (y - y_{center})^2}\ . \qquad (17)$$

For these equations, $x_{center} = 243.8$ and $y_{center} = 240.5$.

To derive the x,y pixel position corresponding to a given angular position θ, ϕ, in degrees, the equations are:

$$X = X_C + P \times Sin(\pi\phi_P/180) \qquad (18)$$

$$Y = Y_C + P \times Cos(\pi\phi_P/180) \qquad (19)$$

where P and ϕ_p are defined by

$$\mathrm{P} = 2.932\,\theta - 0.0002749\,\theta^2 - 0.00003042\,\theta^3 - 0.004269\,\theta\,\mathrm{Cos}(\pi\phi/90) + 0.03171\,\theta\,\mathrm{Sin}(\pi\phi/90) \qquad (20)$$

$$\phi_{\mathrm{p}} = \phi - (0.05787 - 0.004426\,\mathrm{P}\,\mathrm{Cos}(\pi\phi/90) + 0.0002416\,\mathrm{P}\,\mathrm{Sin}(\pi\phi/90)) \qquad (21)$$

A3.6. Site 5 Night Real Time Cloud Algorithm

This section documents the Site 5 Night real time cloud algorithm status.

A3.6.1 Overview of Earlier Deliveries: There were no earlier deliveries of the night algorithm for this site.

A3.6.2 Date Installed: The night algorithm that handles both starlight and moonlight was installed on August 26 2008, and further updated on September 23 2008. Data prior to September 23 2008 will be processed and delivered as archival data. Data starting on this date may be considered valid, until further updated.

A3.6.3 Solar Zenith Angles Processed: 104 and greater

A3.6.4 Moon Zenith Angles Processed: 0 and greater.

A3.6.5 Algorithm Used: This algorithm is ProcWSID Version 3.2, documented in AV08-051

A3.6.6 General Comments:

These algorithm inputs are extracted using the data from the period February 1, 2007 – August 4, 2008. The data from July 1 – August 4, 2008, have been tested to verify that the algorithm inputs apply well to the current data.

A3.6.7 Equations to relate Pixel Position to Angle:

The same equations used for the day algorithm, and provided in Section 5.6, may be used for the night algorithm.

A3.7. Site 7 Day Real Time Cloud Algorithm

This section documents the Site 7 Day real time cloud algorithm status.

A3.7.1 Overview of Earlier Deliveries: The day algorithm was updated in 2005, and has not been updated since this time. I believe the earlier deliveries are not of interest at this time, however in the sections below I will document the 2005 delivery.

A3.7.2 Date Installed: The real time algorithm was installed on 10 November 2005. We plan to extract the inputs for the updated algorithm in the near future, and will reprocess all of the data up to that data and deliver it as archival data. Data starting on 10 November was initially valid, but we don't know at what rate the required inputs may have changed.

A3.7.3 Solar Zenith Angles Processed: 0 – 79

A3.7.4 Algorithm Used: This algorithm is ProcWSID Version 1.0

A3.7.5 General Comments:

These algorithm inputs are extracted using the data from July and August 2005, and are documented in Memo AV05-031t, AV05-032t, and AV05-038t. The algorithm worked reasonably well at that time, but if the filters decayed, it would be less good in later periods. This version of the algorithm also did not include the adaptive algorithm.

A3.7.6 Equations to relate Pixel Position to Angle:

The following equations may be used to convert between image coordinates and spherical coordinates. The zenith and azimuth are in degrees, and azimuth is clockwise with respect to True North in real space (not in image space). That is, the bottom of the image is North, and the right side is East, as explained in Memo AV08-037t.

The equations for azimuth, ϕ, and zenith, θ in degrees, given pixel location x,y are:

$$\phi = -0.3116 + \rho - 0.002360\,\rho\,\mathrm{Cos}(\pi\phi_0/90) + 0.002635\,\rho\,\mathrm{Sin}(\pi\phi_0/90) \tag{22}$$

$$\theta = 0.3400\ \rho - 1.3661\times10^{-5}\ \rho^2 + 5.366\times10^{-7}\ \rho^3 - 0.003086\ \rho\,\mathrm{Cos}(\pi\phi/90) - 0.002681\ \rho\,\mathrm{Sin}(\pi\phi/90) \tag{23}$$

where $\phi_0 = \arctan\left[\dfrac{(x - x_{center})}{(y - y_{center})}\right]$ and $\rho = \sqrt{(x - x_{center})^2 + (y - y_{center})^2}$.

For these equations, $x_{center} = 247.8$ and $y_{center} = 249.1$.

To derive the x,y pixel position corresponding to a given angular position θ, ϕ, in degrees, the equations are:

$$X = X_C + P \times Sin(\pi\phi_P/180) \tag{24}$$

$$Y = Y_C + P \times Cos(\pi\phi_P/180) \tag{25}$$

where P and ϕ_p are defined by

$$\mathrm{P} = 2.961\theta - 0.00080\,\theta^2 - 2.222\times10^{-5}\ \theta^3 + 0.02259\,\theta\,\mathrm{Cos}(\pi\phi/90) + 0.01941\,\theta\,\mathrm{Sin}(\pi\phi/90) \tag{26}$$

$$\phi_\mathrm{p} = \phi - (-0.3116 - 0.002360\,\mathrm{P}\,\mathrm{Cos}(\pi\phi/90) + 0.002635\,\mathrm{P}\,\mathrm{Sin}(\pi\phi/90)) \tag{27}$$

A3.8. Site 7 Night Real Time Cloud Algorithm

This section documents the Site 7 Night real time cloud algorithm status.

A3.8.1 Overview of Earlier Deliveries: The night algorithm currently deployed at Site 7 is an older, contrast-based version of the software that produces medium resolution cloud decision imagery. Memos AV05-031 and AV05-037 document the delivery of night algorithm results for the period July-August, 2005.

A3.8.2 Date Installed: The real time algorithm was installed prior to 2005, with additional minor upgrades installed on 10 November 2005. We plan to extract the inputs for the updated high-resolution algorithm in the near future, and will reprocess all of the data up to the present time and deliver it as archival data.

A3.8.3 Solar Zenith Angles Processed: 104 and greater.

A3.8.4 Moon Zenith Angles Processed: 0 and greater.

A3.8.5 Algorithm Used: This algorithm is ProcWSID Version 1.0

A3.8.6 General Comments: The contrast-based night algorithm works reasonably well for imagery that does not show the moon in the field of view. Imagery with the moon at medium to high brightness are not typically handled well in this version of the software. The transmittance-based software will eliminate many of the issues found in the earlier version of the night algorithm. Thus these data should only be used for no moon. Also, the geometric calibration has probably long since changed, so data starting around 2007 should not be used without checking to see if it makes sense or not.

A3.8.7 Equations to relate Pixel Position to Angle:

The same equations used for the day algorithm, and provided in Section 7.6, may be used for the night algorithm.